Universidad Politécnica de Cartagena

Departamento de Tecnologías de la Información y las Comunicaciones

Contribución a los protocolos anticolisión y técnicas de dimensionamiento para sistemas de identificación por radiofrecuencia

María Victoria Bueno Delgado

Director
Javier Vales Alonso

2010

Technical University of Cartagena

Department of Information Technologies and Communications

A contribution to anti-collision protocols and deployment techniques for radio frequency identification systems

María Victoria Bueno Delgado

Supervisor
Javier Vales Alonso

2010

A mi familia

Abstract

The RFID technology has reached a peak since the adoption in 2005 of the EPCglobal Class 1 Gen 2 standard (EPC-C1G2). RFID has replaced other automatic identification systems like barcodes in some sectors. Besides, it has attracted the attention of scholars in RFID technology. The future of RFID looks promising, with a wide range of application fields, such as home automation, checkout systems, healthcare, public transport, and so forth. Currently, developments are underway in various areas of RFID: physical design, development of middleware, anti-collision algorithms, optimal network planning, etc. These investigations seek to improve RFID performance and reduce costs of deployment and operation.

The contribution of this thesis is twofold. First, the anti-collision mechanisms are studied in depth, and new solutions are suggested both for active and passive RFID systems. Second, the co-existence of several readers in dense reader environments is also investigated in this work. The major outcomes are described next.

One of the main goals of this thesis has been to analyze the performance of the anti-collision mechanisms in passive RFID. Standards as well as relevant proposals based on *Frame Slotted Aloha* (FSA) have been modeled using *Discrete Time Markov Chains* (DTMC). From these models the most relevant performance metrics in the identification process are computed. Namely, the Mean Identification Time (and throughput) in static scenarios, and the Tag Loss Ratio for semi-static and dynamic cases. Based on these results, optimal configuration criteria are provided.

Moreover, since FSA algorithms are inefficient under variable populations of tags, Dynamic FSA (DFSA) are regarded as an efficient solution to cope with this issue. A comprehensive survey of DFSA mechanism is developed in this work, including a DTMC characterization of the optimal DFSA mechanism, and a comparative analysis of current proposals performed via simulation. In addition, we propose a new anti-collision algorithm, the *Multi-Frame Maximum-Likelihood* DFSA algorithm (MFML-DFSA), which outperforms the previous ones, and has a lower computational cost which enables a feasible implementation in current readers.

On the other hand, for active tags, the goal of minimizing power consumption is added to the design constraints of anti-collision protocols. Despite the increased capabilities of these equipments, conventional FSA approaches have been the most extended so far. Since active devices already integrate carrier sensing, two new anti-collision algorithms are suggested based on this observation. A non-persistent *Carrier Sense Multiple Access*

(CSMA) mechanism based upon the quasi-optimal Sift distribution, which is indented to minimize the mean identification time and to reduce the activity periods of the tags. And a p-persistent CSMA, which is able to minimize energy waste switching off a majority of tags during contention slots.

Finally, dense RFID reader environments are studied in this doctoral thesis. In some installations, a single reader is not enough to cover a large identification area, or several identification gates may be present. Hence, several readers are required, and the overall performance is negatively affected by two types of collisions: *Reader to Tag Collisions* (RTC) and *Reader to Reader Collisions* (RRC). Our focus was on the review of the scheduling solutions aimed at minimizing these types of collisions. The performance of the different mechanisms is studied in order to provide comparative results of efficiency and network usability. The drawbacks extracted are used to suggest the key design properties of an efficient scheduler.

Resumen

Desde la aprobación en el año 2005 del estándar EPC Global Class 1 Gen 2, la tecnología RFID ha experimentado un gran auge, sustituyendo, en ciertos sectores, a otros sistemas de identificación automática como el código de barras. Asimismo, se ha despertado un mayor interés de investigadores y de la comunidad científica en la tecnología RFID. El futuro es prometedor, con un amplio abanico de ámbitos de uso, por ejemplo, en domótica, sistemas de control y pago, sanidad, transporte publico, etc. Actualmente se están llevando a cabo desarrollos en diversas áreas de RFID: diseño físico, desarrollo de *middleware*, algoritmos anti-colisión, planificación óptima de la red, etc. Estas investigaciones persiguen mejorar el desempeño de RFID y reducir los costes de despliegue y operación.

Esta tesis aporta contribuciones en dos campos de la tecnología RFID. En primer lugar, los mecanismos de control de acceso al medio han sido estudiados en profundidad, proponiendo nuevas soluciones tanto en RFID activa como pasiva. En segundo lugar, la coexistencia de varios lectores en un entorno es también abordada en este trabajo. A continuación se describen en mayor detalle los resultados fundamentales obtenidos.

Uno de los principales objetivos de esta tesis ha sido analizar el funcionamiento de los mecanismos anti-colisión en sistemas RFID pasivos. Éstos, tanto en el estándar como en las propuestas afines, se basan en *Frame Slotted Aloha* (FSA) y se pueden modelar mediante cadenas de Markov de tiempo discreto (*Discrete Time Markov Chain*, DTMC). A partir de estos modelos se calculan las métricas de rendimiento más importantes del proceso de identificación. A saber, el tiempo medio de identificación (y el *throughput*) en los escenarios estáticos, y el ratio de pérdida de etiquetas para escenaros semi-estáticos y dinámicos. En base a dichos resultados, se proporcionan criterios de configuración óptima.

Por otra parte, los algoritmos FSA no son eficientes si el número de etiquetas en el proceso de lectura varía. En este caso los sistemas FSA dinámicos (DFSA) son considerados como una buena solución para hacer frente a este problema. En este trabajo presentamos un estudio detallado de los mecanismos DFSA existentes, incluyendo una caracterización mediante DTMC del mecanismo de DFSA óptimo, y una comparativa de las propuestas actuales realizada mediante simulación. Además, se propone un nuevo algoritmo anti-colisión DFSA llamado *Multi-Frame Maximum-Likelihood* (MFML-DFSA), que supera a los anteriores y tiene un coste computacional reducido. Por tanto su implementación en los lectores actuales es viable.

En el ámbito del RFID activo, el objetivo de reducir al mínimo el consumo de energía se añade a las restricciones de diseño de los protocolos anti-colisión. En RFID activo se ha empleado FSA convencional hasta la fecha, a pesar de que las capacidades de las etiquetas activas son mucho mayores. Dado que los dispositivos activos ya integran mecanismos de detección de portadora, se han propuesto en este trabajo dos nuevos algoritmos anti-colisión. El primero está basado en *Carrier Sense Multiple Access* (CSMA) no persistente unido a la distribución quasi-óptima Sift. Así, se consigue minimizar el tiempo de identificación y reducir los períodos de actividad de las etiquetas. El segundo mecanismo es un CSMA p-persistente, que es capaz de reducir al mínimo el gasto de energía apagando la mayoría de las etiquetas en las ranuras de contienda.

Por último, los entornos con múltiples lectores de RFID son estudiados en esta tesis doctoral. En algunas instalaciones un único lector no es suficiente para cubrir una gran área de identificación, o es posible que existan varias puertas de identificación. Por lo tanto, varios lectores pueden ser necesarios, y el rendimiento global del sistema se ve afectado negativamente al aparecer dos nuevos tipos de colisiones: colisiones Lector-Etiqueta (*Reader to Tag Collisions*, RTC) y Lector-Lector (*Reader to Reader Collisions*, RRC). Las soluciones destinadas a minimizar estos tipos de colisiones han sido revisadas, y su rendimiento se ha comparado en términos de eficacia y de uso de la red. De este estudio se han extraido las características claves que ha de tener un planificador eficiente.

List of Contents

List of Figures

List of Tables

Chapter 1

Introduction

This chapter provides an overview of the basic principles and the major technical aspects related to the Radio Frequency IDentification (RFID) technology and its standardization. This review includes a brief discussion of the main open issues and ongoing activities of research in active and passive RFID, as well as the motivations and goals of this thesis. Finally, the structure of this thesis and its main contributions are summarized.

1.1 Introduction

Radio Frequency IDentification (RFID) enables the identification of distant objects or people by means of a Radio-Frequency (RF) communication link [Finke03]. The communication takes place between a population of small and portable devices called tags or transponders, attached to the items to be tracked, and one or more reader devices which collect and manage information about these items. In general, the tags are simple devices composed by an antenna and a basic electronic circuit with a memory to store information about the object they are attached to. Tags are intended to label people, animals, pallets, etc. Readers are more complex, they transmit continuously electromagnetic waves, creating *checking areas*. When tags pass through the checking areas they send their stored information back to the reader, thereby identifying the objects. The identification is carried out by means of a communication protocol, such as ISO/IEC18000 [ISO03], EPCglobal Class-1 Gen-2 (EPC-C1G2) [EPCgl05], etc.

RFID, compared with other identification technologies like barcodes, permits automatic identification with no human participation and without the need for a line of sight link between reader and tags.

Over the last years, the advances in communications and microelectronics, the huge decrease in the cost of the technology and the global standardization of EPC-C1G2 have motivated institutions and researchers to work actively on RFID, developing RFID systems adapted to the new standard and working to adopt RFID in a wide variety of environments and applications, *e.g.* animal identification, toll road control, checkpoint systems, security and access control, digital card mail, toy industry, etc.

Although the effort to reach the global implementation of RFID is clear, the integration is not being as quickly and satisfactory as experts expected. There are many factors affecting directly to RFID adoption, mainly the lack of clear information regarding the actual advantages of RFID in comparison with current identification systems, and the lack of confidence in some industrial sectors. In addition, some open issues in the EPC-C1G2 global standard are still under active research: hardware design, communication protocols, security, privacy, etc.

1.2 Historical Development of RFID

RFID was born as the combination of radar and radio broadcast technologies. The first known work on RFID dates back to 1948, the landmark paper written by Harry Stockman “Communications by Means of Reflected Power” [Stock48]. In the 1950s, different sectors started working on RFID for high range transponders, known as “Identification Friend or Foe’ (IFF), for the aeronautic industry. Developments of 1950s and 1960s such as F.L. Vernon’s “Application of the Microwave homodyne” [Verno52] and D.B. Harris, “Radio transmission system with modulatable passive responder” [Harri60], contributed significantly to the evolution of RFID. Also in 1960s the Electronic Article Surveillance (EAS) introduced RFID to protect against thefts in large department stores. In the 1970s, RFID was progressively applied to logistics, transportation, vehicle tracking, livestock tracking and in industrial automation. However, it is only in 1973, that the first RFID patent was filed by Charles Walton, a former IBM researcher, for a radio-operated door lock [Charl73]. Starting from the 1980s, commercial implementations in the USA focused on the access control and transport. In Europe, RFID was intended to improve industrial applications and to enable short-range systems for animal control. In Japan, RFID was used for contactless payments in transportation systems, *e.g.*, the Felicity Card (FeliCa). RFID development took advantage of progresses in related fields: microelectronics, antenna design, software and microprocessors. The fields of application of RFID were substantially extended thanks to companies like Texas Instruments or Philips, which promoted the development and marketing of RFID devices. Currently, the Auto-ID Labs [AutoID] is the leading organization for the development and implementation of RFID. The Auto-ID Labs is a consortium founded in 1999 by hundreds of companies, universities and research centers from all over the world. Auto-ID Labs consists of six laboratories located at different prestigious universities such as the Massachusetts Institute of Technology (MIT) in the USA, the University of Cambridge in UK, the University of Adelaide in Australia, Keio University in Japan, Fundan University in China and the University of St. Gallen in Switzerland. In 2005, the Auto-ID Labs, the European Article Number (EAN) International, the Uniform Code Council (UCC) and a large number of multinational companies developed the EPC^{TM} net and its components, including the EPC-C1G2 [EPCgl05] standard, considered the worldwide standard for RFID systems.

1.3 Components of a RFID system

A typical RFID system consists of three components: (i) RFID tags or transponders (ii) one or more readers and antennas which control data transmission and tags identification and (iii) the processing software, commonly called middleware (see Figure 1.1). In the following sections, we describe each of these components in depth, especially readers and tags.

1.3.1 Tags

Tags store information about the object to which they are attached to. This information includes their unique serial number (called ID), their standardized identification codes, history of transactions or measurements, for example, the temperatures monitored by a sensor, the manufacturing date, the expiration date, etc. When tags are within the range of some reader, they transmit their identification data to the reader, which stores and/or processes the information according to the needs of the service or final application. There are many criteria to classify RFID tags such as their size, the energy source, their durability, the operating frequency, the polarization, the communication protocol, etc. However, the tags are usually classified by their source of energy. Namely, the can be passive, active, or semi-passive.

- *Passive* tags are extremely simple and inexpensive devices (*e.g.* less than 0.10 € in [Alien]) which do not incorporate batteries and are powered by the signals emitted by the reader. This energy activates the circuit of the tag and produces a response signal that includes the information in the tag's memory. The maximum communication range spans from some centimeters to a few meters.

- *Active* tags have a fully autonomous power source which, in most cases, can be replaced. The cost of these devices is much higher than passive ones (*e.g.* from 20 € in [Altic09]) because they incorporate circuits with a microprocessor and a memory to read, write, rewrite or erase data from an external device. The main advantage of active tags is the long reading distance, more than 100 meters.

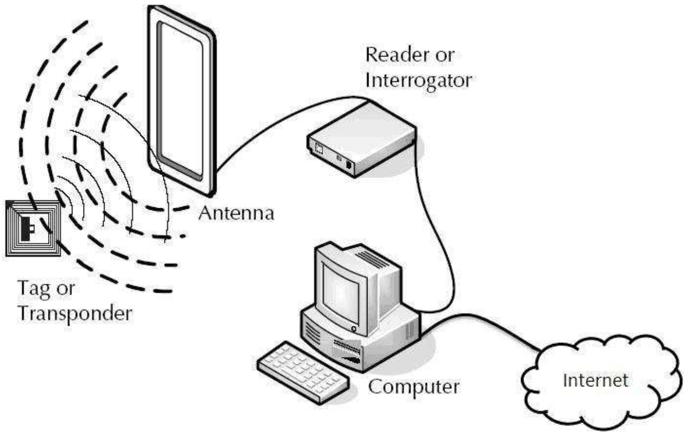

Figure 1.1: RFID system

- *Semi-passive* tags have built-in batteries to power the tags' integrated circuit. The electromagnetic waves from the reader are only used to activate tags in coverage. Then, the tag's response is generated using the energy from the batteries, which is faster than circuitry activation in passive tags.

Another classification commonly used for RFID tags is based on their read and write capabilities, distinguishing five classes [EPCgl05]:

- *Class 0*. Read-only tags. This is the simplest type of tags. The data, usually the identification number, are written into the tag only once during the manufacturing process. Then, the memory is disabled for future write updates.

- *Class 1*. Write-once/Read-only. The tag's memory can be written only once. After this, tags can only be read.

- *Class 2*. Read/Write. In these devices, data can be written and read by the operator an undefined number of times.

- *Class 3*. Read/Write on board sensors. These tags are active or semi-active and contain on-board sensors to store different measures of interest, which depend on the type of sensor, *e.g.* temperature, humidity, pressure. These tags are used in Wireless Sensor Networks (WSN)[Akyld95].

- *Class 4*. Read/Write with integrated transmitters. These active tags can communicate with each other. They are typically applied in ad-hoc networks.

Finally, RFID tags can be further classified in terms of their format and size. Tag size is strongly affected by the RF operating frequency, which determines the dimensions of the antenna. Nowadays, several tag formats can be found in the market: smart card tags, coin tags, embedded tags, paper tags, etc.

1.3.2 Readers

The RFID reader is the key element in a RFID system. It is the interface to access tag information. The reader must be able to convert the data received from the tags into useful information for the final application. Readers can be classified according to tag type as follows:

- Readers for systems with active tags (active RFID systems). In active RFID systems, any tag can act as a reader, since active tags are able to communicate between them. The active tag in the role of reader must be connected to a computer or a network (via a wired or wireless link) to dump the data received from other active tags in coverage.
- Readers for RFID systems with passive tags (passive RFID systems) have to meet a key requirement: their transmission power must be enough to feed the surrounding passive tags. The tags obtain energy using a technique called *backscattering* [Finke03], allowing them to send back a response to the reader. Backscattering consists in reflecting the reader's carrier wave, while modulating a signal that contains the tag data. Then, the reader detects the backscattered response, processes the signal and reads the information sent by the tag.

Readers for active RFID systems are less restrictive than those for passive RFID systems. Next paragraphs will focus on the latter. Some selection criteria for commercial passive RFID readers are:

- Standards of communication between the reader and the associated tags. Although EPC-C1G2 standard is the most extended and adopted, there are also other standards in use such as family ISO-18000 [ISO03], and proprietary protocols (*e.g.* PSG RFID protocol [PSG09]). Therefore, the reader should support multi-protocol/standard operation.
- Operating frequency: Ultra High Frequency (UHF), Low Frequency (LF), or High Frequency (HF) (see section 1.4.1) are used in RFID communications.
- Number of RF ports to connect antennas. Usually, one reader allows up to four antennas.
- Maximum power delivered to each RF port. The antennas can be configured to transmit at different power levels.
- Networking to host protocol: RS-232, Wireless, Ethernet, TCP/IP.
- Reader-to-Reader connection. Readers must be able to coexist together in the same coverage area or in the same network.
- Fixed or portable reader. Readers can be located at a static point in a strategic area, or can be portable and being carried by operators. Portable readers (also called *handled* readers), collect the tag information when the operator passes close to the tag. Then, the reader sends the information to an application by means of a wireless link such as Wifi or Bluetooth.

Frequency	Read range	Read rate	Cost (as of 2009)	Applications
LF: 100-500 KHz	< 50 cm	200 bps - 1 kbps	< 15 cent.	Access control, animal identification, inventory control, etc.
HF: 10-15 MHz	< 1 m	25 Kbps	< 15 cent.	Access control, smart cards, etc.
UHF: 850-950 MHz, 2.4-5.8 GHz	< 10 m	28-600 Kbps	30-50 cent.	Product traceability, supply chains, etc.

Table 1.1: Operating frequencies: characteristics and applications of passive tags

1.3.3 Antennas

Antenna designs differ according to the operating frequency. For low range applications, such as LF or HF range, the antennas are embedded in the readers, whereas in UHF applications antennas are external. On the other hand, polarization is a critical antenna parameter, which affects directly to the performance of the RFID system. In RFID, two types of polarization are used:

- *Linear-Polarization*: the electrical field component of the RF signal is propagated in a plane, and tags must be also orientated in that direction to establish the communication. Evidently, this technique requires also linearly polarized tags.

- *Circular-Polarization*: the electromagnetic waves are emitted in a circular pattern. These antennas are used in situations where the relative orientation between tag and reader is uncontrolled. Both circularly polarized tags and linearly ones work seamlessly with this polarization. Besides, circular-polarized antennas have a shorter read range than linearly polarized antennas.

1.3.4 Middleware

RFID middleware is the set of software tools which interfaces a RFID system with the existing enterprise information systems. For instance, a tag identifier can be used to query the database to obtain information about the item, such as shipment orders, invoices, repair logs, and so forth. EPCglobal specifications define a standard middleware for RFID systems [EPCne04]. However, despite vendors' claims [Al-Jar09], there is no general-purpose plug-and-play middleware solution and the general functionality must be tailored to the particulars of an application or an enterprise. Moreover, it should be noted that RFID applied to industrial environments (*e.g.* traceability) remains an immature and evolving technology. RFID middleware should be flexible enough so that it could be adapted to the future changes with minimal efforts.

1.4 Communications in RFID

1.4.1 Operating Frequencies

The communication frequencies used by RFID systems, both passive and active, range from 125 KHz to 2.45 GHz depending on the application, as Table 1.1 shows. Operating

Region	LF	HF	UHF	Microwaves
Region 1	125 KHz	13.56 MHz	868-870 MHz	2.446-2.454 GHz
Region 2	125 KHz	13.56 MHz	902-928 MHz	2.40-2.4835 GHz
Region 3	125 KHz	13.56 MHz	950-956MHz	2.427-2.470 GHz

Table 1.2: Regional Frequency allocations for RFID

frequency is directly related to the desired radio coverage. Four carrier frequencies are standardized:

- LF: Low Frequency, 125 KHz.
- HF: High Frequency, 13.56 MHz.
- UHF: Ultra High Frequency, 850-950 MHz.
- Microwaves: 2.45 GHz.

The International Telecommunication Union-Radiocommunications sector (ITU-R) is responsible for the management of the frequency spectrum worldwide. It divides the world into three regions:

- *Region 1* is regulated by the European Conference of Postal and Telecommunications (CEPT) whose main responsibilities include frequency and output power assignment. This region includes Europe, Africa and the Middle East.
- *Region 2* is regulated by the Federal Communications Commission(FCC). The region includes North and South America and Pacific Rim East, comprising the countries located on the east coast of the Pacific Ocean.
- *Region 3* is regulated by the Ministry of Public Management, Home Affairs, Posts and Telecommunication (MPHPT) of Japan. The region includes Asia, Australia and the Pacific Rim West, comprising the countries located on the west coast of the Pacific Ocean.

RFID tags and readers usually do not require a transmission license, since they are classified as Short Range Devices (SRD) but have to comply with different local regulations to prevent interferences with frequencies in the Industrial, Scientific and Medical (ISM) equipment band. The frequency allocations per region are shown in Table 1.2.

1.4.2 Near Field and Far Field Communications

Passive RFID communications can be categorized into Near-Field and Far-Field Communications [Finke03] according to the way tags are powered from the reader (see Figure 1.2). In Near-Field Communications (NFC) the tag extracts the energy from the magnetic field generated by the reader. Tags incorporate a small coil, where an electric current is induced by this magnetic field. The voltage between the two coil ends is rectified and coupled to a capacitor. Then, the charge accumulated is used to power the tag. NFC strategy is common for RFID systems in the LF or HF bands. In Far Field Communications (FFC), the incident electromagnetic radiation causes a difference of potential at the tag antenna which charges a capacitor that powers the tag. FFC strategy is used in UHF and microwave bands.

The theoretical boundary between NFC and FFC depends on the frequency used. For UHF RFID antennas (whose size is comparable to the wavelength), the approximate boundary between FFC and NFC is given as $\frac{2D^2}{\lambda}$ meters, where D is the antenna side size and λ is the wavelength. In LF and HF, the boundary between FFC and NFC is established at $\frac{\lambda}{2\pi}$ meters. An overview of FFC and NFC can be found in [Leckl05].

1.4.3 Modulation Procedures

RFID systems operate according to three different modulation techniques [Finke03]. We briefly introduce them:

- *Amplitude Shift Keying* (ASK). Amplitude modulation can provide a high data rate but with low noise immunity. For a given reference, a higher amplitude is assumed as a “1” and a lower one as a “0”.

- *Frequency Shift Keying* (FSK). This modulation uses two different frequencies to transmit data. FSK provides very strong noise immunity, but the data rate achieved is lower than with other modulations.

- *Phase Shift Keying* (PSK). This modulation technique is similar to FSK except that only one frequency is used, and the shift between “0” and “1” is accomplished by shifting the phase of the backscatter clock by π radians. PSK provides fairly good noise immunity, suitable for a moderate simple reader, and a faster data rate than FSK.

EPC-C1G2 allows to use all of them, although current readers operate only in one modulation.

1.5 Standards

Lack of standardization has traditionally been one of the main impediments for the wide scale adoption of RFID technology. Standards guarantee the interoperability among readers and tags of different manufacturers. However, the coexistence of multiple standards may cause the opposite effect by confusing the market.

In the past, each country used to sanction its own regulation for RFID frequencies and transmission specifications. The proliferation of local and regional standards prevented to some extent the spread of RFID technology. In recent years, several regulatory bodies, standard development organizations, and industry consortia such as the European Telecommunications Standards Institute (ETSI) [ETSI-R], EPCglobal [EPCgl05] and the International Standardization Organization (ISO) [ISO03], collaborated on a single global

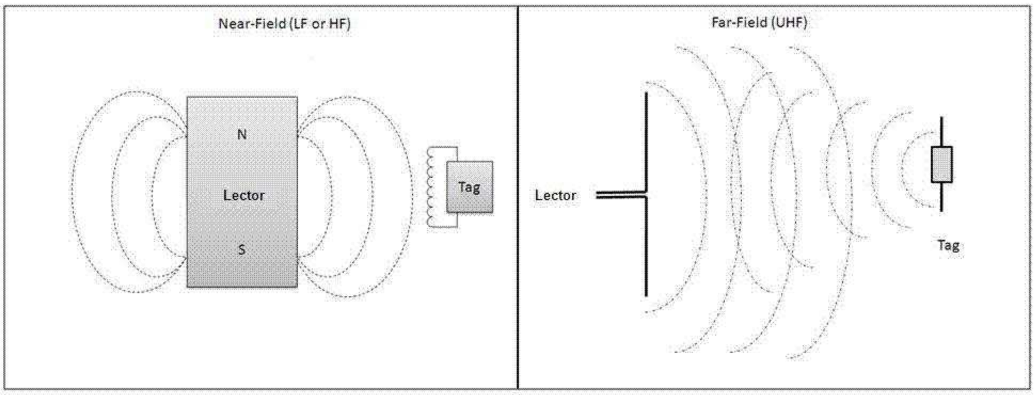

Figure 1.2: Near-Field and Far-Field Communication in RFID

standard for active and passive systems: EPC-C1G2, which joined characteristics from previous standards [Kleis05].

EPCglobal was created in 2004 as a consortium to lead the development of industry-driven standards for the EPC that supports RFID. The members of EPCglobal include industry leaders and organizations such as EAN International, UCC, the Gillete Company, Procter & Gamble, Wal-Mart, Hewlett Packard, Johnson & Johnson, Checkpoint Systems, Auto-ID Labs, and others. The main goal of EPCglobal is to increase visibility and efficiency of supply chains and to improve the quality of the information flows among companies and their trading partners.

EPC-C1G2 is regarded as the “worldwide standard to RFID systems” because it has been implemented to satisfy all the needs of the final customer, irrespective of the geographic location. Thus, an EPC-C1G2-compliant tag conforms other group of standards: ETSI EN 302 208-1, ETSI EN 302 208-2, ISO/IEC Directives-2, ISO/IEC 3309, ISO/IEC 16961, ISO/IEC 15962, ISO/IEC 15963, ISO/IEC 18000-1, ISO/IEC 18000-6, ISO/IEC 19762, Code of Federal Regulations (CFR) (Title 47: Telecommunication, Chapter 1: Federal Communications Commission, Part 15: Radio Frequency devices) and EPCglobal Tag Data Standards (Fast Moving Consumer Goods, FMCG, RFID Physical Requirements Documents, EPC-C1G2 UHF RFID Implementation Reference).

Although EPC-C1G2 was designed also for active RFID systems, it has not been introduced by manufacturers. Instead, ISO/IEC 18000-7 (also known as DASH7) is the most extended standard [ISO03]. It has been widely deployed in the USA Department of Defense (DoD). In addition, it consolidated its use in non military sectors in numerous markets. ISO/IEC 18000-7 has rapidly become the *de facto* global standard for active UHF RFID solutions.

ISO/IEC 18000-7 defines the Physical and Medium Access Control (MAC) layer as well as the communication protocol for active RFID systems communicating at 433 MHz.

Although ISO/IEC 18000-7 standard was ratified in 2004, and underwent subsequently modifications in 2008 and 2009, several open issues can be still found in *e.g.* data encryption, tag-to-tag communications and other aspects that may impact interoperability.

With the aim at improving ISO/IEC 18000-7 and extending its use, more than 20 RFID vendors, users and researchers have formed the Dash-7 Alliance [Dash7], an independent industry action group whose purpose is to promote the use of ISO/IEC 18000-7 active RFID technology.

The identification procedure of both EPC-C1G2 and ISO/IEC 18000-7 standards is studied deeply in Chapters 2 and 5.

1.6 Privacy and security

The RFID technology raises concerns regarding the privacy issues for individuals and organizations because the tags can be read by external parties without the owner's knowledge [Juels06, Peris06]. RFID threats affect individuals and businesses. The main risk to personal privacy is that a tag with a unique identification number can be used to track a person. In the case of commercial entities, corporate espionage threat is the most important risk. Policy and regulation-based solutions have been proposed to improve privacy protection in RFID systems in [Sarma03, Juels07]. Nevertheless, these proposals are not easy to implement and to manage. Some of the technical solutions suggested in scientific literature are described briefly here:

- *EPC Kill*. The Auto-ID Center designed the EPC Kill command as a pro-privacy technology. The principle of this command is "dead tags do not talk" and so it is applied. For instance, when tags pass through a checkpoint in a shop, they receive a "kill" command from the reader to deactivate themselves permanently. As an alternative to killing, tags can be attached to a product price tag and discarded at the point of sale.

- *Encryption*. The idea behind this solution is to store encrypted serial numbers into the tags. However, this procedure presents some problems regarding the distribution and management of keys. In addition, encryption does not protect from tracking because an encrypted serial number is, in essence, a static identifier that can help to track a tag.

- *Passwords*. Current tags have enough resources to verify passwords. The idea is simple: a tag does not send information unless it receives the right password. The problem is that a reader would not know the password to send without determining the tag's identity beforehand. However, this approach would be applied in specific environments where only one reader interacts with a known group of tags.

- *Pseudonyms*. Besides the product data, tags store a list of pseudonyms. Every time a tag must be identified by a reader, the tag selects one pseudonym from its list and sends it to the reader. The reader maintains the corresponding lists of pseudonyms for each tag. When the reader receives the pseudonym, it checks the lists to confirm the tag's identity. This makes the solution vulnerable to an attack where the same tag is scanned repeatedly to force it to reveal all the pseudonyms that it stores.

- *Blocker tags*. The idea behind them is that a group of tags (*e.g.*, tags attached to consumer items in a supermarket) create an RF environment that is hostile to unauthorized readers. A blocker tag is specifically configured to be read only by authorized scanners, for example, the readers installed in a given supermarket. This mechanism requires that a list of valid readers are known previously by the tags.

1.7 Collision problems

When two or more tags/readers transmit simultaneously, a collision may occur. Several collision types exists:

- *Single reader-multiple tags* collisions. Multiple tags are in the reading range of the same reader and respond simultaneously. The reader is unable to interpret the signals received.
- *Multiple readers-single tag* collisions. Only one tag is in the read range of multiple readers. The interferences occur when the outgoing signals from the neighboring readers collide with the tag transmission.
- *Reader-reader* collisions. Multiple readers are configured to operate in the same channel, interfering each other.

Collisions cause the loss of identities and control commands, producing delays in the identification process, and may even cause that tags leave the workspace unidentified. In order to minimize collisions, the RFID systems incorporate anti-collision mechanisms. Several proposals have been introduced with the aim of minimizing the collision problems in RFID systems, suggesting new anti-collision protocols that outperform current standards. These collision resolution methods depend on the RFID technology: in active RFID, the collision resolution is not only mandatory to reduce the identification time, but also to decrease the tag energy consumption in order to maximize the batteries lifetime. In this case, tag hardware permits putting forward sophisticated anti-collision mechanisms. On the other hand, in passive RFID, the extreme simplicity of the tags is a hard constraint in order to design new collision resolution methods. However, some approaches have been proposed, where the anti-collision complexity relies exclusively upon the reader.

Discussion of these three types of collisions resolution methods is addressed in Chapters 2, 5 and 4.

1.8 Energy consumption

Active RFID systems are demanding in terms of power consumption. Therefore, energy saving is mandatory to increment the operation lifetime. The major sources of energy waste are related to radio communication issues [Akyld02]: namely collisions, idle listening, and overhearing. In [YeW04] it is stated that idle listening is the dominant factor. It arises if active tags are continuously listening to the channel. Thus, a key mechanism to save energy is to turn off the radios during periods of inactivity [Akyld02, Stemm97, Schur08]. Other energy saving methods initially intended for WSN, such as [ZhouF04, Kubic03, Takag84, ChenY03], can be implemented (with slight modifications) in active tags. A detailed discussion of the energy consumption problem in active RFID is addressed in Chapter 5.

1.9 Advantages of RFID *vs.* Barcodes

Despite of privacy issues and collision problems, RFID has several advantages over the traditional identification systems based on barcodes, the original technology that drove the revolution in automatic identification systems. The main advantages of RFID compared with barcodes are:

- Read/Write Data. Tags can store data about the objects to which they are attached to. Information can be written or read by a reader at distances that can reach up to a few hundred of meters in the case of active tags.
- Storage capacity. A passive tag is able to store 30 times more data than a barcode and active tags 100 times more data [Finke03].
- Environmental information. Active tags can obtain real-time information about the carrier object through different sensors: temperature, vibrations, etc.
- Simultaneous identification. With traditional identification systems using barcodes, items must be read individually and manually to guarantee their successful identification. RFID provides simultaneous identification of a potentially large number of tags placed in its read range.
- Line-of-sight-free limitations. Tags can be identified without the need for line-of sight communication, even in the presence of obstacles.
- Resilience to forgery. Identifiers with barcodes can be easily replicated, by simply scanning and printing them. On the contrary, copying an RFID tag is not trivial for unskilled people.

Table 1.3 summarizes the main features that distinguish RFID from barcode technologies.

1.10 Research topics in RFID

Despite RFID spread, there is still a number of technical open issues and ongoing activities of research in passive and active RFID fields. Some of the most important points on passive technology are:

Characteristics	RFID	Barcodes
Writeable	Read/Write	Read only
Quantity of data	Up to Kbytes	Up to 100 bits
Read speed	ms	s
Read distance	Up to 100 m	Up to 2 cm
Data Format standard	Few	Many
Dirt influence	No effect	Very high
Sight obstruction	No effect	Very high
Effects of degradation /wear	None	Susceptible
Unauthorized copy	Ciphering	Susceptible
Cost	Depends on the tag	Inexpensive

Table 1.3: Comparison of RFID *vs.* Barcodes

- To enhance the Physical layer performance:
  - Decreasing the absorption and reflection effects caused by the metals and liquids. In many applications, the carrier of the tag contains liquids and/or metals. Also metallic environments, where RFID systems are commonly installed, increase the reflection effects, degrading the communications. Research is carried out in the design of new antennas as well as new shapes, sizes and materials to make tags less sensitive to these phenomena.
  - Attenuating electromagnetic noise and improving signal detection. RFID systems are usually installed in noisy scenarios: industrial warehouses, production chains, etc. Researchers study how to minimize interferences in these environments, studying the effect of antenna orientation, tag position, etc.
- To enhance the MAC and upper layers performance:
  - Designing new middleware platforms which permit to interconnect and exchange data from thousand of RFID systems and mixed applications.
  - Solving security and privacy problems. RFID technology exhibits confidence problems due to the lack of privacy. Institutions study new ways for data encryption and secure communication protocols.
  - Improving reading efficiency with new anti-collision algorithms which minimize collisions among tags. Optimizing the configuration parameters of the protocols. Previously to those actions, the mathematical characterization of the systems is mandatory.
  - Minimizing collisions in dense reader environments, that is, scenarios sensitive to collisions among readers. Since standards do not endorse efficient mechanisms to work properly in these scenarios, researchers study new schedulers and protocols to manage and allocate resources among readers with the aim of minimizing collisions and maximizing efficiency.

In active RFID, the research topics are mainly focused on:

- In Physical layer, enhancing energy savings: *e.g.* switching off tags during inactivity periods and with new hardware designs, etc.

- In MAC and upper layers, research topics are similar to passive RFID, including energy constraints.

All these topics affect notably the RFID performance. In the next sections the motivations and specific goals of this doctoral thesis are discussed. Finally, we describe the structure of following chapters, indicating the scientific contributions.

1.11 Motivation and goals of this thesis

Anti-collision methods for RFID have been extensively studied yielding to different proposals with the aim of enhancing reading procedures. One of the goals of this thesis has been to analyze and compute the reading performance of the relevant proposals, including standards and providing suitable criteria to select among them. In addition, new anti-collision algorithms, which outperform the previous ones, have been proposed in this work. Such new algorithms have a lower computational cost which enable feasible implementation in current readers. Besides, we have detected that the lack of previous studies about the optimal configuration of the standard protocols in passive RFID systems. Hence, another goal of this thesis has been to discuss the optimal configuration methodology for specific scenarios where a passive RFID system can be installed. Finally, in passive dense reader environments, the objectives have been to review scheduling strategies that minimize multi readers-single tag and reader-reader collisions. From the comparative results, the key properties for an efficient scheduler are extracted, as well as some network requirements disregarded in previous works: network topology, reader transmission power, etc.

1.12 Structure and contributions

The rest of the thesis is organized as follows:

- Chapter 2 reviews the most relevant anti-collision algorithms to handle/avoid collision in passive RFID systems. This analytical study is focused on scenarios with one reader and multiple tags and probabilistic algorithms, computing their efficiency and their computational cost. The shortcomings extracted from the study help us to propose a new feasible anti-collision algorithm, *Multi-Frame Maximum-Likelihood Dynamic Frame Slotted Aloha* (MFML-DFSA), which outperforms and solves some of the problems detected. This chapter is supported by the following publications [Anger10], [Bueno08a], [Bueno09a], [Bueno09c], and [Vales10c].

- Chapter 3 analyzes the identification performance of passive EPC-ClG2 RFID systems in different scenarios. Besides, the *Capture Effect* (CE) phenomenon is introduced in the study of the reading performance. The analysis is addressed by means of *Discrete Time Markov Chains* (DTMC), and relevant results are extracted to meet the best identification performance. The analytical results are confirmed by means of simulations and by a set of measurements performed on a real passive RFID system. The work of this chapter has been published in [Bueno08b], [Bueno09b], [Bueno10b], [Vales10a] and [Vales10b].

- Chapter 4 studies in depth the collision problems in passive *Dense Reader Environments* and the solutions proposed by the current standards, by the European regulations, in research proposals as well. Most of them intend to minimize collisions by means of simple techniques: transmission power control in readers, disconnection of interfering readers, resources allocation (frequencies, time units) following a determined scheme, etc. These alternatives are compared in terms of *usability* and *efficiency*, and key design properties for schedulers are identified. The following publications [Bueno09d] and [Bueno10a] present the outcomes of this chapter.

- Chapter 5 reviews the current anti-collision standards for active RFID systems: ISO/IEC 18000-7 and EPC-C1G2, as well as the proposals suggested for WSN that can be applied to active RFID. We take into account the carrier sense capabilities of active tags to suggest two anti-collision procedures: a p-persistent CSMA option which enables to minimize the period of tag activity, and a non-persistent CSMA which uses the optimal mechanism described in [TayYC04] to minimize collisions. Both proposals are evaluated analytically and achieve a notable energy reduction. The publications related to this chapter are: [EgeaE07a], [EgeaE07b], [EgeaE08], [Rodel07], [Vales07a], [Vales07c], [Vales08b] and [Vales08c], [Vales08d].

- Finally, Chapter 6 presents the main conclusions drawn in this thesis and discusses future works.

Chapter 2

Anti-collision protocols in passive RFID systems

In this chapter we give an overview of the most extended anti-collisions proposals for passive RFID systems, at the Physical and MAC layers, as well as of the EPC-C1G2 standard. As we will discuss, proposals for the Physical layer are not cost-effective due to passive RFID technology restrictions. For that reason, collision solutions are commonly implemented at the MAC layer. This chapter studies the MAC mechanisms based on Aloha protocols, more specifically on Dynamic Frame Slotted Aloha (DFSA) protocols, since their reading efficiency outperforms any other mechanisms. We point out some faulty formulae of previous works which may lead to incorrect algorithm behavior and their incompatibilities with the current standard. These shortcomings have led us to propose the Multi Frame Maximum Likelihood DFSA (MFML-DFSA), a new feasible DFSA algorithm which can be seamlessly integrated in current RFID readers. The performance of the algorithm proposed is evaluated and compared with the best alternatives studied, also performing a computational cost analysis. MFML-DFSA improves current DFSA proposals in terms of better average identification time and computational cost.

2.1 Anti-collision mechanisms at the Physical layer

Numerous multi-access and anti-collision protocols have been developed with the aim of separating colliding signals at the Physical layer. FDMA, TDMA, SDMA, CDMA and CSMA are the most extended and available alternatives [Finke03]. They will be briefly reviewed in the next paragraphs:

- *Frequency Division Multiple Access* (FDMA). The channel is divided in different sub-channels and tags are distributed among them. In RFID systems, this technique adds complexity (and cost) to the readers, since dedicated receivers for each channel are required. Besides, tags should be able to distinguish between different frequencies and select the sub-channel of interest. Only active tags achieve such functionality.

- *Time Division Multiple Access* (TDMA). A single channel is divided in time slots that are assigned to tags. One of the most important features of this technique is that the tags must be synchronized to send their information in the slot selected. This technique can be directly applied to RFID. For passive RFID systems, the simplicity of tags requires the reader to control the (centralized) synchronization. For active RFID systems, synchronization can be either centralized or distributed (tags control synchronization themselves).

- *Space Division Multiple Access* (SDMA). This technique reuses resources (channel, time-slots, etc.) over separated areas, providing a high increase in efficiency. It can be applied in scenarios with a single reader using multiple antennas with reduced read range. The main drawback is the cost of implementing the array of antennas.

- *Code Division Multiple Access* (CDMA) uses spread-spectrum modulations to transmit the data over the entire spectrum. CDMA is the ideal procedure for many applications, *e.g.* navigation systems. However, CDMA complexity is not affordable in passive RFID systems, nor in many active devices.

- *Carrier Sense Multiple Access* (CSMA). In this case, tags sense the channel before sending their information. If there is no ongoing transmission, they begin their own identification message. This mechanism can only be used with active tags because passive tags cannot monitor the channel.

New reactive inter-layer procedures are currently being explored, which extract useful information from colliding signals and apply it in anti-collision procedures at the MAC layer:

- The application of *Radar-Cross-Section* (RCS) mechanisms was proposed in the field of RFID in [Khasg09]. The number of collided tags is estimated by RCS analysis. Then, a *Minimum Distance Detector* (MDD) is used to decode colliding signals. However, this technique is only useful for collisions where just two tags are involved. In fact this mechanism has only been suggested for ISO/IEC 18000-6C as the underlying standard [ISO03].

- Constellations analysis computes *In-phase-Quadrature* (IQ) constellations produced by additive simultaneous tag responses, and determines symbol decoding regions of incoming transmissions. This technique has been described for LF RFID systems in [ShenD09] and for UHF in [Anger10].

Finally, we should remark that although many of these techniques are still immature, they are feasible and compatible with current protocols and tags.

2.2 Anti-collision protocols at the MAC layer

The protocols reviewed in this section have specifically been proposed for RFID systems at the MAC layer so as to reduce collisions in scenarios with a single reader and multiple tags.

2.2.1 Tree based tag anti-collision protocols

Tree-based anti-collision protocols put the computational burden on the reader. The reader attempts to recognize a set of tags in the coverage area in several interrogation cycles. Each interrogation cycle consists of a *Query* packet, sent by the reader, and the response of tags in range. If the set has more than one tag, a collision occurs and the mechanism splits the tags into two subsets. The reader keeps on performing the splitting procedure until eventually each set has a single tag. Tree-based protocols are not efficient when the number of tags to recognize is large, due to the increase in identification delay. Tree based anti-collision protocols can be classified into two groups:

- *Query Tree protocols* [HushD98, Jacom99, LawC00]. These protocol work as follows (see Figure 2.1): the reader starts splitting a set of tags by sending a *Query* packet with one bit set to 0 or 1. Tags in coverage receive the packet and those tags whose prefix matches the bit sent by the reader transmit their identification number. If there is a collision, the reader adds another bit set to 0 or 1 to the prefix of the last *Query* packet and sends a new *Query*. The mechanism continues expanding the query tree until a successful response takes place. It means that a branch of the query tree has been built and that one tag has been identified. Then, to identify the rest of tags, the reader must send new *Query* packets with other combination of bits in the prefix until all tags have been recognized. Query Tree protocols are also called 'memoryless' protocols because tags do not need to have additional memory.

- *Binary Tree protocols* [HushD98, ShihD06, Myung06]. These mechanisms follow the same procedure that the Query Tree protocols but using additional features in tags: a random number generator and a counter. These protocols operate as follows: the reader sends a *Query* packet announcing that a time slot starts. If there is only one tag in range, it is successfully identified. Otherwise, tags in range respond during that slot and a collision occurs. The colliding tags randomly generate a sample that can be 0 or 1. Note that tags are aware of the collision because not acknowledgement is received from the reader. Based on the particular value, the

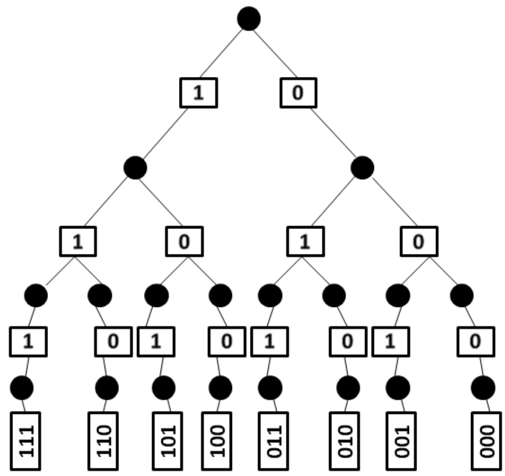

Figure 2.1: Query-tree Protocols

set of tags is split into two subsets of tags. The set of tags which generated the 0 value send their identifier number in the following slot. If there is more than one tag in the subset another collision will occur, and the subset will be split again. This procedure continues recursively until the subset is reduced to one tag, that is identified without collisions.

2.2.2 Aloha protocols

Aloha protocols - also called probabilistic or random access protocols - are the most extended and used in active and passive RFID (in the UHF band). The popularity of Aloha protocols comes from the type of scenario where a RFID system works. These protocols are designed to be used in situations where the reader does not know exactly when tags will pass through its coverage range. In these scenarios, Tree based protocols performs with a high identification delay that is not suitable for RFID. Aloha protocols are classified in four main groups:

- The first one is the widely known Pure-Aloha [LeonA96] protocol, which is considered the simplest anti-collision scheme for passive tags with read-only memory. This protocol operates as follows: the reader sends a *Query* packet. Tags in range are energized by the electromagnetic waves from the reader's signal and wake up, sending back the information stored. However, readers can not avoid/handle collisions.

- The second group is the Slotted-Aloha protocol [Weise88]. It is based on Pure-Aloha but time is divided in time units called slots. The mechanism is as follows:

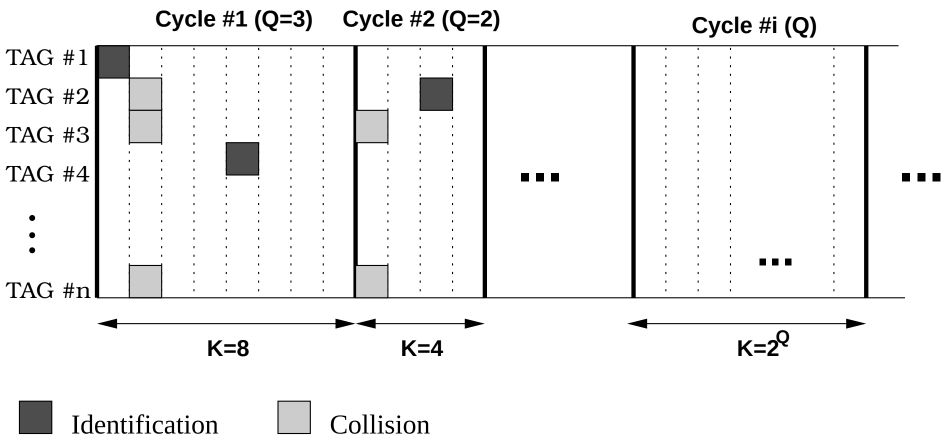

Figure 2.2: Dynamic Frame Slotted Aloha procedure

The reader, announces the beginning of a slot by means of a *Query* packet. Every tag decides whether to transmit in that slot or to wait for another. Therefore, packets may either completely overlap (and, hence, collide) or not overlap at all. Slotted-Aloha outperforms Pure-Aloha at the cost of requiring a reading system that manages slotted time synchronization.

- The third group, FSA, is a variation of Slotted-Aloha. In FSA, time is also divided in slots but they are confined to a super-structure called ”frame´´ (or ”cycle´´). Each frame has a static length of K slots, and tags randomly select a slot within the frame to send their information to the reader. FSA has been implemented in many commercial products and has been standardized in ISO/IEC 18000-6C, ISO/IEC 18000-7 [ISO03] and EPC-C1G2 [EPCgl05]. In FSA, when the number of tags is much larger than the number of slots, identification delay increases considerably. On the other hand, if the number of tags is low and the number of slots is high, many slots can be empty after the identification process, which leads to increased identification time [Finke03].

- In Dynamic FSA (or DFSA), the number of slots per frame is variable (see Figure 2.2). When a frame finishes, an identification cycle concludes and the reader has to decide whether to increase, decrease or maintain the number of time slots in the next frame. According to *Schoute et al.* in [Schou83], the optimum throughput (η) (mean number of tags identified per slot) in a cycle i of a DFSA protocol is achieved if the number of tags n_i equals the number of slots K_i in that cycle i, and this throughput is given by η=$e^{-1} \approx 0.36$. Since the number of tags in range per cycle is commonly unknown, the reader must estimate the number of tags that are going to compete in that cycle beforehand possibly through the statistical information collected on previous cycles. Then, the reader adjusts the frame size to achieve maximum throughput. Note that it is equivalent to minimize total identification delay.

In short, FSA is clearly inefficient: if tags outnumber slots, collisions will be frequent. Otherwise, there will be many empty slots. Both situations are undesirable. Therefore, DFSA techniques are more appropriate, although the reader must have a method to guess somehow the number of tags in competition. In the following sections we describe and analyze the most relevant DFSA proposals, which were comprehensively studied in [Bueno09c] and [Bueno08b]. We point out some faulty formulae in previous studies which lead to incorrect algorithm behavior. Finally the MFML DFSA algorithm is introduced. Besides, since most proposals are based on EPC-C1G2, we firstly introduce the standard and its procedures.

2.3 EPCglobal Class-1 Gen-2

As stated in the previous chapter, EPCglobal is an institution focused on the development of industry-driven standards, such as the EPC-C1G2 standard. For passive RFID systems, EPC-C1G2 includes a set of specifications for the hardware of the passive tags and for both hardware and software in readers (where the complexity of the identification procedure can be found).

EPC-C1G2 also defines the format of the data stored in the memory of tags, the *Electronic Product Code* (EPC). Figure 2.3 illustrates it. EPC data consist of a unique identifier of 96 bits divided in three fields. The Header is 8 bits long and contains the tag identifier. The Global Trade Item Number (GTIN) is the second field and comprises two subfields: the identification number of the company or manufacturer ID (EPCManager, 28 bits long) and the manufacturer's product ID (ObjectClass, 24 bits long). Finally, a Serial Number of 36 bits codes the information related to an individual item such as price, weight, expiration date, etc. With its 96 bits code (note that 8 bits are reserved for Header), a total of 268 million companies (2^{28}) can categorize up to 16 million different products (2^{24}), where each product category contains a maximum of 687 billion individual items (2^{36}).

EPC-C1G2 proposes an anti-collision mechanism based on a variation of FSA. Figure 2.4 illustrates EPC-C1G2 operation: In the stationary-state (no ongoing identification process), the reader monitors the environment to detect new tags, using continuous *Broadcast* packet transmissions. Tags in range reply immediately. In case several tags answer simultaneously, a collision takes place. When the reader detects the collision, it starts a new identification cycle, *i.e.* it allocates a new frame which is in turn subdivided in slots, following an FSA scheme. EPC-C1G2 establishes two identification procedures:

- *Fixed frame length procedure* (Fixed EPC-C1G2): all identification cycles (frames) have the same number of slots. It is common to find commercial systems with this configuration.

- *Variable frame length procedure* (Variable EPC-C1G2): the number of slots per frame can be changed by the reader in each identification cycle (DFSA operation).

In the following subsections both procedures are reviewed.

2.3.1 Fixed frame length procedure

An identification cycle starts when the reader transmits a *Query* packet, including a field of four bits with the value $Q \in [0, \ldots, 15]$, stating that the length of the frame will be

Figure 2.3: Standardized Data format in an Electronic Product Code

of K=2^Q slots. Tags in coverage receive this packet and generate a random number r in the interval $[0, 2^Q - 1]$. The r value represents the slot within the frame where the tag has randomly decided to send its identification number ID=r. Inside each frame, the beginning of each slot is controlled by the reader via transmission of a *QueryRep* packet, except in the first slot (slot 0), which starts automatically right after the *Query* packet. Tags use the r value as a counter, which is decreased upon reception of a new *QueryRep*. When counter r reaches 0, the tag transmits its identifier ID, which corresponds to the random value initially calculated for contention. Note that it must be also equal to the slot number in the frame. After transmitting the ID, three situations are possible:

- If several tags select the same slot, a collision occurs. The reader detects it and reacts starting a new slot with a *QueryRep* packet (see slot #0 in Figure 2.4). Involved tags update their counter to $r = 2^Q - 1$. That means that they will not contend again until the next frame.

- If the reader receives the ID which matches the current slot number, the reader responds with an *Ack* packet. Although all tags receive the packet, only the winner answers with a *Data* packet (including its EPC code). If the reader receives the *Data* packet correctly, it answers with a *QueryRep* packet, thus starting a new slot. Besides, the winner tag quits the identification process (see slot #1 in Figure 2.4). However, if the reader does not receive a correct *Data* packet after a certain time, it considers that the slot has expired and sends a *Nack* packet. Again, only the involved tag updates its counter value to r=$2^Q - 1$. Thus, this tag will not contend again in this identification cycle (see slot #2 in Figure 2.4). After this, the reader also sends a new *QueryRep* packet to begin the new slot.

- If the reader does not receive a packet before a given deadline, it is assumed that the slot is empty, and the reader starts a new one sending a new *QueryRep* packet.

This procedure continues until the identification cycle finishes. Then, the reader send a new *Query* packet to start a new cycle. Unidentified tags compete again in the new cycle, selecting a new random r value. Eventually, all tags are identified and the procedure ends. This happen when all the slots in a frame are empty.

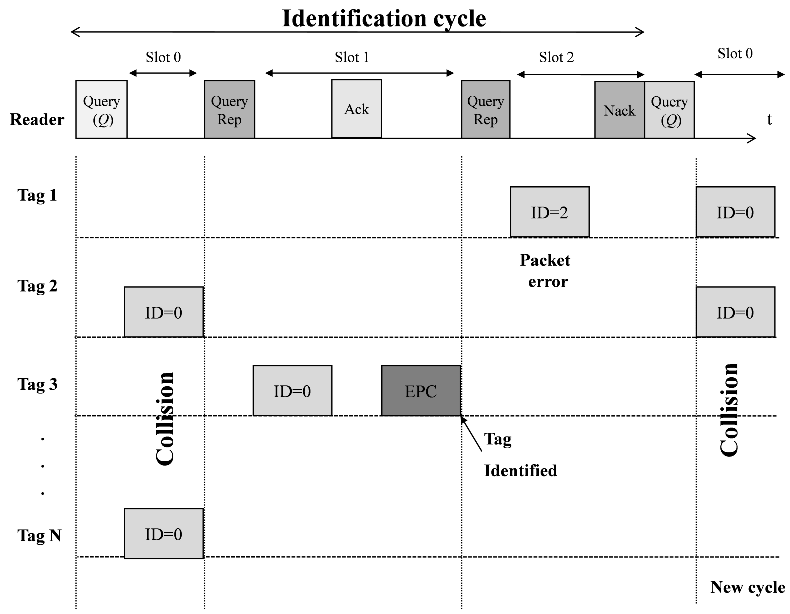

Figure 2.4: EPCglobal Class-1 Gen-2: Fixed frame length procedure

2.3.2 Variable frame length procedure

To mitigate the poor efficiency of static frame length EPC-C1G2, the standard suggests a variable frame length procedure called variable EPC-C1G2 or variable EPC, that selects the Q value in each cycle/slot by means of an arbitrary function. As Figure 2.5 shows: when a slot ends, the reader checks if it was empty, successful or with collision. Accordingly, the reader increases, decreases or keeps a floating point variable Q_{fp} unmodified. Then, the nearest integer to Q_{fp} is selected as Q, and a new *Query* packet with that value is sent. Variable $C \in (0.1, 0.5)$ (see Figure 2.5) controls frame length selection, and can be adjusted to improve performance.

2.4 A Classification for DFSA protocols

Establishing a clear classification of all DFSA protocols is not straightforward. In this section different perspectives are considered [Bueno09c]:

How is the protocol operation modified? Frame structure can be adjusted in two ways: (i) controlling the number of slots in the frame with Q, or (ii) resetting the identification cycle at any time, by sending a new *Query* packet with the same (or a new) Q value. Throughout this chapter, we call them *Q-control* and *Q-reset* operation, respectively.

Which data is used to compute length or reset the frame? DFSA readers can monitor different variables to take operative actions. In a given cycle, it is possible to extract three variables: the number of slots filled with exactly one transmission (henceforth, id), the number of empty slots (e), and the number of slots with collision (c). Let us remember that K is used to denote the frame length. Notice that it is possible to relate the previous variables since $K = 2^Q = id + e + c$. Therefore, two variables in the set $\{id, e, c\}$ give full information about a cycle. In fact information of several cycles may also be used, in which case we will label the variable corresponding to the ***i***-th cycle with an i subscript $(K_i, Q_i, id_i, e_i, c_i)$. To summarize, we endorse a classification according to the monitored set: SFSP, or Single-Frame Single-Parameter (id, e, or c); SFFP, or Single-Frame Full-Parameter (two in id, e, c); MFSP, or Multi-Frame Single-Parameter; and MFFP, or Multi-Frame Full-Parameter. Clearly, the performance of the algorithm will be directly related to the cardinality of this set and the quality of the information. Single-frame makes sense in case of continuous tag flow, since frame information quality degrades with age. Instead, multi-frame is advisable if new tag populations do not appear until the previous set has been completely identified. The reader may also enforce this behavior. For instance, if a conveyor belt carries the tags, the reader can control it.

How is frame length selected? Every time a new *Query* packet is sent, the DFSA protocol computes its Q parameter. Depending on how this value is selected we classify protocol operation into two categories: (i) $Direct$ and (ii) *Indirect Q* selection. In the former, some heuristic returns the value of Q. Many of these heuristics also determine if the current frame must be reset or not, *i.e.* they operate using *Q-reset*. In the latter, the algorithm first estimates the number of tags $\hat{n}$ that competed in the previous cycle. The expected number of competitors in the next cycle will be ($\hat{n} - id$). Then, Q is selected as a function of $\hat{n}$. There are different ways of calculating $\hat{n}$: heuristically, through Bayesian inference, through Maximum Likelihood (ML) estimation, etc. With Bayesian inference, the goal is to compute the *a-posteriori* distribution of the number of competing tags. In fact, this distribution can be upgraded cycle-by-cycle to obtain a more precise estimation (for multi-frame information sets). Q can be calculated as the value that maximizes the expected identification rate for the next cycle, or even as the value that minimizes some loss function defined over the n domain. In the ML estimation, the probability of observing a given sample set is computed as a function of n. Let $\hat{n}$ reach its maximum and let Q also maximize the expected identification rate.

2.5 Analysis of DFSA protocols

Table 2.1 shows a classification of the main DFSA proposals, according to the criteria of the previous section. We consider four major groups of protocols, each one stemming from a different root or operative foundation: variable EPCglobal protocols, indirect Q heuristics, Error Minimization estimators and ML estimators.

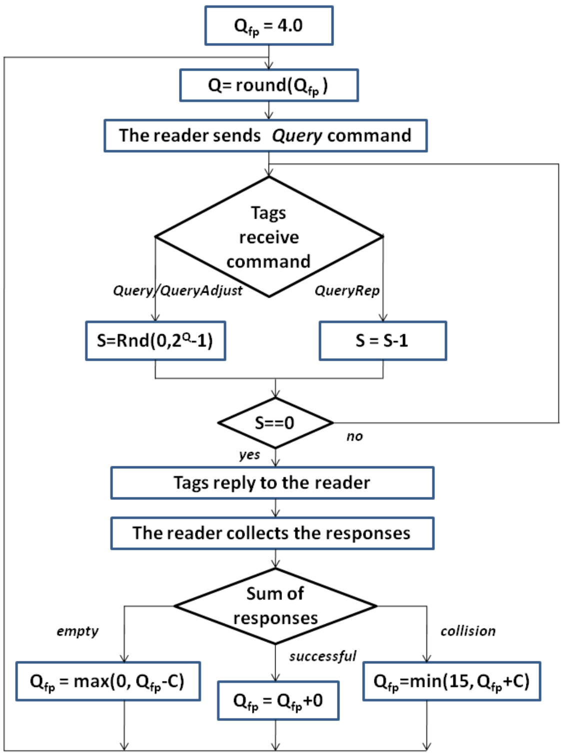

Figure 2.5: EPCglobal Class-1 Gen-2, variable frame-length procedure

2.5.1 Variable EPCglobal protocols family

As already discussed, EPC-C1G2 [EPCgl05] proposes the variable frame-length mechanism as an alternative to the fixed frame-length scheme. It adjusts the frame length slot-by-slot (*Q-reset* operation), following the heuristic shown in Figure 2.5. In this scheme, the value of C directly affects the slot-by-slot mechanism. The standard does not specify the selection of C. It only recommends using high values if the previous Q value was low and vice versa. This lack of definition has led to many different alternatives.

In [LeeD07] the authors propose the Q^{+-} algorithm. Since the *Query* packet length (22 bits) exceeds *QueryRep* packet length (4 bits), *Query* packets are only sent if the calculated Q value differs from the previous one. Otherwise, a *QueryRep* packet is transmitted. Besides, the C variable is replaced by two new variables: C_i and C_c. The former is used when the reader detects an empty slot. The latter is applied when the reader detects a collision. The authors propose computational methods to obtain them regardless of whether the number of competing tags is known (or can be estimated). However, they neither propose a way to determine the number of tags, nor suggest how to estimate it. In fact the authors only compare the Q^{+-} algorithm with the EPC-C1G2 in its fixed frame length procedure, instead of the variable one. Thus, their results are not conclusive. In [JoeI07] the authors describe the *Optimum-C* protocol, which calculates the optimum C value and compares it to the previous Q value. The authors simulate a passive RFID system for $Q \in [0, \ldots, 15]$, and, for each Q, for $C \in [0.1, \ldots, 0.5]$, only in 0.1 steps. Finally, they offer the value that achieves the best identification delay. As in [LeeD07], the *Optimum-C* protocol is compared with fixed EPC-C1G2 and the protocol in [Vogt02].

The *Slot-Count-Selection* (SCS) algorithm in [Danes07] improves the variable EPC-C1G2 procedure. As in [LeeD07], there are two control parameters (C_1 and C_2) instead of a single C. They are calculated slot-by-slot, as a function of other parameters that mainly depend on reader-to-tag (R-T) and tag-to-reader (T-R) data rates. It is suggested to set $C_2 \in [0.1, 1]$ and $C_1 = 0.1$. Authors claim a great improvement of performance in comparison to the variable EPC-C1G2 procedure. They assume that R-T is set to 64 kbps and T-R is constant for each simulation, in the range 16 kbps $\leq$ T-R $\leq$ 128 kbps. However, *this assumption is not correct*, since the R-T value set affects the final T-R. In particular, with R-T= 64 kbps, T-R must be 170 kbps $\leq$ T-R $\leq$ 640 kbps. The correct value of T-R actually depends on the modulation and data encoding assumed [EPCgl05], but the authors did not compute T-R this way. Following the standard's specifications, C_1 and C_2 should be computed assuming T-R and R-T data rates of 40 and 80 kbps, respectively. Moreover, in variable EPC-C1G2 tests, they set C=3, but the standard recommends establishing variable values regarding the C value, in order to get a better response. Therefore, results in [Danes07] have to be reanalyzed.

2.5.2 Indirect Q Heuristic family

Indirect Q heuristics compute $\hat{n}$ by means of some heuristic, and then adjust the frame length (K) to achieve the best throughput. They only use information of the last frame. The first DFSA indirect Q heuristic was proposed in [Schou83] (called *Schoute* in this thesis) and its authors selected the number of competing tags ($\hat{n}$) in the *i*-th frame as:

$$\hat{n}_i = 2.39 \cdot c_i \tag{2.1}$$

and established the next frame length to:

$$K_i = round(\hat{n}_i - id_i) \tag{2.2}$$

Equation (2.1) is computed assuming that the number of competing nodes follows a Poisson distribution of mean 1. Evidently, this does not hold in general. Actually, the frame length from equation (2.2) does not satisfy the power-of-two constraint imposed by the standard. Recent analysis in [DengX08, Rives87, ChaJR05, TongQ07] have also adopted the same heuristic to compute $\hat{n}$, stating that frame length must be selected according to the standard constraints. However, none of these studies indicate how to compute the optimal Q value. Another heuristic, the *Lower Bound* estimation [Vogt02], defines:

$$\hat{n}_i = id_i + 2 \cdot c_i \tag{2.3}$$

This trivial (every collision involves at least two tags) and inaccurate lower bound has deserved some attention [Abder07].

In the estimation method proposed in [ChaJR06], as a simplification, the authors assume a binomial distribution of the number of tags that select each slot (with success probability $p = \frac{1}{K}$). They define the *C-ratio* as the ratio between the number of slots with collision and the frame size. Since the collision event is the complementary of the empty slot or single-tag ones, the *C-ratio* is calculated at the end of every i frame as:

$$C_{ratio} \triangleq \frac{c_i}{K_i} = 1 - \left(1 - \frac{1}{K_i}\right)^{n_i} \left(1 + \frac{n_i}{K_i - 1}\right) \tag{2.4}$$

The second part of equation (2.4) is evaluated for each $n_i \geq 2 \cdot c_i + id_i$ and $\hat{n}$ is the value that gives the closest approximation to the *C-ratio*. However, this formula is undefined when the numbers of collision slots and frame slots coincide, c_i=K_i. This may occur for short frames and many competing tags. Despite this, other works such as [Abder07] have considered this estimation.

The estimation method in [Wang07] (called *Wang* in this thesis) also assumes independent binomial distribution of the tags in each slot as follows:

$$\frac{c_i}{K_i} = \sum_{j=2}^{n_i} \binom{n_i}{j} \left(\frac{1}{K_i}\right)^j \left(1 - \frac{1}{K_i}\right)^{n_i - 1} \tag{2.5}$$

Unlike the previous proposals, the simple $\hat{n}$ estimator in [ChenW06a] (called *Chen-1* in this thesis) is the following SFFP estimator:

$$\hat{n}_i = (Ki - 1)\frac{id_i}{e_i} \tag{2.6}$$

Nevertheless, this estimator has shortcomings. If id_i=0, it selects $\hat{n}_i$=0, but it must be $\hat{n}_i \geq 2 \cdot c_i$. For e_i=0, the value of $\hat{n}_i$ is undefined. In this case, the authors suggest applying an upper bound to estimate the number of tags.

Finally, we must remark that these heuristics do not provide any procedure to select the optimal Q value for the next frame.

2.5.3 Error Minimization estimator

In [Vogt02] the author proposes a SFFP procedure based on Minimum Squared Error (MSE) estimation, the *MSE-Vogt* estimator. It minimizes the Euclidean norm of the vector difference between actual frame statistics and expected values. Equation (2.7) assumes n tags in the access procedure. Let the value of n that minimizes the error be:

$$\hat{n}_i = \underset{\boldsymbol{n}}{\operatorname{argmin}} \left\{ \left| \begin{pmatrix} id_i \\ c_i \\ e_i \end{pmatrix} - \begin{pmatrix} E\left\{\mathbf{id}|n_i\right\} \\ E\left\{\mathbf{c}|n_i\right\} \\ E\left\{\mathbf{e}|n_i\right\} \end{pmatrix} \right| \right\} \tag{2.7}$$

where random variables e, id and c represent the number of empty, successful and collision slots respectively. Their expected values are computed assuming independent binomial distribution of the tags in each slot as follows:

$$E\left\{\mathbf{e}|n_i\right\} = K_i \left(1 - \frac{1}{K_i}\right)^{n_i} \tag{2.8}$$

$$E\left\{\mathbf{id}|n_i\right\} = n_i \left(1 - \frac{1}{K_i}\right)^{n_i - 1} \tag{2.9}$$

$$E\left\{\mathbf{c}|n_i\right\} = K_i - E\left\{\mathbf{id}|n_i\right\} - E\left\{\mathbf{e}|n_i\right\} \tag{2.10}$$

Let $\hat{n}$ be the value of n that minimizes equation (2.7). A limitation in [Vogt02] is that the performance of the algorithm is only compared against a heuristic from the same study, which is compatible with the I-code system [ICODE], but it has not been evaluated for the EPC-C1G2 standard.

In [Knerr08] the authors propose a Minimum Squared Error estimator based on a slot-by-slot procedure (MSE-Knerr), modifying the estimator of [Vogt02] in order to improve its response. They propose a *Q-reset* operation based on the error function in equation (2.7). However, they do not specify when the reader must reset the cycle to get the best performance. The statistical information of several previous cycles improves the estimation (MFFP operation), using the following equation:

$$\hat{n}_i = \underset{\boldsymbol{n}}{\operatorname{argmin}} \left\{ \left| \begin{pmatrix} id_i \\ c_i \\ e_i \end{pmatrix} - \begin{pmatrix} E\left\{\mathbf{id}|n_i\right\} \\ E\left\{\mathbf{c}|n_i\right\} \\ E\left\{\mathbf{e}|n_i\right\} \end{pmatrix} \right| + \sum_{p=1}^{i-1} \left| \begin{pmatrix} id_p \\ c_p \\ e_p \end{pmatrix} - \begin{pmatrix} E\left\{\mathbf{id}|n_p\right\} \\ E\left\{\mathbf{c}|n_p\right\} \\ E\left\{\mathbf{e}|n_p\right\} \end{pmatrix} \right| \right\} \tag{2.11}$$

That equation minimizes the cumulative error function. Although this is proposed as an enhancement to [Vogt02], it is instead compared against the heuristic in [Schou83] and the ML estimator by the same authors [Knerr08-2].

2.5.4 Maximum Likelihood Estimators

The main idea behind this group of estimators is to compute the conditional probability of some observed event (or set of events) assuming that *n* nodes are undertaking the identification process, and select the *n* that maximizes such probability. The main chores of these algorithms are the exact formulation of this conditional probability, and the extra computational cost, which may render them unusable.

In [ChenW06b] the authors proposed a ML algorithm derived from the occupancy problem described in [Feller70] (called *Chen-2* in this thesis). The estimator is a *Q-control* SFSP mechanism. When a cycle ends, the reader calculates the probability to find e_i empty slots and selects $\hat{n}$ as follows:

$$\hat{n}_i = \arg \min_{\boldsymbol{n_i \geq id_i + 2c_i}} \{P\left(K_i, e_i | n_i\right)\} \tag{2.12}$$

$$Pr\left(K_i, e_i | n_i\right) = \frac{(-1)^{e_i} K_i!}{e_i! K_i^{n_i}} \sum_{j=e_i}^{K_i} (-1)^j \frac{(K_i - j)^{n_i}}{(j - e_i)! (K_i - j)!} \tag{2.13}$$

Note that this is an exact computation, unlike previous groups of protocols, which assumed independent identically distributed (*iid*) binomial or Poisson distributions of tags in each slot. As a drawback, its performance has only been tested against the heuristic in [Vogt02] and EPC-C1G2 with fixed frame length procedure [EPCgl05].

[Khande07] presents an algorithm similar to the one proposed in [ChenW06b], pointing out the computational unsuitability for large values of K_i and n_i and proposing the heuristic estimator of equation (2.12) as an alternative. Nevertheless, this heuristic is erroneous when $e_i = 0$, because $log(0)$ -which is not defined- appears in the numerator.

$$\hat{n} = \frac{log\left(\frac{e_i}{K_i}\right)}{log\left(1 - \frac{1}{K_i}\right)} \tag{2.14}$$

In [Knerr08-2], the authors improve the study published previously in [Knerr08], proposing the Slot-by-Slot Maximum Likelihood (SbS) estimator that uses the number of empty slots as well as the number of identified tags in its calculations. The authors propose this algorithm as a *Q-reset* mechanism. However, they do not provide any decision rule regarding cycle restart. The probability formula in [Knerr08-2] can be reduced to:

$$\begin{aligned} Pr(K_i, e_i, id_i | n_i) = \frac{k_i! n_i!}{e_i! id_i! k_i^{n_i}} & \sum_{j=0}^{min\{c_i,(n_i - id_i)\}} \frac{(-1)^z}{z!} \\ \sum_{j=0}^{min\{c_i - z_i, n_i - id_i\}} \frac{(K-1)^j}{j!} & \frac{(c_i - z - j)^{n_i - id_i - j}}{j! (c_i - z - j)! (n_i - id_i - j)!} \end{aligned} \tag{2.15}$$

However, both the original and the reduced formulae are erroneous: they return negative probabilities in some cases (*e.g.* $c_i = 1$, $id_i = 1$ $e_i = 1$, $K_i = 4$, for $n_i \geq id_i + 2 \cdot c_i$), and we have found out that in other configurations where results are positive, they do not coincide with the simulated results.

Protocol	Operation	Data	*Q* selection	Order
Variable EPC-C1G2	Q-reset	SFSP	Direct	Constant
Q^{+-}	Q-reset	SFSP	Direct	Constant
Optimum-C	Q-reset	SFSP	Direct	Constant
SCS	Q-reset	SFSP	Direct	Constant
Schoute	Q-control	SFSP	Ind., Heuristic $Q = N$	O(n)
Lower Bound	Q-control	SFSP	Ind., Heuristic $Q = N$	O(n)
C-ratio	Q-control	SFSP	Ind., Heuristic $Q = N$	O(n)
Wang	Q-control	SFSP	Ind., Heuristic	O(n^2)
Chen-1	Q-control	SFFP	Ind., Heuristic $Q = N$	O(n)
MSE-Vogt	Q-control	SFFP	Ind., MSE $Q = N$	O(n)
MSE-Knerr	Q-reset	MFFP	Ind., MSE $Q = N$	O(n)
Chen-2	Q-control	SFFP	Ind., ML $Q = N$	O(n)
SbS	Q-reset	MFFP	Ind., ML $Q = N$	O(n)
Chen-3	Q-control	SFFP	Ind., ML $Q = N$	O(n)
Floerker	Q-control	MFFP	Ind., ML $Q = N$	O(n^2)

Table 2.1: Comparison of DFSA protocols

[ChenW09] models the probability of event $\{id, e, c\}$ as a multinomial distribution problem (an approximation to the actual probability). From equations (2.8), (2.9) and (2.10), the probabilities of empty, successful and collision slot are $p_0 = E\{\mathbf{e}|n_i\}$, $p_1 = E\{\mathbf{id}|n_i\}$ and $p_{\geq 2} = E\{\mathbf{c}|n_i\}$, respectively. The algorithm is called *Chen-3* in this thesis.

$$Pr\left(K_i, e_i, id_i, c_i|n_i\right) = \frac{K_i!}{e_i!id_i!c_i!} p_0^{e_i} p_1^{id_i} p_{\geq 2}^{c_i} \tag{2.16}$$

As in [ChenW06b], the author only compares this estimator with the heuristics proposed in [Vogt02] and [Schou83]. The estimator in [Floer06] uses statistical information of several frames (it is the only MFFP estimator proposed so far) to update the tags probability distribution according to a Bayesian methodology. That is, the *a posteriori* distribution (distribution at the end of cycle i) is derived from the *a priori* tag probability distribution (distribution at the end of cycle $i-1$), according to expression (2.16). The algorithm is called *Floerker* in this thesis.

$$Pr\left(n_i|ciclos_{1:i}\right) = \alpha Pr\left(n_i|ciclos_{1:i-1}\right)\left(k_i, e_i, id_i, c_i|n_i\right) \tag{2.17}$$

where α is a normalizing constant, whose value is not indicated by the authors. In this algorithm, at the end of each frame, the reader extracts the information as the mode of the *a-posteriori* distribution. However, in the first iteration, since the *a priori* distribution is not available, these authors directly assume that the likelihood is the *a posteriori* distribution. This is false since likelihood functions are not mass probability functions (the sums of probabilities are not equal to one).

We obtained simplified versions of that expression [Floer06], but the final form is unnecessarily complex (available in [Floer06]). Besides, as in previous studies, the comparison only considers the heuristics in [Vogt02, Schou83].

2.6 Performance Evaluation of DFSA protocols

In this section we compare the performance of the previously discussed DFSA algorithms. As already stated, this has not been clearly -and, in our opinion, fairly- achieved so far.

2.6.1 Evaluation rules

We have selected conditions and parameters representing an actual system implementation:

- The physical configuration parameters correspond to a commercial passive RFID system, Alien 8800 [Alien], which is a widely used EPC-C1G2 RFID equipment. We have validated our simulation results with laboratory test beds based on this system [Bueno08b], [Bueno09b].

- The EPC-C1G2 frame length constraint (power of two) holds. For each number of competing tags N, there is an optimal Q that maximizes throughput. Conversely, for each Q there is a (closed) set of N values, for which the expected performance will be optimal. Table 2.2 summarizes the values of Q (see section 2.7.3). These values have not been evaluated in any previous study. When any of the algorithms under evaluation has to select the next frame size we just pick the correct value from this table. Note that this does not add complexity to the algorithms.

- In our simulation, exactly N tags enter the reader range. Identification proceeds until all tags are detected.

- The number of slots (L) is measured in each simulation. For each N the same setup is simulated (as many independent runs) until a confidence interval of 10% of the mean values of L with a confidence degree of 90%.

Some algorithms leave some parameters open or are clearly faulty. In such cases we assume the following:

- EPC-C1G2 in its variable frame length procedure [EPCgl05]: since the standard only recommends to set high C values if the last frame's Q is low (and vice-versa), we set $C = 0.2$, if $Q > 8$ and $C = 0.4$, if $Q < 8$.

- Q^{+-} algorithm [LeeD07]. The computing methodology for C_c is unknown. The authors only state that $C_c \in [0.1, 0.5]$. Therefore our assumption was the the same as the previous one.

- SCS algorithm [Danes07]: C_1 and C_2 are computed assuming T-R and R-T data rates of 40 and 80 kbps, respectively.

- The *C-ratio* algorithm [ChaJR05] fails if C_{ratio}=1, and the algorithm defined in [ChenW06a] is undefined under some conditions (see section 2.5.2). In those cases, we took the lower bound estimation [Vogt02].

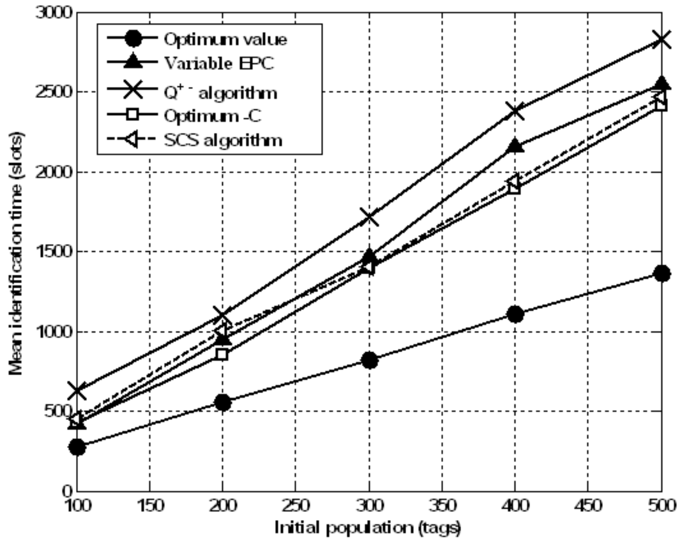

Figure 2.6: Variable EPC family. Mean Identification time versus initial tag population

- MSE-Knerr [Knerr08] and SbS-ML [Knerr08-2] do not specify how often the frame must be reset. We have assumed a cycle-by-cycle operation. In addition, "negative" probabilities in [Knerr08-2] are treated as zeros (see section 2.5.3).

- *Indirect-Q* algorithm frame size is selected as in Table 2.2.

2.6.2 Evaluation results

Figures 2.6, 2.7, 2.8, and 2.9 show the mean identification time versus the initial tag population size (N), up to 500, for the four groups of protocols introduced in the previous section. We observe in all cases that the more initial tags, the larger the differences between the identification time of all proposals and that of the optimum. Besides, we have also computed the effect of non-optimal Q selection. All algorithms have been tested under the original assumption of select 2^Q as the closest value to $\hat{n}$. This renders 5-10$\%$ performance degradation in Heuristics, MSE and ML algorithms. Note that the variable EPCglobal protocol family is not affected by this issue, since Q is directly computed.

In short, the best algorithm proposals (considering large N values and optimal Q selection) are: *Optimum-C* [JoeI07], *Lower-bound* [Vogt02], MSE-Knerr [Knerr08], and *Chen-3* [ChenW09]. Figure 2.10 compares them. *Chen-3* [ChenW09] ML estimator offers the the closest results to the optimal algorithm for large N values. Note that this protocol actually uses an approximation to compute likelihood and a more accurate computation may lead to a better response. In contrast, the mixed ML-Bayesian strategy of the *Floerker* estimator from [Floer06] has an excellent performance for lower values of N, but it degrades as the initial population grows.

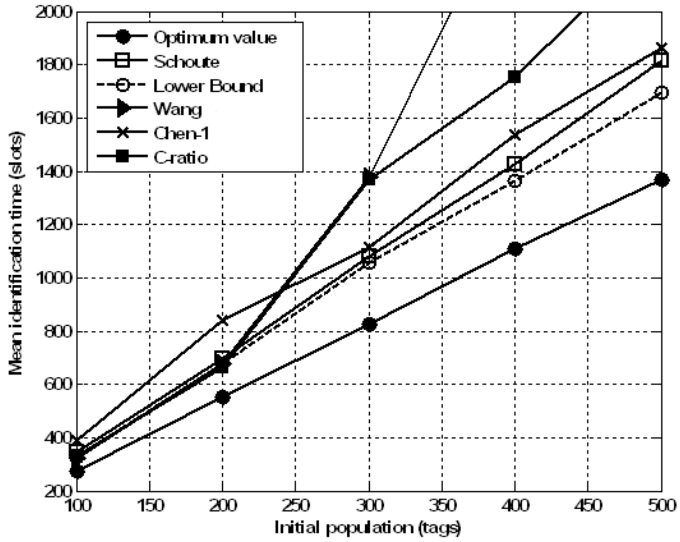

Figure 2.7: Heuristic estimators. Mean identification time versus initial tag population

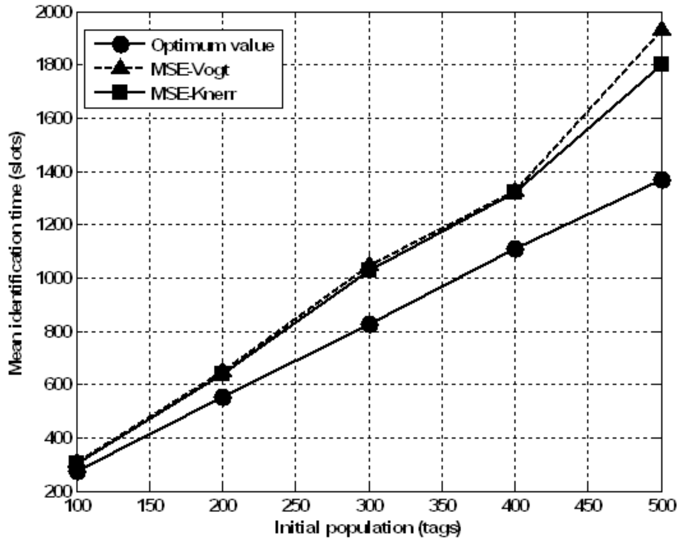

Figure 2.8: MSE estimators. Mean identification time versus initial tag population

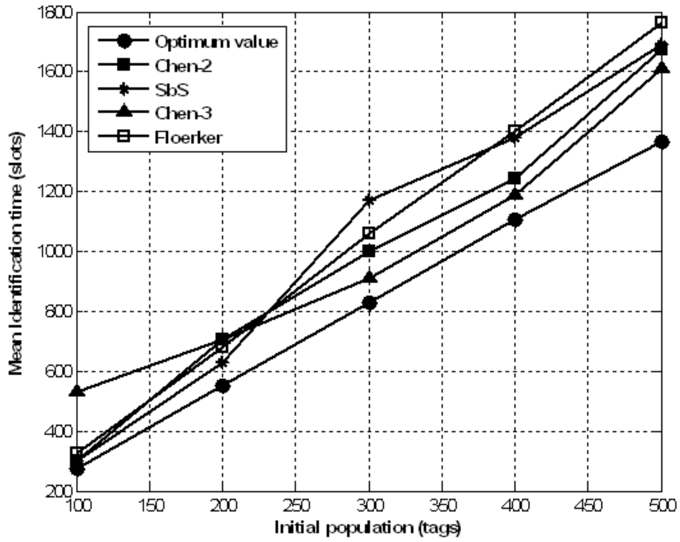

Figure 2.9: ML estimators. Mean Identification time versus initial tag population

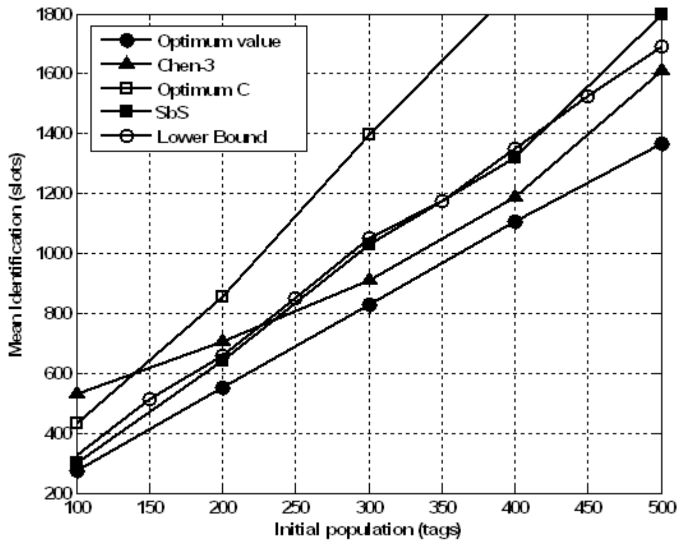

Figure 2.10: Comparison of the best algorithm proposals. Mean identification time versus initial tag population

2.6.3 Computational cost

The results of identification time in the previous section do not include the computation time needed for tags estimation, Q selection, etc. The calculations for the decisions have to be carried out at the end of every cycle (or slot), before sending a new *Query* or *QueryRep* packet. Although the reader can delay the transmission of these packets (tags do not act until some packet is received) overall identification time may also increase. We address the issue in this section

First, we have derived the computational order of each proposal examining the calculations involved. Results are summarized in table 2.3. The Variable EPC family has a constant order, *i.e.*, the number of computations does not depend on the tag population. In the other cases, all proposals have order $O(n)$, except *Wang* [Wang07] and *Floerker* [Floer06] which are $O(n^2)$. That is, the number of computations grows as a function of n or n^2 respectively. This order is related to the scalability of the anti-collision procedure for large populations of tags. In addition, to provide insight into performance in real situations we have selected two examples and measured the exact number of computations involved. The scenarios are:

- Scenario 1. At the end of a cycle (with K_i=128), the reader collects the following statistical information: e_i= 48, c_i= 30, id_i=22. Note that, with this configuration, $n_i \geq 2c_i$+ id_i=82. Algorithms iterate for each possible value of n_i up to a given n_{max} and the optimum is extracted. In this scenario we have established n_{max}= 100. Then, the worst case requires 100-82=18 iterations.

- Scenario 2. At the end of a cycle (K_i= 512), the reader collects the following statistical information: e_i= 170, c_i= 192, id_i= 170. In this case, we have established n_{max}= 1000, then 1000-554=446 iterations are necessary.

We have considered the following additional assumptions:

- A computational power of 1 Giga FLOating Point Operations per Second (GFLOPS) (10^9 FLOPS) is considered, representing the performance of an average Digital Signal Processor (DSP). DSPs are common in RFID hardware devices like the Alien 8800 reader used as reference.

- We have assumed that Multi-Frame algorithms do not require re-computing the sum of all iterations, from the first to the last one. Instead, they only update computations to take the last cycle into account.

- Finally, we have assumed a computational cost of 50 FLOP for powers, logarithm, and exponential operations. And 100 FLOP for factorials.

Table 2.3 summarizes the approximate number of computations required per cycle for both examples. Additionally, the increase of time required to perform these computations is expressed relative to that of frame length, in $\%$. As a conclusion, despite being $O(n)$, some proposals (*e.g. Chen-2* and SbS) suffer from a high computational cost, which degrades total identification time. SbS [Knerr08] and *Floerker* [Floer06] have an unacceptably high computational cost in some cases, which prevents actual implementation in the current form of the algorithms. The variable EPC and Heuristic families are computationally more efficient due to their intrinsic nature.

2.7 MFML-DFSA Anti-Collision Algorithm

In the previous section the most relevant DFSA algorithms have been thoroughly analyzed and compared. Significant results have been achieved regarding current DFSA proposals, and their strengths and weaknesses have been identified. Comparisons have demonstrated that Maximum-Likelihood algorithms give the best performance in terms of mean identification time, that Multi-Frame proposals are scarce and that more detailed statistical information would lead to better estimators. The shortcomings in previous research have led us to propose a new feasible DFSA algorithm that improves estimation while decreasing computation time for estimating the number of tags.

In this section, a new algorithm (MFML-DFSA) is proposed. At the end of every cycle, MFML-DFSA computes the optimal frame length that maximizes throughput, based on a Multi-Frame (MF) Maximum-Likelihood (ML) estimator. The MFML-DFSA estimator is used to compute the most likely number of competing tags. Thus, frame length is accordingly set for the next frame, following the EPC-C1G2 standard restrictions; namely, that frame length cannot be an arbitrary natural number, but a number in the set $\{K=2^Q : Q=1,\ldots,15\}$. Therefore, the MFML-DFSA may be directly adopted in current RFID reader equipments, without tag modifications. Results show that MFML-DFSA achieves better identification time than previous DFSA proposals. Its computational feasibility is explicitly addressed in this study.

2.7.1 Algorithm procedure

Let n be the number of tags entering the identification area. In our model we assume all tags remain in the identification area at least until their identities are correctly received, and that no new tags enter during the reading process. The goal is to identify the n tags in the shortest time (equivalently in as few slots as possible). The identification process requires a series of consecutive reading frames (i=1, 2, ...) until all tags are identified. Let us denote n_i as the number of tags competing on frame i, and $K_i=2^{Q_i}$ as the frame length on cycle i, $Q_i \in[1,\ldots,15]$. At the end of frame i, the reader knows the number of identified tags (id_i), the number of slots with collisions (c_i) and the number of empty slots (e_i). Note that $K_i=2^{Q_i}=id_i+c_i+e_i$. Then, at the end of frame i, the MFML-DFSA algorithm proceeds as follows:

- $\widehat{n}$, the most likely number of tags at the beginning of the identification process, is computed by means of the ML estimator, as a function of the set $\{(Q_j, id_j, c_j, e_j); j=1,\ldots, i\}$ (see section 2.7.2).
- The most likely number of tags that will compete in the next frame (i+1) is $\widetilde{n_{i+1}}=\widehat{n}-\sum_{j=1}^{i} id_j$ (the total number of tags minus those already identified).

- Then, K_{i+1}=$2^{Q_{i+1}}$ is accordingly selected to maximize the expected throughput in frame i+1 (see section 2.7.3).

2.7.2 Computation of $\widehat{n}$

To compute the probability $Pr(n, K, id, c, e)$, henceforth $Pr(n, K)$, we apply a technique from [Milen04], where the authors formulate probabilistic transforms for urn models that convert the dependent random variables describing urn occupancies (slot in our case) into independent random variables. Due to the independence of random variables in the transformed domain (codomain) it is simpler to compute the statistics of interest, and invert the transform.

Let us denote $Pr(n, K)$ as the probability of interest, and $\boldsymbol{Pr}(\lambda, K)$ as its transformation, with λ being a meaningful parameter only in the transform domain. In fact there is no dependence on the number of balls, n, in the transform domain.

The calculation procedure is as follows: first, the appropriate transform for a particular urn model is selected. In our case, the K urns (slots) are distinguishable and the n balls (tags) are undistinguishable, since we are only interested in the number of balls within each urn. In this case, the $Z_1, \ldots, Z_K$ independent random variables describing the occupancy of an urn (number (b) of balls inside) in the transform domain, are geometrically distributed with mean λ [Milen04]. That is, $Pr(Z_i = b) = (1-\lambda)\lambda^b$. Second, the probability of interest, $\boldsymbol{Pr}(\lambda, K)$, is computed in the transformed domain. In our case, given a frame of length K, the probability of having id urns with one ball, c urns with several balls and e empty urns is:

$$\begin{aligned}\boldsymbol{Pr}(\lambda, K) &= \frac{K!}{id!c!e!}Pr(Z=1)^{id}Pr(Z>1)^{c}Pr(Z=0)^{e} = \\ &= \frac{K!}{id!c!e!}((1-\lambda)\lambda)^{id}\lambda^{2c}(1-\lambda)^{e}\end{aligned} \tag{2.18}$$

We have to express this statistic as an power series in λ, in order to compute the inverse transform as the coefficient of the λ^n term from the following expression:

$$Pr(n, K) = \binom{K+n-1}{n}^{-1}[\lambda^n]\{\boldsymbol{Pr}(\lambda, K)/(1-\lambda)^n\} \tag{2.19}$$

with $[\lambda^n]\{h(\lambda)\}$ denoting the coefficient of λ^n in the power series $\{h(\lambda)\}$. In our case, rewriting equation (2.18) as power series in λ,

$$\begin{aligned}Pr(n, K) = \frac{K!}{id!c!e!}&\binom{K+n-1}{n}^{-1}[\lambda^n]\{ \\ &\sum_{l=0}^{\infty}\binom{K-id-e+l-1}{l}\lambda^{l+id+2c}\}\end{aligned} \tag{2.20}$$

and extracting the coefficient of λ^n for the appropriate n value, $n = l + id + 2c$, we obtain this result:

$$
\begin{aligned}
&Pr(n,K,id,c,e) = \\
&= \frac{K!}{id!c!e!}\binom{K+n-1}{n}^{-1}\binom{n-id-c-1}{n-id-2c} = \\
&= \frac{K!(K-1)!}{id!c!e!(c-1)!}\frac{\prod_{a=n-id-2c-1}^{n-id-c-1} a}{\prod_{b=n+1}^{n+K-1} b}
\end{aligned}
\tag{2.21}
$$

Equation (2.21) can be computed for $n \geq id + 2c$, since n is at least the sum of the tags identified plus the colliding ones (at least 2 per collision). After the first cycle of the identification process, the probability of the event $\{(Q_1, id_1, c_1, e_1)\}$ being n tags contending is calculated as follows:

$$
prob\{(Q_1, id_1, c_1, e_1)\} = Pr(n, 2^{Q_1}, id_1, c_1, e_1) \tag{2.22}
$$

After the second cycle:

$$
\begin{aligned}
&prob\{(Q_1, id_1, c_1, e_1),(Q_2, id_2, c_2, e_2)\} = \\
&=Pr(n, 2^{Q_1}, id_1, c_1, e_1)Pr(n-id_1, 2^{Q_2}, s_2, c_2, e_2)
\end{aligned}
\tag{2.23}
$$

Note that reading cycles are independent, and so is the probability of the observed events. Then, after i frames, if the initial number of tags is n, the probability of a given set of events $\{(Q_j, id_j, c_j, e_j) : j = 1, \ldots, i\}$ is calculated as

$$
\prod_{j=1}^{i} Pr(n - \sum_{u=1}^{j} id_{u-1}, 2^{Q_j}, id_j, c_j, e_j) \tag{2.24}
$$

Let us remark that in reading cycle j the number of tags still unidentified is $n - \sum_{u=1}^{j} id_{u-1}$, having s_0 equal to 0 for consistency. Therefore, $\widehat{n}$ is computed as the value that maximizes the probability of equation (2.24), yielding its ML estimator:

$$
\widehat{n} = \underset{\{n \geq \max\limits_{j=1,\ldots,i} n_j\}}{\arg\max} \prod_{j=1}^{i} Pr(n - \sum_{u=1}^{j} id_{u-1}, 2^{Q_j}, id_j, c_j, e_j) \tag{2.25}
$$

where n_j is the minimum number of competing tags detected at frame j, n_j = $2c_j + \sum_{u=1}^{j} id_u$.

2.7.3 Q_i selection

The throughput of a FSA system (η) reaches its maximum η=e^{-1} when the number of tags (n) matches the number of slots (K) [Bueno09c]. However, the number of slots per frame for EPC-C1G2 must lie within $\{2^Q : Q = 0, \ldots, 15\}$.

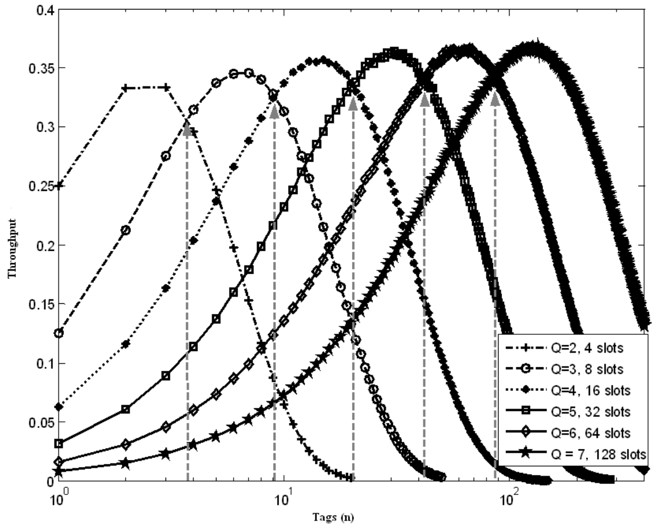

Figure 2.11: Throughput (Identification rate) per cycle for different N and Q values

$$\eta = \frac{n}{K}\left(1-\frac{1}{K}\right)^{n-1} = \frac{n}{2^Q}\left(1-\frac{1}{2^Q}\right)^{n-1} \tag{2.26}$$

For each Q there is a set of values of n, for which throughput is maximum. These sets have the form $[n_{min}(Q), \ldots, 2^Q, \ldots, n_{max}(Q)]$. We can compute them, since $n_{max}(Q^* - 1) = n_{min}(Q^*) - 1$, and $n_{max}(Q^* - 1)$ must be the largest integer fulfilling inequality (2.27). Table 2.2 summarizes the results for an arbitrary frame *i*.

$$\begin{aligned} &\frac{n_{max}(Q^*-1)}{2^{Q^*-1}}\left(1-\frac{1}{2^{Q^*-1}}\right)^{n_{max}(Q^*-1)-1} > \\ &> \frac{n_{min}(Q^*)}{2^{Q^*}}\left(1-\frac{1}{2^{Q^*}}\right)^{n_{min}(Q^*)-1} \end{aligned} \tag{2.27}$$

In addition, note that there is not information available (id, e, c) to select Q_1, and it must be selected using other criteria. The readers on the market currently select Q_1=4, independently of the population of tags in range. This study demonstrates that better values of Q_1 can be selected if the amount of contending tags in the first frame is known to lie within a certain interval (see section 2.7.5).

2.7.4 Implementation issues

Regarding algorithm implementation feasibility, the following iterative method is proposed. Knowing that maximizing probability in equation (2.25) is equivalent to maximizing its logarithm, the products of equation (2.21) can be expressed as a sum of logarithms. To speed up computations, the RFID reader keeps an array with pre-defined computations of $\sum_{z=1}^{n} log(z)$ for $n = 1, \ldots, 2^{15} + n_{max}$. Let A_z be the z-th position of this array, let us

Q_i	$\widetilde{n_i}$ range
0	$\widetilde{n_i} = 1$
1	$1 < \widetilde{n_i} \leq 3$
2	$3 < \widetilde{n_i} \leq 6$
3	$6 < \widetilde{n_i} \leq 11$
4	$11 < \widetilde{n_i} \leq 22$
5	$22 < \widetilde{n_i} \leq 44$
6	$44 < \widetilde{n_i} \leq 89$
7	$89 < \widetilde{n_i} \leq 177$
8	$177 < \widetilde{n_i} \leq 355$
9	$355 < \widetilde{n_i} \leq 710$
10	$710 < \widetilde{n_i} \leq 1420$
11	$1420 < \widetilde{n_i} \leq 2839$
12	$2839 < \widetilde{n_i} \leq 5678$
13	$5678 < \widetilde{n_i} \leq 11357$
14	$11357 < \widetilde{n_i} \leq 22713$
15	$22713 < \widetilde{n_i}$

Table 2.2: OptimalQ_i versus $\widetilde{n_i}$ range

initialize an all-zero array B_n with n_{max} positions, and let n_{min} = 1. Then, just at the end of cycle i, it is necessary to:

1. Update n_{min}, n_{min} = $\max\{n_{min}, 2c_i + \sum_{j=1}^{i} id_j\}$
2. Compute the logarithm of equation (2.25) for n = $n_{min}, \ldots, n_{max}$. Note that this is the sum of a constant:

$$\begin{aligned} & log\left(\frac{K_i!(K_i-1)!}{id_i!c_i!e_i!(c_i-1)!}\right) = \\ & = A_{K_i} + A_{K_i-1} - A_{id_i} - A_{c_i} - A_{e_i} - A_{c_i-1}, \end{aligned} \tag{2.28}$$

   plus a factor that varies with n:

$$\begin{aligned} & log\left(\frac{\prod_{v=n-id_i-2c_i-1}^{n-id_i-c_i-1} v}{\prod_{v=n+1}^{n+K_i-1} v}\right) = \\ & = A_{n-id_i-c_i-1} - A_{n-id_i-2c_i-2} - A_{n+K_i-1} + A_n \end{aligned} \tag{2.29}$$

   Therefore, this step requires at most $5 + 4n_{max}$ sums.

3. Then, the sum of logarithmic probabilities is updated, $B_n = B_n + log(Pr(n - \sum_{j=1}^{i} id_{j-1}, 2^{Q_i}, id_i, c_i, e_i))$, and the index -belonging to $[n_{min}, n_{max}]$- with the largest component in the array minus $\sum_{j=1}^{i} id_j$ is returned as $\widetilde{n_{i+1}}$. This step requires n_{max} sums and comparisons.
4. Finally, the best value of Q_{i+1} is selected from Table 2.2 as a function of $\widetilde{n_{i+1}}$.

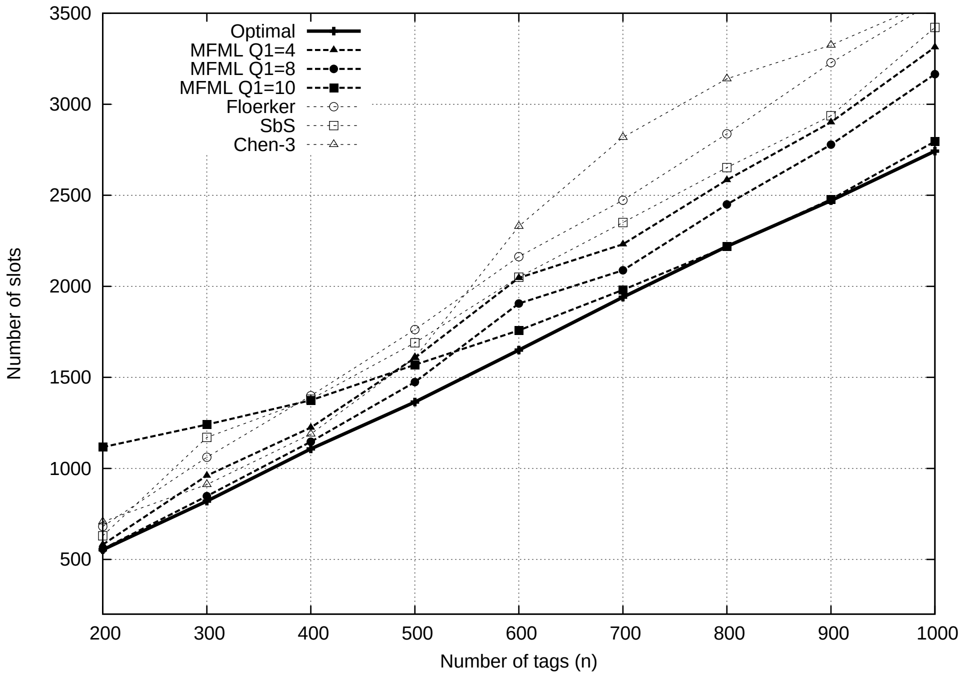

Figure 2.12: Average number of slots required for identification, L versus n

2.7.5 Performance evaluation

The performance of MFML-DFSA and its main alternatives (see section 2.5) have been evaluated by means of a discrete-event simulator. As in the previous performance evaluation, we have taken the physical configuration parameters from the commercial Alien 8800 system [Alien]. This simulator has been validated by means of laboratory test beds based on this system [Bueno09b].

Figure 2.12 shows the performance of MFML-DFSA starting with Q_1=4, 8, 10, compared with the best DFSA algorithms [Knerr08-2, ChenW09, Floer06]. These algorithms start with Q_1=4. The optimal Q_i is selected from the expected $\widehat{n_i}$ in all cases. As a reference, we also depict the performance of an ideal algorithm, *i.e.* with perfect knowledge of the competing tags within each frame. Our proposal outperforms previous ones. Regardless of the initial Q_1, MFML-DFSA performs better when $n > 500$. Indeed, MFML-DFSA lies very close to the optimal bound in a range of values of n (*e.g.* for 700$< n <$1000 if Q_1=10), illustrating that just a rough knowledge about the initial number of tags (*i.e.* a relatively wide range) is advantageously exploited by MFML-DFSA.

Computation requirements have also been evaluated for the examples of section 2.6.3, assuming the same constraints. Table 2.3 summarizes the results. MFML-DFSA achieves a low computational cost in both scenarios. Therefore, we can state that MFML-DFSA process as a whole is not computationally demanding and also that current commercial *Central Processing Units* (CPUs) can analyze extremely large ranges in $\sim$1μs (note that 2.5 ms is the typical slot length).

		Scenario 1		Scenario 2	
Protocol	**Order**	**FLOP/cycle**	%	**FLOP/cycle**	%
Schoute	$O(n)$	10^2	$< 0.1\%$	10^3	$< 0.1\%$
Lower Bound	$O(n)$	10^2	$< 0.1\%$	10^3	$< 0.1\%$
C-ratio	$O(n)$	10^3	$< 0.1\%$	$2.5 \cdot 10^4$	$< 0.1\%$
Wang	$O(n^2)$	$18 \cdot 10^3$	$< 0.1\%$	$1.1 \cdot 10^7$	$< 1\%$
Chen-1	$O(n)$	$3 \cdot 10^2$	$< 0.1\%$	$3 \cdot 10^3$	$< 0.1\%$
MSE-Vogt	$O(n)$	$1.1 \cdot 10^4$	$< 0.1\%$	$2.7 \cdot 10^5$	$< 0.1\%$
MSE-Knerr	$O(n)$	$3.7 \cdot 10^4$	$< 0.1\%$	$2.7 \cdot 10^5$	$< 0.1\%$
Chen-2	$O(n)$	$3.8 \cdot 10^5$	$< 0.1\%$	$4.1 \cdot 10^7$	$\approx 3\%$
SbS	$O(n)$	$1.3 \cdot 10^7$	$\approx 3\%$	$3.7 \cdot 10^8$	$\approx 24\%$
Chen-3	$O(n)$	$7 \cdot 10^5$	$< 1\%$	$7 \cdot 10^6$	$< 1\%$
Floerker	$O(n^2)$	$4.4 \cdot 10^7$	$\approx 11\%$	$3.6 \cdot 10^9$	$> 100\%$
MFML-DFSA	$O(n)$	10^3	$< 0.1\%$	$6 \cdot 10^5$	$< 0.1\%$

Table 2.3: Comparison of computational cost

2.8 Conclusions

The most relevant anti-collision protocols for passive RFID have been analyzed and evaluated in this chapter. The study has focused on DFSA algorithms, pointing out their strengths and weaknesses, also introducing and analyzing a new proposal: the MFML-DFSA algorithm. MFML-DFSA uses a Maximum Likelihood estimator to compute the expected number of competing tags. The results show that MFML-DFSA outperforms other current DFSA proposals, achieving better identification time, with an extremely low computational cost achieved by the efficient implementation proposed. Besides, MFML-DFSA does not impose tag modifications, while satisfying the frame length constraints of EPC-G1C2.

We would like to finish this chapter encouraging further research regarding the following issue: The MFML-DFSA estimator can be modified to estimate the number of tags under the assumption of the Capture Effect phenomenon, which is studied in Chapter 3.

Chapter 3

Characterization of the identification process in passive RFID Systems

Passive RFID systems on the market implement the anti-collision protocol EPC-C1G2 [EPCgl05], based on a variation of FSA. As we described in Chapter 2, the FSA throughput (tags identified per time unit) depends on the relationship between the number of competing tags (N) and the frame length (K). The anti-collision protocols based on FSA perform optimally if K=N for every cycle. However, readers do not adjust K depending on N and EPC-C1G2 restricts the frame length to $\{K = 2^Q : Q = 0, \ldots, 15\}$.

This chapter takes into account these aspects to analyze the identification process in passive RFID systems and to propose suitable criteria to maximize the throughput. The analysis is carried out by means of *Discrete Time Markov Chains* (DTMC) in static, semi-static and dynamic scenarios. In static scenarios a group of tags enters the checking area and remains until all of them have been successfully identified. Besides, new tags do not enter the checking area. In these scenarios the mean identification time is the parameter of main interest. The second scenario is similar to the fist one, but tags stay in the workspace only for a bounded time (sojourn time, or time in coverage). In this scenario, the goal is to minimize the ratio of tags that leave the checking area unidentified *Tag Loss Ratio* (TLR), either configuring the sojourn time or the number of tags entering the workspace. Finally, in the dynamic scenario, a continuous flow of new tags is considered, as well as a bounded sojourn time, and TLR must be minimized. Finally, identification process is also analyzed in a static scenario assuming the Capture Effect phenomenon. To confirm the analytical results of all the previous analysis, experimental measurements have been addressed with a real passive RFID system: the development kit Alien 8800 [Alien]. The results obtained can assist manufacturers and system operators improving their RFID system performance.

3.1 Overview of RFID readers in the market

The current passive RFID readers available on the market implement EPC-C1G2. Some of them only permit to work with one of the two procedures explained in Chapter 2: fixed frame length procedure or variable frame length procedure. Besides, some readers do not permit to configure internal parameters such as the initial frame length (the Q_1 value). Depending on the level of configuration allowed, the readers can be classified as follows:

- Readers with fixed frame length, non-customizable, such as those commercialized by Symbol [Symbol], ThingMagic [ThingMagic], Caen [Caen], Awid [Awid] and Samsys [Samsys]. In these readers, the length of every identification cycle is fixed and set up by the manufacturer. It is not possible to modify it and it is usually fixed to 16 slots. Therefore, in these readers it is not feasible to optimize the frame length.

- Readers with fixed frame length, customizable, such as those commercialized by Samsys [Samsys], Intermec [Inter] and Alien [Alien]. Before starting identification procedures, the system operator can configure the frame length, choosing among several options which depend on the manufacturer. Afterwards, the identification cycle length cannot be changed. If the reader manager wants to establish a different value of frame length, it is necessary to stop the identification procedure and restart it with the new frame length.

- Readers with variable frame length such as those also commercialized by Samsys [Samsys], Intermec [Inter] and Alien [Alien]. The system operator only configures the frame length for the first cycle. For successive cycles the frame length is self-adjusted trying to adapt it to the best value at each moment, following the standard proposal (see page 24).

Readers with fixed frame length do not allow to achieve the maximum throughput per cycle, although N and/or K can be set to minimize the mean identification time of the whole identification process. Namely, in those readers with fixed frame length non-customizable, N can be selected (*e.g.* setting the tags per pallet that pass through the checking areas). Moreover, in customizable systems either N or K can be modified. That is, selecting the number of tags per package N, or selecting the optimal value of K, if N is known. In addition, readers with variable frame length implement an internal mechanism to adjust K in every cycle/slot, as we discussed in the previous chapter. Note that, since adjustment is based on estimations of N, the performance is sub-optimal.

3.2 Identification process in static scenarios

Static scenarios are characterized by a block of tags (modeling a physical container like a pallet, a box, etc.) that enter the checking area and remain until all of them are successfully identified. Two related performance measures are commonly considered:

- The identification time, defined as the mean number of time units (slots, cycles, seconds, etc.) until all tags are identified.

- The system throughput or efficiency, defined as the inverse of the mean identification time, *i.e.*, the ratio of identified tags per time unit.

3.2.1 Markovian analysis

The identification process in a static scenario is determined by the number of remaining unidentified tags. Thus, the identification process can be modeled as a homogeneous DTMC, X_s, where each state in the chain represents the number of unidentified tags, being s the cycle number. Thus, the state space of the Markov process is $\{N, N-1, \ldots, 0\}$, being N the number of tags unidentified. Figure 3.1 shows DTMC state diagram from the initial state, X_0=N. The transitions between states represent the probability of identifying a certain quantity of tags t or, in other words, the probability of having $(N-t)$ tags still unidentified.

The transition matrix P depends on the anti-collision protocol used and its parameters. For EPC-C1G2, the parameter K denotes the number of slots per frame (frame length). To compute the transition matrix P, let us define the random variable μ_t, which indicates the number of slots being filled with exactly t tags in a reading cycle. Its mass probability function is [Vogt02]:

$$Pr_{K,N}(\mu_t = m) = \frac{\binom{K}{m} \prod_{z=0}^{m-1} \binom{N-zt}{t} G(K-m, N-mt, t)}{K^N} \tag{3.1}$$

Where m=0, ..., K and G is an auxiliary function defined as follows,

$$G(a,l,v) = a^l + \sum_{z=1}^{\lfloor \frac{l}{v} \rfloor} \left\{ (-1)^i (a-z)^{l-zv} \frac{1}{z!} \prod_{y=0}^{z-1} \left\{ \binom{l-yv}{v} (a-y) \right\} \right\} \tag{3.2}$$

When $t=1$, *i.e.* how many slots contain a successful identification, the equation (3.1) can be simplified:

$$Pr_{K,N}(\mu_1 = m) = \frac{K!N!}{m!K^N} \sum_{z=0}^{N-m} \frac{(-1)^z (K-m-z)^{N-m-z}}{(N-m-z)!z!(K-m-z)!} \tag{3.3}$$

The equation (3.3) is equivalent to the equation proposed in [Feller70], where the author computes this probability by an alternative method.

In [Vogt02], the author assumes all tags compete in every identification cycle. However, in EPC-G1C2 tags identified in a cycle will not compete in the following ones. Hence, the transition matrix P must be transformed, yielding to:

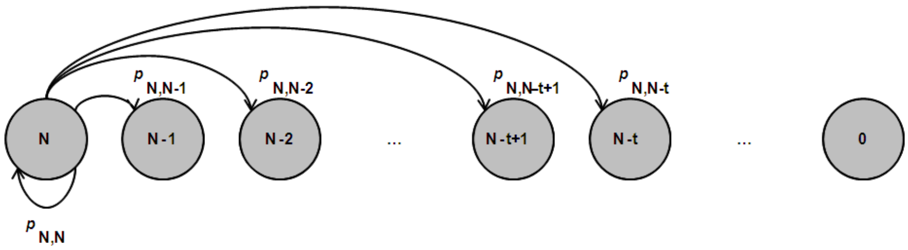

Figure 3.1: Partial Markov Chain

$$p_{i,j} = \begin{cases} Pr_{K,i}(\mu_1 = i - j) & , i - K \leq j < i \\ \\ 1 - \sum_{y=i-1}^{i-K} p_{i,y} & , j = i \\ \\ 0 & \text{, otherwise} \end{cases} \tag{3.4}$$

for $i = 1, \ldots, N$.

Since a static scenario is assumed, the Markov chain clearly has a single absorbing state, X_s=0. The mean number of steps until the absorbing state is the mean number of identification cycles $(\bar{s})$. It can be computed by means of the fundamental matrix, D, of the absorbing chain [Kemen60]. The fundamental matrix D is obtained from the canonical form of the transition probability matrix P. In our case, since there is only one absorbing state it has the form:

$$P = \left(\begin{array}{c|c} 1 & 0 \\ \hline Q & F \end{array} \right) \tag{3.5}$$

where F denotes the submatrix of P with the transient states (note that the size of F is $N \times N$). Thus, the fundamental matrix D is:

$$D = (I - F)^{-1} \tag{3.6}$$

being I the identity matrix of size $N \times N$.

From D the mean number of identification cycles $\bar{s}$ can be calculated as follows:

$$\bar{s} = \sum_{y=0}^{N-1} D_{0,y} \tag{3.7}$$

Note that the mean number of identification cycles expected before absorption equals the total number of steps to make to all the non-absorbing states from an initial state i. This is calculated as the sum of all the entries in the i-th row of D. In this analysis, the calculation starts from the initial state, X_0, hence, $\bar{s}$ is calculated as the sum of the elements of row 0 in D.

From the previous analysis we can compute the mean number of cycles ($\bar{s}$) to identify a population of tags (N) as well as the mean number of slots $\bar{L}$=$\bar{s} \cdot K$. Using the physical

Tags (N)	$\bar{s}$	L	T_{total}
10	2.44	39.04	0.0395
20	4.11	65.76	0.0738
30	6.15	98.4	0.1126
40	8.97	143.52	0.1564
50	13.03	208.48	0.2151
60	19.3	308.08	0.2914
70	29.41	470.56	0.3988
80	46.0	736	0.5662
90	73.81	1.1 10^3	0.8348

Table 3.1: Average identification time

and FSA standard parameters (see Table 3.2) we can also transform the identification time from cycles to seconds.

Let us define T_{id} the duration of a slot with a valid data transmission (EPC code) and T_e and T_c the duration of an empty and collision slot, respectively. Thus, the identification time in seconds is approximated by [Bueno09b]:

$$\bar{T}_{total} \approx \bar{s} \cdot [\bar{T}_e\bar{e} + \bar{T}_c\bar{c} + \bar{T}_{id}\bar{id}] \tag{3.8}$$

where $\bar{e}$, $\bar{c}$ and $\bar{id}$ denote the mean number of empty, collision and successful slots, respectively. These variables depend on the particular FSA algorithm and its configuration, and on the population size. For instance, setting M=4 (see Table 3.2), $\bar{T}_{id}$=2.505 ms and $\bar{T}_e$=$\bar{T}_c$=0.575 ms. Since an empty slot and a collision slot have the same duration, the previous equation can be simplified:

$$\bar{T}_{total} \approx \bar{s} \cdot [\bar{T}_c(\bar{e} + \bar{c}) + \bar{T}_{id}\bar{id}] \tag{3.9}$$

Since,

$$\bar{e} + \bar{c} \approx K\bar{s} - \bar{id} \tag{3.10}$$

Then,

$$\bar{T}_{total} \approx \bar{s} \cdot [\bar{T}_c(K\bar{s} - \bar{id}) + \bar{T}_{id}\bar{id}] \tag{3.11}$$

In Table 3.1 we show an example of identification time calculation in seconds from the mean number of cycles and slots obtained by the Markovian analysis. The analysis has been carried out setting K=16 and different tag populations.

3.2.2 Analytical and simulation results

The analysis introduced in the previous sections has been evaluated using the Montecarlo methodin Matlab. Besides, an RFID simulator has been developed with the OMNeT++ (Objetive Modular Network Testbed in C++) tool [Varga01]. The simulator implements the functionality of the readers available on the market: the standard EPC-C1G2 and its anti-collision procedures. The parameters used in the simulator are summarized in Table 3.2.

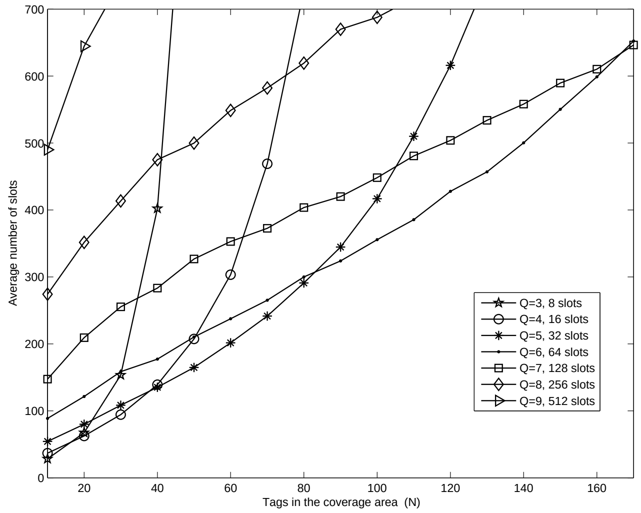

Figure 3.2: Reader with fixed frame length in static scenario: Average identification time (number of slots) vs. number of tags

The identification time (average number of slots) has been computed for a single reader RFID system with fixed frame length and different tag populations (N). The reader has been configured with different frame-lengths $\{K = 2^Q : Q = 3, \ldots, 9\}$. The mean identification time (in number of slots) is shown in Figure 3.2. For every Q there is an interval where the identification time is lower than with the other Q values. The intersection points between curves define the boundaries (minimum and maximum number of tags in coverage) of optimal configurations.

3.2.3 System Throughput

The throughput (η) can be computed from the previous Markovian analysis, just as the inverse of the identification time. Another way is described in this section. Let us remark that, obviously, the result of both methods is equal, and the second one is provided for completeness. Given N tags, and K slots, the probability that t tags respond in the same time slot is binomially distributed:

$$Pr(t) = \binom{N}{t} \left(\frac{1}{K}\right)^t \left(1 - \frac{1}{K}\right)^{N-t} \tag{3.12}$$

for $t = 0, \ldots, N$.

Then, $Pr(t = 0)$ is the probability of an empty slot, $Pr(t = 1)$ the probability of a successful slot, and $Pr(t \geq 2)$ the probability of collision:

$$Pr(t = 0) = \left(1 - \frac{1}{K}\right)^N \tag{3.13}$$

Parameter	Symbol	value
Electronic Product Code	EPC	96 bits
Initial Q value	Q_0	4
Reference Time interval for a data-0 in Reader-to-Tag signalling	TARI	$12.5us$
Time interval for a data-0 in Reader-to-Tag signalling	DATA0	1.0 TARI
Time interval for a data-1 in Reader-to-Tag signalling	DATA1	1.5 TARI
Tag-to-Reader calibration symbol	TRcal	64 us
Reader-to-Tag calibration symbol	RTcal	31.25 us
Divide Ratio	DR	8
Backscatter Link Frequency	LF	DR/Trcal
Number of subcarrier cycles per symbol in Tag-to-Reader direction	M	1,2,4,8
Reader-to-Tag rate	Rtrate	64 Kbps
Tag-to-Reader rate	Trrate	LF/M
Link Pulse Repetition Interval	T_{pri}	1/LF
Tag-to-Reader preamble	TRP	$6T_{pri}$
Tag-to-Reader End of Signalling	$T \rightarrow R\,EoS$	$2T_{pri}$
Delimiter	Del	12.5 us
Reader-to-Tag preamble	RTP	Del + DATA0+ TRcal + RTcal
Reader-to-Tag Frame Synchronization	RTF	RTP - RTcal
Time for reader transmission to tag response	T_1	$Max(RTcal, 10T_{pri})$
Time for tag response to reader transmission	T_2	$5T_{pri}$
Time a reader waits, after T_1 before it issues another command	T_3	$5T_{pri}$
Minimum time between reader commands	T_4	2RTcal
Query packet	Query	22 bits
QueryAdjust packet	QueryAdjust	9 bits
QueryRep packet	QueryRep	4 bits
Ack packet	Ack	18 bits
Nack packet	Nack	8 bits

Table 3.2: Typical values of EPC-C1G2 parameters

$$Pr(t=1) = \frac{N}{K}\left(1-\frac{1}{K}\right)^{N-1} \tag{3.14}$$

$$Pr(t \geq 2) = 1 - Pr(t=0) - Pr(t=1) = 1 - \left(1-\frac{1}{K}\right)^{N}\left(1-\frac{N}{K-1}\right) \tag{3.15}$$

Since all identification cycles are composed of K slots, the throughput is:

$$\eta = K \cdot Pr(t=1) = N\left(1-\frac{1}{K}\right)^{N-1} \tag{3.16}$$

3.2.4 Identification process analysis considering the Capture Effect phenomenon

The Capture Effect phenomenon occurs in RFID systems when the signals of two or more tags arrive at the reader simultaneously, (in the same time slot) but with different power levels. Sometimes the stronger signal can be successfully decoded by the reader. The Capture Effect has a considerable influence on the RFID system throughput, because it is not is achieved if the number of tags N equals the number of slots K in every cycle, but when $K \approx N + \delta c$, being c the number of colliding slots and δ the probability of recovering the signal of one tag from a colliding slot. Note that δ depends on the physical characteristics of the system, distance among tags, etc.

The Capture Effect has been extensively studied for decades. However, there are only a few works focusing on the analysis of the Capture Effect on RFID [AutoID] or FSA procedures [Weise88]. The main way to model the Capture Effect for the analysis of RFID is the Signal-to-Interference-Ratio (SIR) model: The Capture Effect occurs when the SIR is higher than a threshold. In this case, the signal recovered corresponds to the tag with maximum signal strength and the remainder are considered interferences. The capture probability is determined by the following equation:

$$\delta(t) = Pr(SIR > C_r) = Pr\left(\frac{Pw_v}{\sum_{y=1, y\neq v}^{z} Pw_y} > C_r\right) \tag{3.17}$$

Where t is the number of tags colliding, C_r is the capture ratio and Pw is the power of the signal received from tag i. In [AutoID], the SIR model has been analytically evaluated for different parameters. The authors conclude that the capture probability strongly depends on the number of tags colliding and C_r (which depends on the scenario assumed). We can simplify equation (3.17) as follows:

$$\delta(t) = q^t \tag{3.18}$$

Being $q \in [0, 1]$ a parameter related directly to C_r [AutoID]. Note that $\delta(z)$ decreases as the number of tags colliding z increases and *vice versa*.

Let us then define $\gamma(t)$ as the random variable (*r.v.*) "number of slots with t simultaneous tag transmissions where one transmission can be successfully decoded". Its mass probability function, given that the number of slots filled with exactly i tags is μ_t (introduced in section 3.2.1) is the binomial distribution function:

$$Pr(\gamma_t = \gamma | \mu_t) = \binom{\mu_t}{\gamma} \delta(t)^{\gamma} (1 - \delta(t))^{\mu_t - \gamma} \tag{3.19}$$

For $z \geq 2$.

Note that if there are N tags competing in K slots, then, $\sum_{z=0}^{N} \mu_z = K$. On the other hand, $\sum_{t=0}^{N} \gamma_t \leq K$.

3.2.4.1 Markovian Analysis

We have analyzed the identification process of a RFID system in a static scenario considering the Capture Effect phenomenon, as in the previous wounder EPC-C1G2 in fixed frame length procedure. The analysis can also be modeled as a homogeneous DTMC. In contrast to the analysis of section 3.2.1, the transition from state i to j depends not only on the number of slots filled with exactly one tag (μ_1) but also on the slots (γ_t) where the reader can decode the signal of one tag from a collision of t tags.

In fact, the transition from state i to j depends on the *r.v.* number of empty (e), successful (id), collision slots (c) and collision slots with a successful tag signal (r) as follows:

$$e = \mu_0 = \gamma_0 = K - \sum_{t=1}^{N} \mu_t \tag{3.20}$$

$$id = \mu_1 = \gamma_1 \tag{3.21}$$

$$c = \sum_{t=2}^{\lfloor \frac{N-\mu_1}{2} \rfloor} \mu_t - \gamma_t \tag{3.22}$$

$$r = \sum_{t=2}^{\lfloor \frac{N-\mu_1}{2} \rfloor} \gamma_t \tag{3.23}$$

where $K = e + id + c + r$.

The number of tags successfully identified in a cycle (in the transition state from i to j) depends on the number of slots with a successful identification id, and on the number of slots with collision decoded (r), that is, $(i - j) = id + r$.

Let us denote the set of all possible stages of (e, id, c, r) as $\Phi = \{\mu | \sum_{t=0}^{i} \mu_t \wedge i = \sum_{t=0}^{i} t\mu_t\}$. For each μ, there will be a set of possible γ, denoted as $\Psi = \{\gamma | r = \sum_{t=2}^{\lfloor \frac{i-\mu_1}{2} \rfloor} \gamma_t \wedge c = \sum_{t=2}^{\lfloor \frac{i-\mu_1}{2} \rfloor} \mu_t - \gamma_t\}$.

Thus, the transition matrix P is given by:

$$p_{i,j} = \begin{cases} Pr_{K,i}(id + r, e, c) & , j - 2K \leq j < i \\ 1 - \sum_{y=i-1}^{i-K} p_{i,y} & , j = i \\ 0 & , \text{otherwise} \end{cases} \tag{3.24}$$

where,

$$\begin{gathered} Pr_{K,i}(id + r, e, c) = Pr_{K,i}(id + r, c) = \\ \sum_{\forall \mu \in \Phi} Pr_{K,i}(id + r, c|\mu) Pr_{K,i}(\mu) = \sum_{\forall \mu \in \Phi} \sum_{\forall \gamma \in \Psi} Pr(\gamma|\mu) Pr_{K,i}(\mu) \end{gathered} \tag{3.25}$$

Equation (3.25) depends on $Pr(\gamma|\mu)$, defined previously in equation (3.19) and $Pr_{K,i}(\mu)$ is given in equation (3.1).

Note that, when the number of tags competing is high the computation of the above algorithm can be unfeasible, (*e.g.* if N=10^5, there are 10^{10} stages). To cope with this complexity, it is possible to assume $\delta(z) = 0$, for $z > Y$, where Y=$2, 3, 4, \ldots, \frac{N}{2}$. The Y value selected will depend on the q value set, see equation (3.18).

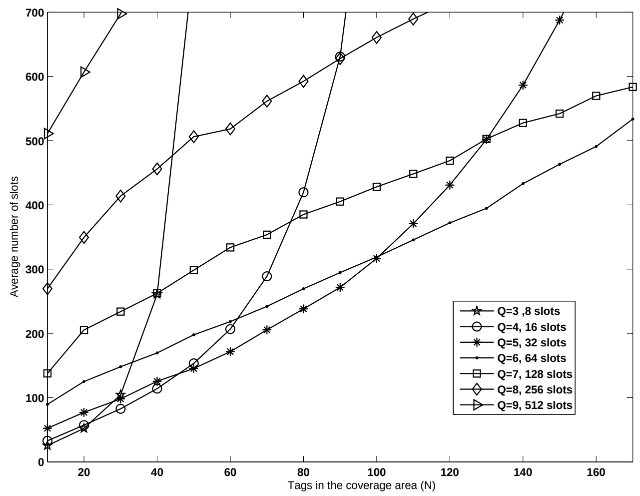

Figure 3.3: Reader with fixed frame length considering the Capture Effect phenomenon: Average identification time (number of slots) vs. number of tags

3.2.5 Analytical and simulation results

The identification time has been computed considering the Capture Effect phenomenon. In the simulations a collision ratio of C_r=6 dB has been used, which is equivalent to set q=0.5 in the analysis [AutoID]. The results are shown in Figure 3.3. In comparison with the previous results (see section 3.2.2), the Capture Effect provides a remarkable improvement in the identification process, achieving a lower identification time. For instance, Figure 3.2 shows that setting the reader to Q=6 and assuming 100 tags in coverage, the identification time is close to 350 slots. In the same scenario but assuming the Capture Effect, Figure 3.3 shows that the identification time is reduced in 50 slots. Note that when the number of tags in coverage increases, the improvement considering Capture Effect is more noticeable, *e.g.*, if N=170 tags and Q=6, the identification time with capture effect is around 530 slots whereas without capture effect it is around 660 slots, or some 24$\%$ more time.

Simulation has been performed with the same assumptions considered in the analytical model either with or without the Capture Effect phenomenon. The readers with variable frame length are evaluated setting Q_1=4. The results are plotted in Figure 3.4, together with fixed frame length results. Note that variable frame length readers achieve the best performance when Capture Effect is considered, as expected.

3.3 Identification process in semi-static scenarios

Many real RFID applications (*e.g.* a conveyor belt installation) work in semi-static scenarios, which are characterized by tags confined in groups (pallets or similar), entering and leaving the workspace through RFID enabled gates (see Figure 3.5). When tags enter the checking area, they keep on there for a specific time (sojourn time, or time in coverage).

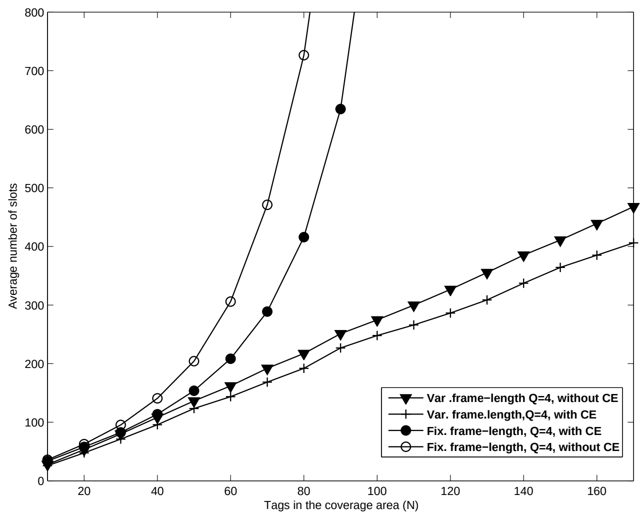

Figure 3.4: Reader with variable frame length with and without considering the Capture Effect phenomenon. Comparison with fixed frame length

New groups of tags do not enter the checking area until the previous one has left.

For these types of systems, the goal is to minimize the tags leaving the workspace unidentified. Consequently the key parameter is the *Tag Loss Ratio* (TLR), defined as the ratio of tags leaving the workspace unidentified to the rate of incoming tags. Note that since the identification time is an unbounded *r.v.* in FSA systems (*i.e.* the identification time can be arbitrarily high), it is impossible to establish a sojourn time that guarantees the identification of all tags. Instead, the sojourn time can be configured to guarantee an *Identification Confidence Level* (ICL), that is, the percentage of successful identifications as close as zero as required (but not null). Based on the demand of ICL, the sojourn time can be computed. This analysis is developed in the following sections.

3.3.1 Computation of ICL

The analysis and computation of ICL in semi-static scenarios is addressed by DTMC. The Markovian analysis to compute the transition probabilities is the same as static-scenarios. Hence, we start the analysis from equation (3.4). Then, for each cycle s, the distribution probability of the DTMC is calculated as follows:

$$\pi^{(s)} = \pi^{(0)} \cdot h^s \tag{3.26}$$

being $\pi^{(s)}$ the row vector where each element represents the probability of reaching a particular state in the cycle s and $\pi^{(0)}$ is the initial distribution.

Let V denote the *r.v.* that indicates the number of cycles required to identify N tags. Its CDF is:

$$Pr[V \leq K] = \pi_N^{(K)} \tag{3.27}$$

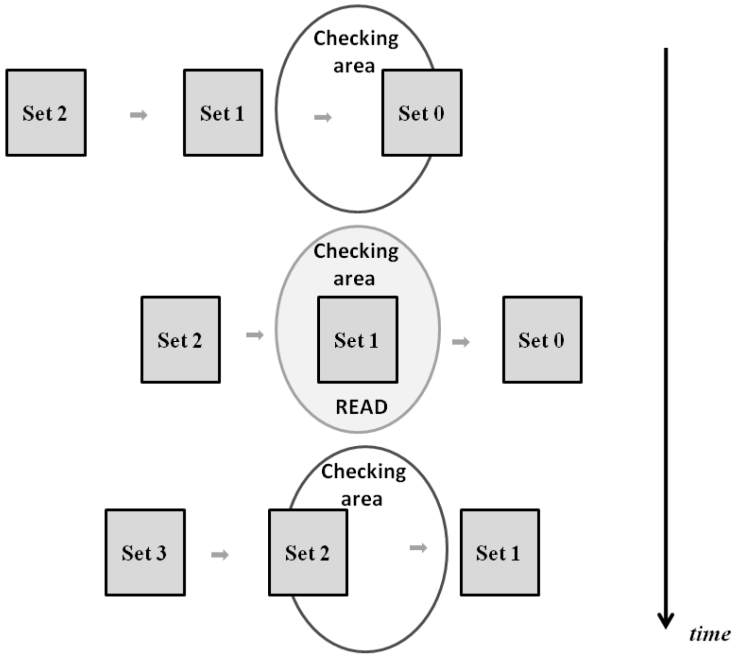

Figure 3.5: Typical identification process in semi-static scenario

The previous expression is the *Cumulative Distribution Function* (CDF) of *r.v.* V. The CDF provides the ICL for a given cycle. It has been evaluated using the Montecarlo method in Matlab. Different sets of tags are considered, from 10 to 100 tags. We compute the average number of cycles required to identify each set of tags and the number of cycles needed setting ICL=0.99 (99$\%$) for K=16. Figure 3.6 shows the results.

Figure 3.7 shows the CDF of the *r.v.* and the mean number of unidentified tags obtained for N=100 and K=16. There is a remarked point where the probability of identifying 100 tags in 120 cycles is 55$\%$, or, in other words, if the time in coverage is set to 120 cycles, 45$\%$ of tags will be unidentified.

This result demonstrates that, if the mean identification time is used as the configuration parameter for the sojourn time, some tags can leave the coverage area unidentified. Hence, instead of the mean identification time, ICL must be used as the parameter to configure the sojourn time.

Figure 3.8 shows a comparative using ICL=0.99 as criterion to select the time in coverage. The experiment has setting K=16 and the population range from 10 to 100 tags. If the mean identification time is used as time in coverage, the number of unidentified tags grows as the population grows; whereas the number of unidentified tags with ICL is almost negligible.

3.3.2 Population Splitting strategy

The aim of this section is to study how the size of the sets of tags in coverage (*e.g.* number of tags in each pallet) influences the identification process performance. Specifically, if

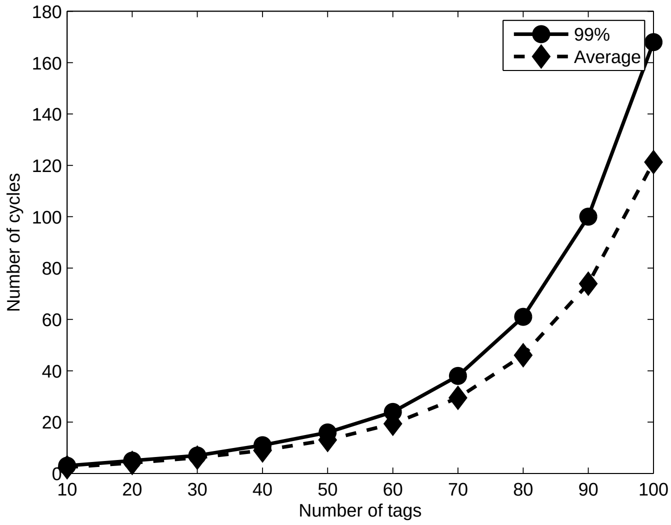

Figure 3.6: Identification time (cycles) for different tag populations and K=16

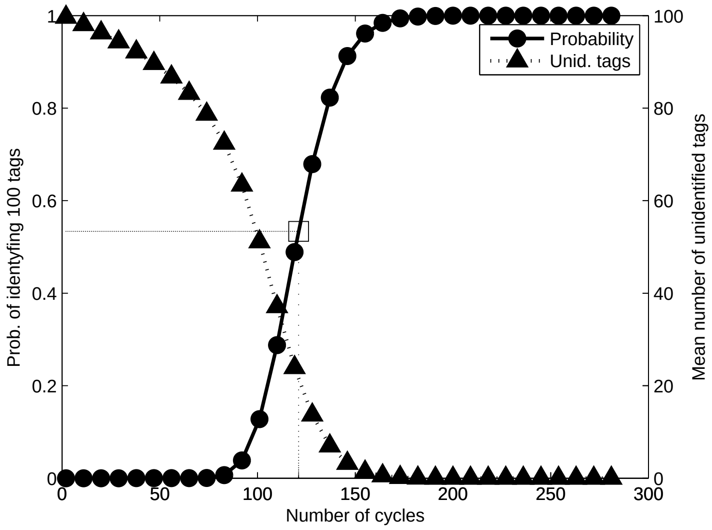

Figure 3.7: CDF with N=100 and K=16

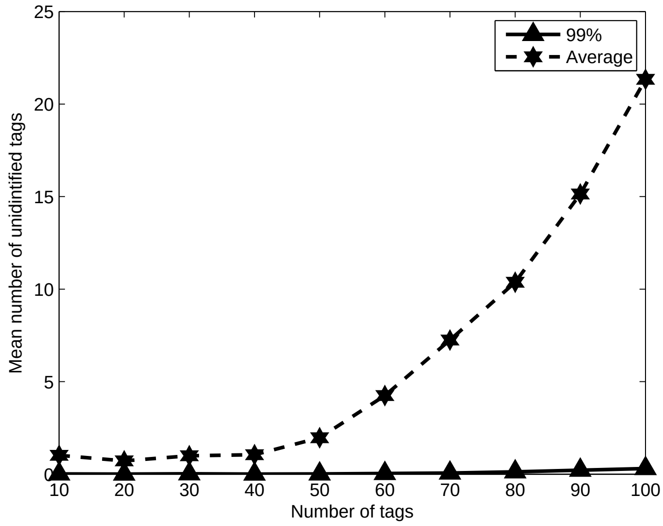

Figure 3.8: Mean number of unidentified tags with K=16

splitting the tags in smaller subsets may reduce the overall identification time. The results can help to decide, for instance, whether it is better to read one set of 400 tags, read 2 sets of 200 tags, read 4 sets of 100 tags, etc. We compute the identification time for a set of N tags and also for the same number of tags, but redistributed into J smaller subsets of $\lceil \frac{N}{J} \rfloor$ tags.

Figures 3.9 and 3.10 show the effect of subdividing the population comparing the CDF of the identification time. Figure 3.9 shows the CDF of the reading time and Figure 3.10 shows the cycles required for a reading time selected with the ICL criterion, the probability of identifying a single population of N=400 tags, and the same population divided into 2 sets of 200, 4 sets of 100 and 8 sets of 50. Every time the population is split, the number of cycles to identify the total population decreases. Figure 3.10 shows the total number of cycles/slots to identify a population of 400 tags, setting ICL=0.99 and K=$\{8, 16, 32, 64, 128\}$. Results demonstrate that with K=16, subsets of 50 tags are the best option, but it is possible to use subsets of 100 tags. If K=32, the difference between subsets of 50 and 100 tags is almost negligible, but better than using subsets of 200 tags. Setting K=64 and K=128 shows that the difference between subsets is negligible as well.

3.4 Identification process in dynamic scenarios

These scenarios are characterized by an incoming flow of tags entering the coverage area of a reader, moving at the same speed (*e.g.*, modeling a conveyor belt). We consider that new tags can enter the workspace *although another group of tags are still being identified*. For this type of systems, the performance analysis must be focused on the *Tag Loss Ratio* TLR. As we introduced in the previous scenario, TLR is the ratio of unidentified tags in the identification process. Depending on the final application, even a low TLR (*e.g.* TLR=10^{-3}) may be disastrous and cause thousands of items lost per day. In this section,

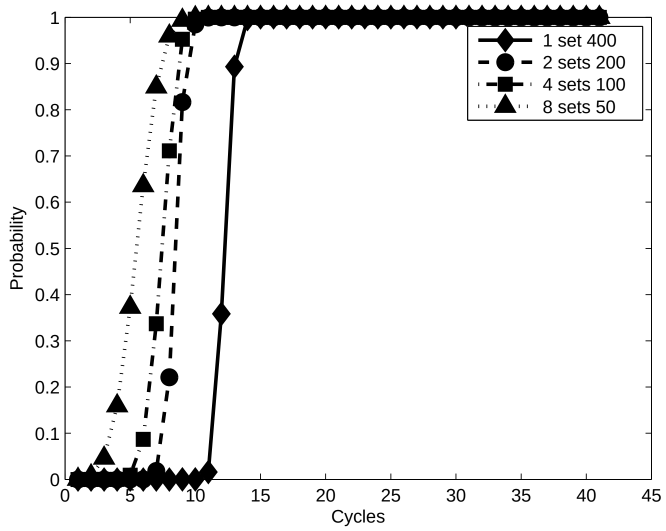

Figure 3.9: Comparison of reading time CDF for N=400, K=128

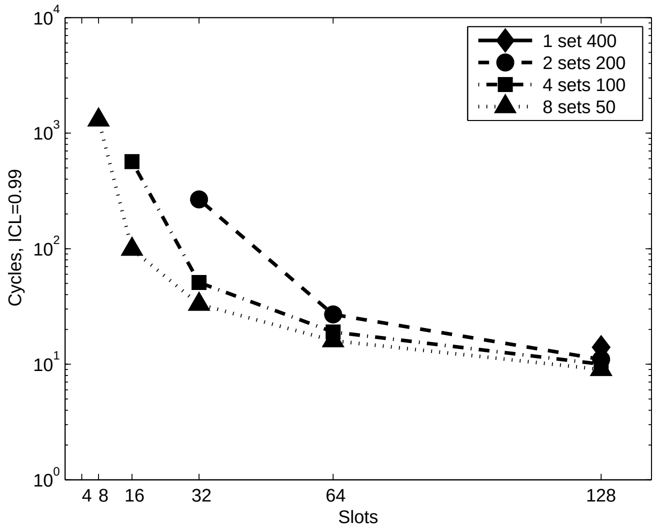

Figure 3.10: Number of cycles for ICL=0.99 and N=400 and its subsets

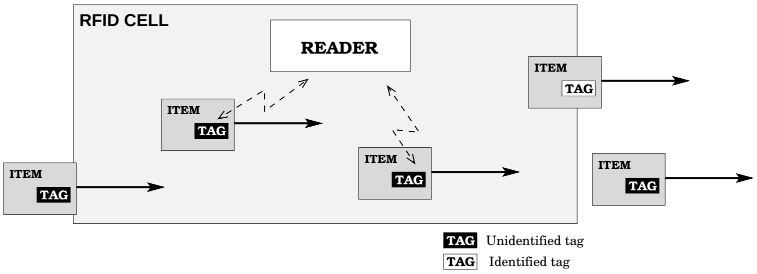

Figure 3.11: RFID cell with tag traffic

the TLR is computed for a RFID scenario similar to the one depicted in Figure 3.11. The analysis has been addressed by DTMC. Before addressing the analysis we introduce the notation and conventions used: a row vector is denoted as $\vec{V}$, the *i*-th component of a vector is denoted $(\vec{V})_i$, and $\sigma(\vec{V})$ denotes the sum of the values of the components of a vector $\vec{V}$. For the sake of simplicity, let us assume tags remain S complete cycles in the reading area. Then, once a tag enter the coverage area, it should be identified in the following S identification cycles. Otherwise (if it reaches the cycle $S+1$), tag is lost.

A truncated Poisson distribution, with parameter λ, has been selected as the tag arrival process in the system. That is, the probability that t tags arrive in a time slot is given by:

$$a(t) = \frac{(\lambda)^t}{t! \sum_{i=0}^{H} \frac{(\lambda)^t}{i!}} \tag{3.28}$$

For $t = 0, \ldots, H$, being H the maximum number of tags entering per cycle. The former assumptions allow to express the dynamics of the system as a discrete model, evolving cycle by cycle, such that,

- Each tag is in a given reading cycle in the set $[1, \ldots, S]$
- After a cycle, identified tags withdraw from the identification process.
- After a cycle, each tag unidentified and previously in the *i*-th cycle moves to the (*i+1*)-th cycle.
- If a tag enters cycle $S+1$, it is considered out of the range of the reader, and, therefore, lost.
- At the beginning of each cycle, up to H new tags are assigned to cycle 1, following a truncated Poisson distribution.

For any arbitrary cycle, the evolution of the system to the next cycle only depends on the current state. Thus, a DTMC can be used to study the behavior of the RFID system. Next section describes this model.

3.4.1 Markovian analysis

Based on previous considerations, the system can be modeled by a homogeneous discrete Markov process X_s, whose state s pace is described by a vector $\vec{E} = e_1, \ldots, e_{S+1}$, where each $e_j \in [0, \ldots, H]$, representing the number of unidentified tags in the ***j***-th cycle. Figures 3.12 and 3.13 illustrate the model. They describe the state of the system for two consecutive cycles, showing tags entering and leaving the system. Therefore, e_j is the number of tags which are going to start their ***j***-th identification cycle in coverage. e_1 component also represents the number of tag arrivals during the identification cycle (which do not contend since they have not received a *Query* packet yet). Finally, component e_{S+1} indicates the number of tags lost at the end of the identification cycle, since tags leave coverage area after $S+1$ cycles.

In addition, let us define the mapping Ψ an enumeration of the possible number of states, defined as:

$$\begin{aligned} \Psi :& [0, \ldots, H] \times {}^{(S+1)} \times [0, \ldots, H] \rightarrow [1, \ldots, (H+1)^{S+1}] \\ & \vec{E} = \{e_1, e_2, \ldots, e_{S+1}\} \rightarrow \Psi(\vec{E}) = 1 + \sum_{j=1}^{S+1} e_j H^{j-1} \end{aligned} \tag{3.29}$$

This allows defining ***i***-th state in our model as the state whose associated vector is given by $\Psi^{-1}(i)$. Let us denote $\vec{E}_i$ as the vector associated to ***i***-th state, ***i.e.***, $\vec{E}_i = \Psi^{-1}(i)$. Finally, let $e_{i,j}$ denote the ***j***-th component of the $\vec{E}_i$ state vector. The goal is to describe the transition probability matrix P for the model, from every state i to another state j. The stationary state probabilities are computed as $\vec{\pi} = \vec{\pi}P$. Let us denote λ_j as the average incoming unidentified tags to cycle j, which can be computed as:

$$\lambda_j = \sum_{i=1}^{(H+1)^{S+1}} e_{ij}\vec{\pi}_i \tag{3.30}$$

Obviously, λ_i is the average incoming traffic in the system and λ_{S+1} is the average outgoing traffic of unidentified tags. Then, TLR can be calculated as:

$$TLR = \frac{\lambda_{S+1}}{\lambda_1} = \frac{\sum_{i=1}^{(H+1)^{S+1}} e_{i(S+1)}\vec{\pi}_i}{\lambda_1} \tag{3.31}$$

To build the transition probability matrix P let us define the auxiliary vectors $\vec{L}_i$ and $\vec{U}_i$ as:

$$\begin{aligned} \vec{L}_i &= \{e_{i1}, \ldots, e_{iS}\}, \\ \vec{U}_i &= \{e_{i2}, \ldots, e_{i(S+1)}\} \end{aligned} \tag{3.32}$$

That is, the $\vec{E}_i$ state vector without either the last or the first component. Let us define the outcome vector as:

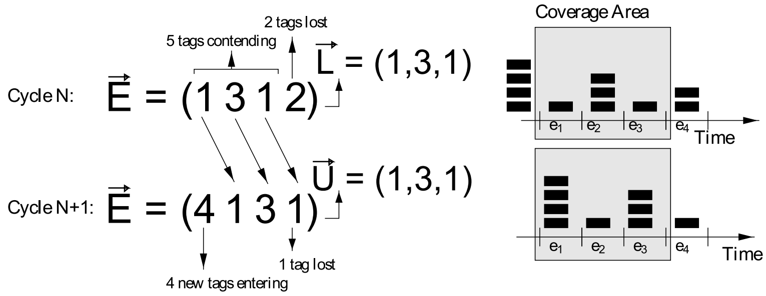

Figure 3.12: Representation of a state transition. Case 1: No identification

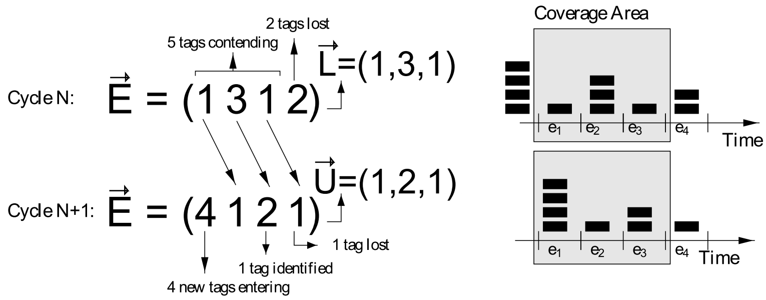

Figure 3.13: Representation of a state transition. Case 2: Identification

$$\vec{O}^{ij} = (\vec{L}_i - \vec{U}_j) = \{o_1^{ij} \dots o_S^{ij}\} = \{e_{i1} - e_{j2}, \dots, e_{iS} - e_{j(S+1)}\} \tag{3.33}$$

Figures 3.12 and 3.13 graphically show this computation. To construct the transition matrix let us define the function $id(i, j)$ that operates on an outcome vector $\vec{O}^{ij}$ providing the number of identified tags in a transition from a state i to a state j, *i.e.*:

$$id(i, j) = \vec{O}^{ij} \cdot \vec{1}^{\text{t}} \tag{3.34}$$

Note that for $\vec{E}_i$ and $\vec{E}_j$, if $e_{iz} < e_{j(z+1)}$ for some $z = 1, \dots, S$, such transition is impossible (new tags cannot appear in stages different from stage 1). These impossible transitions will yield $id(i, j)$ providing a negative value. Besides, let us define the *r.v.* $d(K, N)$ indicating the number of contention slots being filled with a single tag. The *mass probability function* of $d(K, N)$ has been computed in [Vogt02] (see equations (3.1) and (3.2)). Henceforth, $Pr\{d(K, N)\}$=k is denoted as $D_k(K, N)$.

Using FSA, up to K tags may be identified in a single identification cycle. Therefore, possible cases range from $id(i, j)$=0 to $id(i, j)$=K. The probability of $id(i, j)$ successful identifications is uniformly distributed among the contenders, whose distribution depends on the particular state, and hence the transition probability. From equations (3.1) and (3.2) and the previous definitions, the transition matrix P is computed as follows:

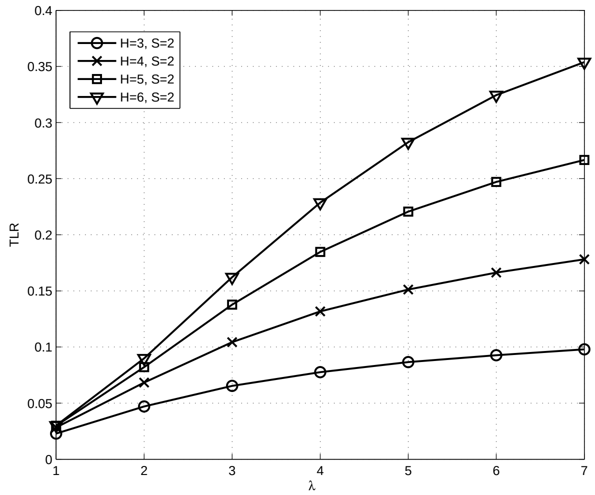

Figure 3.14: TLR results for FSA with 8 slots and Poisson arrivals. S=2, and H=3 to H=6

$$p_{i,j} = \begin{cases} a(e_{j1})D_0(K,N) & , id(i,j) = 0 \\ a(e_{j1})\frac{\Pi_{z=1}^{S}\binom{e_{iz}}{o_z^{ij}}}{\binom{N}{id(i,j)}} D_{id(i,j)}(K,N) & \text{, if } id(i,j) \in [1,K] \\ 0 & \text{, otherwise} \end{cases} \tag{3.35}$$

3.4.2 Experimental evaluation: a postal mail control system

From a practical point of view, TLR evaluation may become critical in some realistic scenarios. As an example, this section evaluates a postal mail control system, where mails are carried over conveyor belts for distribution, with an attached tag. Two configurations for the mail sojourn times of $S = 2$ and $S = 3$ identification cycles have been considered, for a frame length of $K = 8$ slots. The slot time is assumed to be 4 ms based on parameters shown in Table 3.2. Therefore, the sojourn time is around 64 ms for $S = 2$ and 100 ms for $S = 3$. λ range spans from 1 to 7. Results are provided in Figures 3.14 and 3.15.

As expected, for a fixed S, TLR increases as the maximum number of arrivals H increases. In addition, for the parameters analyzed, keeping fixed H decrements TLR if S grows, because there are more opportunities for identification. For example, the maximum number of tags in the system for H=6 and S=2 is 12 tags, whereas for H=6 and S=3 there might be up to 18 tags. The main issue of the previous analysis is that it becomes computationally unfeasible for moderate values of H and S. In this case, simulation is mandatory. Figure 3.16 shows simulations performed for $\lambda = [10, \ldots, 60]$ and $H = [3, 6]$. In this case, envelopes sojourn time is close to 800 ms. We can observe that, if we set H=3, TLR reaches 10^{-4} and does not vary, irrespective of the λ value. On the other hand, with H=6, the TLR reaches up to 10^{-3}. It means that, one out of

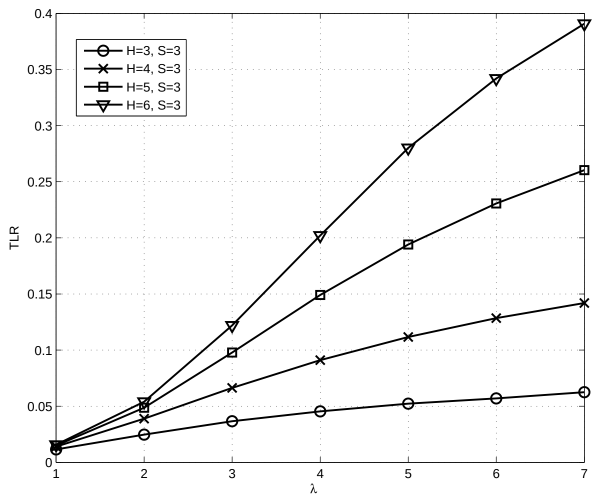

Figure 3.15: TLR results for FSA with 8 slots and Poisson arrivals. S=3, and H=3 to H=6

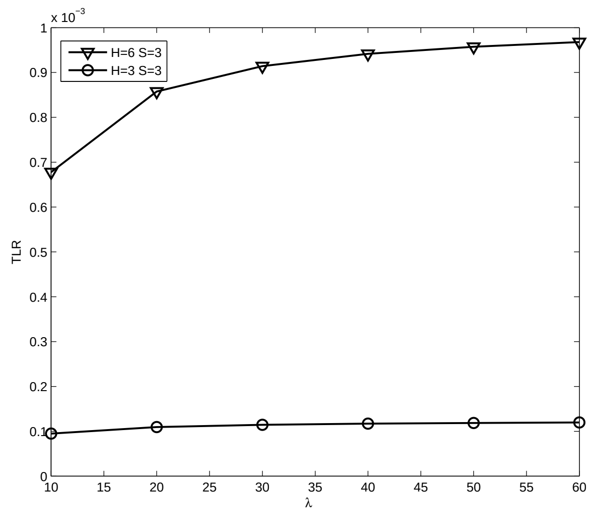

Figure 3.16: TLR results for FSA with 64 slots and Poisson arrivals, S=3 and H=3, H=6

Optimal Q	n range without CE	n range with CE $q = 0.5$
0	$n = 1$	$n = 1$
1	$1 < n \leq 4$	$1 < n \leq 4$
2	$4 < n \leq 8$	$4 < n \leq 9$
3	$8 < n \leq 19$	$9 < n \leq 22$
4	$19 < n \leq 38$	$22 < n \leq 46$
5	$38 < n \leq 85$	$46 < n \leq 100$
6	$85 < n \leq 165$	$100 < n \leq 202$
7	$165 < n \leq 340$	$202 < n \leq 405$
8	$340 < n \leq 720$	$405 < n \leq 820$
9	$720 < n \leq 1260$	$820 < n \leq 1675$
10	$1260 < n \leq 2855$	$1675 < n \leq 3360$
11	$2855 < n \leq 5955$	$3360 < n \leq 7540$
12	$5955 < n \leq 12124$	$7540 < n \leq 14420$
13	$12124 < n \leq 25225$	$14420 < n \leq 27990$
14	$25225 < n \leq 57432$	$27990 < n \leq 59925$
15	$57432 < n$	$59925 < n$

Table 3.3: Optimal Q versus n ranges with and without Capture Effect (CE)

a thousand envelopes will be lost, showing the impact on the final system. In short, last section allows the evaluation of TLR for different protocol parameters, such as the number of slots, the arrival process, the time in coverage (conveyor belt velocity), etc.

3.5 Optimal Q Configuration

As seen in the previous sections, the identification performance depends on the number of tags competing and on the frame length. The best throughput is achieved when there are as many competing tags as slots in the frame, N=K, yielding a maximum throughput of $\frac{1}{e} \approx 0.36$ [Schou83]. However, for EPC-C1G2, K can not be set to any arbitrary natural number, but to powers of two, *i.e.* K=2^Q, for $Q \in [0, \ldots, 15]$.

The optimal Q can be computed to achieve the maximum throughput in both types of readers. In readers with fixed frame length procedure, we cannot set K=N per cycle to reach the maximum throughput because K is fixed. However, we can compute the Q value that provides the minimum identification time when a population of N tags is in coverage. Note that minimizing the identification time in this scenario is equivalent to maximizing the throughput of the whole identification procedure, rather than the individual throughput per cycle. For every Q value, we have computed the minimum and maximum value of N that permits to reach the maximum throughput [Bueno09b]. Figure 3.2 shows the results, and Table 3.3 summarizes them. The optimal Q for readers with variable frame length procedure was introduced in the previous chapter.

3.6 Conclusions

In this chapter we have characterized the EPC-C1G2 identification procedure. The analysis was carried out for typical scenarios such as traceability, inventory control, conveyor belts, etc. in static, semi-static and dynamic scenarios. In static scenarios the mean identification time is the metric of interest, as well as the throughput. Both have been computed in this chapter, considering also the Capture Effect phenomenon. On the other hand, in semi-static scenarios the sojourn time must be related to the *Identification Confidence Level* (CICL). Given a target ICL, we provide the optimal configuration criteria. Moreover, we have studied the benefits of splitting blocks of tags into subsets. In some scenarios this procedure reduces the mean identification time. Finally, dynamic scenarios, reducing *Tag Loss Ratio*(TLR) are mandatory as well. Expressions which relate the system configuration and the incoming traffic of tags with the TLR have been obtained.

Chapter 4

RFID schedulers in passive Dense Reader Environments

Passive RFID is increasingly being used to identify and track objects in supply chains, manufacturing processes and product traceability. In these scenarios, the readers are placed in strategic places creating checking areas. Tags enter and leave the checking areas trying to send back their identifiers to the readers. The size of a checking area depends on the reader transmission power. In Europe, the maximum value of this parameter is 2 Watts [ETSI302]. This limits the maximum distance from the tag to the reader systems (reader-to-tag range) up to 10 meters and may produce reader-to-reader interferences up to 1000 meters (considering the Building Propagation Model) [Leong05]. In some installations, a single reader is not enough to cover a specific identification area, or simply the final application requires the existence of more than one identification gate. In these scenarios several readers are required; the so-called *Dense RFID Reader Environments* (see Figure 4.1). The performance in Dense RFID systems is negatively affected by two types of collisions: *Reader to Tag Collisions* (RTC) and *Reader to Reader Collisions* (RRC).

Current European standards and regulations [EPCgl05][ETSI302] propose some solutions to reduce collision issues, but exclusively focused on minimizing RRC. Besides, some works deal with minimization of RTC, but without considering RRC or assuming they do not happen [WangD06][KimJ07][ChenN09]. Other proposals considering both type of collisions do not make an efficient use of the network resources, require additional hardware or are not even compatible with the current standards [Shail05][Kwang06].

In this chapter we review the European regulations and related works. The performance of the different mechanisms is studied for common reference scenarios in order to

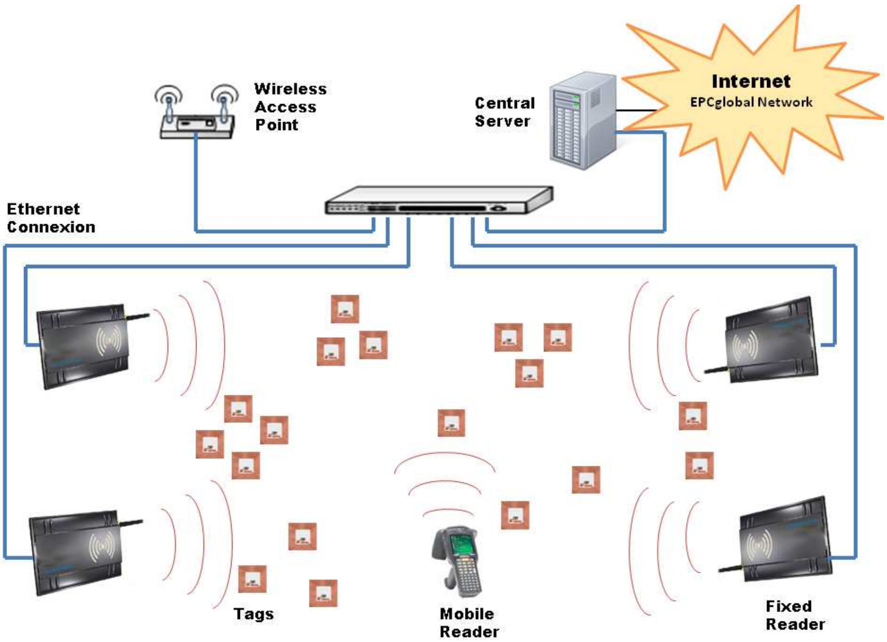

Figure 4.1: Example of Dense RFID Environment

provide comparative results of efficiency and network usability. The drawbacks extracted from the previous comparison help us to suggest the key properties to design an efficient scheduler.

4.1 Reader Collision Environments. Problem description

A dense reader environment is a RFID system composed by two or more fixed or mobile readers. Typically, these readers are connected to a central device (server) by means of a wired (Ethernet) or wireless network (*e.g.* WLAN or 3G). They are continuously monitoring tags within their reading range. As we stated in the introduction, the output transmission power (P_R) delimits the reader ranges. If the readers ranges overlap, collisions occur. Dense reader environments are susceptible to the following *Reader Collision Problems*:

- *Reader-to-Tag Collisions* (RTC) occur when two or more readers overlap their reader-to-tag ranges and try to read the same tag simultaneously. In Figure 4.2 if R and $R^{'}$ try to read tag A simultaneously, A receives electromagnetic energy from both readers. This is a source of RTC, even if both readers are operating at a different frequency. Since tag A is a passive device, it is unable to select a particular reader/frequency to transmit its data.

- *Reader-to-Reader Collisions* (RRC) arise if the reader receives signals from neighbor readers interfering with the weak signal from a tag and hindering identification. In Figure 4.2 if R reads data from tag B and, at the same time, $R^{'}$ sends data to tag C, $R^{'}$ interferes with R.

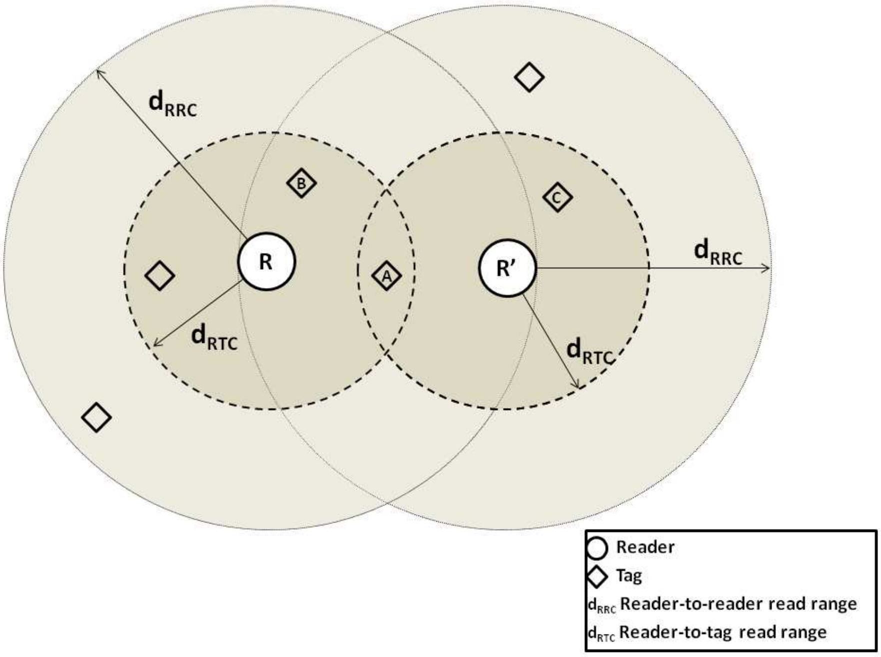

Figure 4.2: Reader Collision Problems

P_R determines the boundaries of RTC and RRC as follows:

- If two or more readers are within two times, the reader-to-tag range (d_{RTC}) either part or the whole reading area overlaps, preventing tags operation. Hence, both RTC and RRC are present. In this case, the readers operation should be allocated at different working times.
- If the distance among readers is larger than d_{RTC} and shorter than d_{RRC} only RRC occurs. The readers operation can be multiplexed either in frequency or in time.
- If distance among readers is larger than maximum d_{RRC}, they will not suffer any collisions.

Table 4.1 summarizes the distance ($d_{i,j}$) between two readers, i and j, and the concurrent operation possibilities.

4.2 Related works

This section is divided into two parts. First, the EPC-C1G2 [EPCgl05] and ETSI EN 302 208 regulation [ETSI302] applicable to passive Dense RFID systems are described. Then, a comprehensive set of existing research proposals found in the literature is reviewed. These are commonly based on variations of the classical FDMA and TDMA techniques (see Chapter 1). CDMA techniques are of difficult application in passive RFID systems, since they require more complex circuitry in the tags. At the end of the Section, Table 4.2 summarizes and categorizes the main aspects of the schemes introduced.

	Frequency =	**Frequency $\neq$**
Time slot =	$d_{i,j} > d_{RRC}$	$d_{i,j} > d_{RTC}$
Time slot $\neq$	Any distance	Any distance

Table 4.1: Restrictions to multiplexation of the readers

4.2.1 Regulations and Standards

The deployment of passive Dense RFID systems is affected by the recommendations and definitions included in two standards: the EPC-C1G2 and ETSI EN 302 208. ETSI EN 302 208 [ETSI302] regulation defines 15 work frequencies. In Europe only 10 channels are available, while the remaining five are used as guard bands. The regulation recommends that each reader selects a channel randomly and listens to it during a prefixed time, following the *Listen Before Talk* (LBT) strategy. If the channel is free, the reader occupies it for up to 4 s. After this time, the channel must be free for at least 100 ms. This mechanism is intended to mitigate the effects of RRC. In its turn, EPC-C1G2 defines a procedure to coordinate a dense RFID reader environment, using the 10 work frequencies defined in the ETSI EN 302 208 regulation. In EPC-C1G2 readers must operate in even-numbered channels and tag responses must be allocated in odd-numbered channels. Hence, only 5 channels are available for readers. Readers randomly alternate among these 5 channels using the *Frequency Hopping Spread Spectrum* (FHSS) technique. In contrast to ETSI EN 302 208 recommendation, in EPC-C1G2 readers do not listen to the channel before accessing to it. Therefore, the system is still vulnerable to RRC when two readers select the same operating frequency at a given time. In addition, this technique does not eliminate the RTC collisions. A tag in range of two or more readers at different frequencies may be energized from all of them at the same time. Despite its drawbacks, EPC-C1G2 is *de facto* standard for passive Dense reader environments.

4.3 Research proposals

In this section the most relevant research proposals for coordinating the readers in passive dense RFID systems are reviewed, emphasizing their requirements, problems and incompatibilities with EPC-C1G2. Since these mechanisms are commonly classified into centralized and distributed, we follow this taxonomy to review them. Table 4.2 compares their relevant characteristics.

4.3.1 Centralized Mechanisms

Centralized mechanisms are designed to be executed in a centralized device (server), which is connected to the readers through a wired or wireless network (see Figure 4.1). The server controls the reader's synchronization and manages the network resources, sharing them among readers.

In [WangD06] the authors propose the use of a non commercial hardware as a centralized server which coordinates the resources (only one channel, instead of five or ten, like in the standard [EPCgl05]) and also manages the reader-to-tag communication through a technique that multiplexes the reader request to specific tags. This technique is not compatible with the current standard. Besides, the proposed multiplexing technique involves the readers have to share tags information among adjacent readers. The authors also assume RRC do not happen in their simulations.

In [Harri60] the authors propose a centralized server to distribute the frequencies among the readers in a pure FDMA scheme so that readers which are closer allocated frequencies more separated from each other. Since no TDMA technique is included, RTC is not eliminated. The authors assume that there are as many frequencies as readers, without considering the frequency restrictions of the standard and regulations. They also suggest reducing the reader output power to decrease the collisions. Obviously this recommendation reduces the size of the checking areas. This is not possible in many real systems where the identification region is strictly defined.

In [KimJ07] the authors propose a similar approach, consisting of controlling the reader output power optimally in order to reduce the RTC (but not considering RRC).

In [ChenN09] readers are supposed to share a unique frequency channel and apply a TDMA technique to coordinate the readers. The mechanism controls in real-time the overlapping of the reader-to-tag read ranges. Then, it decides to disconnect the interfering readers to reduce RTC. Needless to say, this scheme can only be applied to those scenarios which admit the disconnection of a set of the reader systems.

4.3.2 Distributed Mechanisms

In these schemes, the readers communicate directly with their neighbors -usually by means of wireless links- and do not rely on a centralized device to make the allocation of the network resources.

In [HsuCH07] a decentralized mechanism called *Leo* is proposed. In *Leo* each reader detects the maximum number of neighboring redundant readers that can safely be turned off to minimize RTC, preserving the original network coverage, in a manner similar to the OSPF (*Open Shorter Path First*). This is done before running the RFID identification process. In this approach, both tags and reader positions must be known, making a real implementation difficult. Besides, mobile readers are not contemplated.

Pulse [Shail05] is a protocol based on LBT (or CSMA) that makes use of an auxiliary control channel. Readers can listen simultaneously to the control and the reading channel, but only transmit in one of them. Before powering the tags, readers check if any neighbor reader is on. When a reader is activated, it continuously transmits beacons in the control channel before the tag reading process takes place. After a guard period without transmissions in both channels, the reader occupies the control channel filling it with beacons, and shortly afterwards it starts the tag reading process.

In [LiuL08] a similar mechanism is suggested, but only for minimizing RRC, whereas [SungK06] introduces another LBT aimed at minimizing RTC. In the latter, a wireless sensor network is selected for reader-to-reader communications. This network is not used for sensing particular parameters, thus resulting in extra costs.

The previously described proposals [LiuL08, SungK06] only consider a single reading channel, instead of five or ten, as in the European regulations and standards. *DiCa*

[Kwang06] is another single channel distributed algorithm based on LBT, and focused on RTC reduction. It proposes to use a control channel which doubles the range of the reading channel. When a collision with another reader is detected, *DiCa* decreases both channels ranges proportionally. Authors claim that this is an energy saving system. However, since the readers' energy consumption has a minor impact on system operation costs, it is questionable if the energy cost reduction obtained compensates the performance loss and extra hardware complexity.

MCMAC [DaiH07] is a multi-channel LBT strategy combined with FDMA. In a MCMAC system with R readers, R-1 non-overlapping channels for reading and one control channel are used. The control channel is used to distribute the reading channels by means of a random access competitive algorithm. Although this approach can mitigate the effects of RRC, it does not solve the RTC. Besides, if the number of readers (R) is higher than the number of channels (N), MCMAC delays the operation of R-N-1 readers.

Colorwave [Waldr03] is based on a TDMA scheme for mitigating RTC. Time-slots for performing the tag reading process are randomly selected by the readers. Colliding readers repeat the process, since RTC makes tag identification impossible.

HiQ [HoJ06] is a hybrid mechanism (centralized and distributed) that provides a solution to minimize the RTC. It is based on the discovery of collision patterns among readers. Readers measure the instants of collision and broadcast this data, as well as the own channel and time period used, to adjacent readers via a common control channel. Then, each reader computes the best time period and channel for its next reading cycle using an artificial neural network, and each transmits this information to a global server, which arbitrates among readers.

The main drawback of this approach is that readers have to manage a large amount of information, and the results depend on the quality of the neural network training.

Table 1 summarizes the main features of the existing proposals for coordinating RFID readers in dense RFID environments. As shown, proposals that alleviate RTC and RRC effects are scarce and difficult to adapt to the standard.

4.4 Performance Evaluation

The proposals introduced in the previous section can be evaluated using different metrics: detection of redundant readers, number of successful *Query* packets transmitted by the readers (see Chapter 2), throughput (defined as the ratio of successful *Query* packets vs. total *Query* packets sent), reader-to-reader and reader-to-tag collision probability, etc. These metrics are aimed at measuring the mitigation of RRC and RTC. Indeed, the schedulers have to share the resources available efficiently in order to maximize the tags identified per slot. Therefore, we introduce two new metrics to evaluate the schedulers:

- The *Efficiency* (γ), defined as the ratio of resources free of RTC and RRC to the total resources demanded by the readers.

- The *Usability* (μ), defined as the ratio of resources allocated free of RTC and RRC to the total resources available.

	Criterion													
	Minimize RTC	Minimize RRC	Centralized	Distributed	Control Channel	FDMA	TDMA	CSMA	Switch off readers	Readers P_{out} variation	Fixed Readers	Mobile Readers	Extra Hw.	Standard Compatibility
EPC [EPCgl05]		•		•		•					•	•		•
ETSI [ETSI302]		•		•		•		•				•		•
Wang. [WangD06]	•		•		•						•		•	
Harr. [Harri60]		•	•			•				•	•	•	•	
Kim. [KimJ07]	•			•	•					•	•	•	•	
Chen [ChenN09]	•		•						•					•
Hsu [HsuCH07]	•			•					•		•			
Shail [Shail05]	•	•		•	•			•			•	•	•	
Liu [LiuL08]		•		•	•			•				•	•	
Sung [SungK06]	•			•	•							•	•	
Kwang. [Kwang06]	•	•		•	•			•		•		•	•	
Dai [DaiH07]		•		•	•	•		•			•	•	•	
Waldr. [Waldr03]	•			•			•				•	•	•	
Ho [HoJ06]	•		•	•	•	•	•				•		•	

Table 4.2: Comparison of Reader Collision Solutions

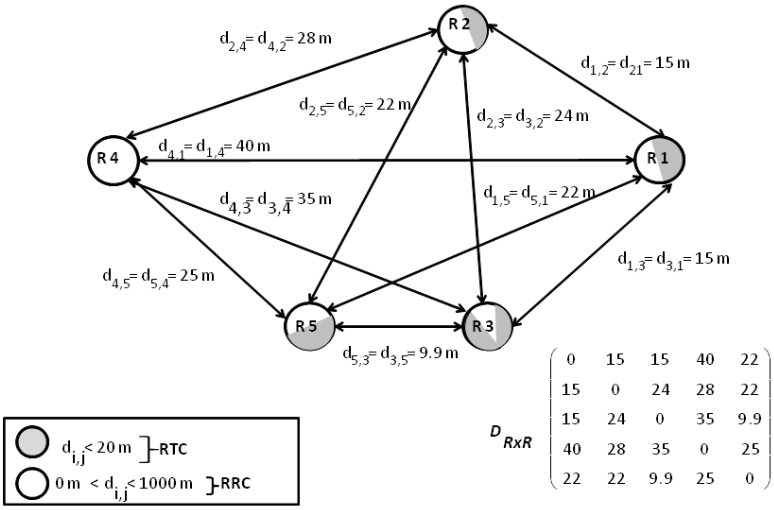

Figure 4.3: Initial simulation scenario

4.4.1 Scenario description and considerations

Let us consider an initial dense reader environment with R=5 fixed readers (as depicted in Figure 4.3). The relative distances among readers are given in matrix D_{RxR}, measured in meters (*e.g.* $d_{2,4}$ is the distance from reader 2 to reader 4). Every reader transmits at the maximum output power permitted in Europe, P_R= 2 W. This value determines reader coverage area, and the overlapping distances caused by RRC and RTC, denoted as d_{RRC} and d_{RTC}, respectively.

The resources available for allocation in the scenario are the number of reading sub-channels, F, and the number of time-slots in each sub-channel, S time-slots. Hence, each frequency is a super-frame with S slots available. The total resources available for allocation in the scenario is given by Z parameter. If all the readers in the system are placed within the d_{RRC} distance, Z is computed as follows:

$$Z = S \cdot F \tag{4.1}$$

Otherwise, they can share the same frequency and slots (*i.e.* there is spatial reuse), then,

$$Z = S \cdot (F + C(d_{RRC} - 1)) \tag{4.2}$$

Where $C(d_{RRC})$ denotes the number of clusters of readers as a function of distance d_{RRC}, that is, the number of sets of readers with at least a reader separated more than

Parameter	**Definition**	**Value**
R	Readers in the workspace	$[5, 10, ..., 50]$
F	Frequencies available	5
S	Slots available per frequency	1600
T_s	Typical slot-length in EPC-C1G2	2.5 ms
P_R	Maximum Output Power in Europe	2 W
d_{RTC}	Maximum overlapping distance for RTC	20 m
d_{RRC}	Maximum overlapping distance for RRC	1000 m
r_i	Resources requested per reader i	$rnd(0.10S, S)$

Table 4.3: Simulation parameters

d_{RRC}. Note that neighbor clusters may share some readers. Indeed, if there is a single cluster, $C(d_{RRC})$=1, and equations 4.1 and 4.2 match. Other assumptions for the evaluation are:

- The RFID system is periodically reconfigured, every T=4 times, as in [ETSI302]. Hence, every frequency is a super-frame with a duration of 4 seconds. Since the duration of a slot in EPC-C1G2 is T_s=2.5 ms [EPCgl05], we assume this value to calculate the total number of slots available per frame (or frequency) $S = \frac{T}{T_s}$=1600.
- Every T times the readers detect the tag population in their coverage area and determine (following an internal procedure) the resources they need to identify the population (in number of slots).
- We assume the number of slots required by each reader i every T times is randomly and uniformly distributed in the interval $[0.10S, S)$.
- The number of resources (slots) free of RTC and RRC allocated to every reader i is denoted as $\beta_i \leq r_i$.

Then, the efficiency (γ) is given by next equation:

$$\gamma = \sum_{i=1}^{R} \frac{\beta_i}{r_i} \tag{4.3}$$

And the usability (μ):

$$\mu = \frac{\sum_{i=1}^{R} \beta_i}{Z} \tag{4.4}$$

Note that with an optimal scheduler and assuming that every reader i requests $\frac{Z}{R}$ slots, then γ=μ.

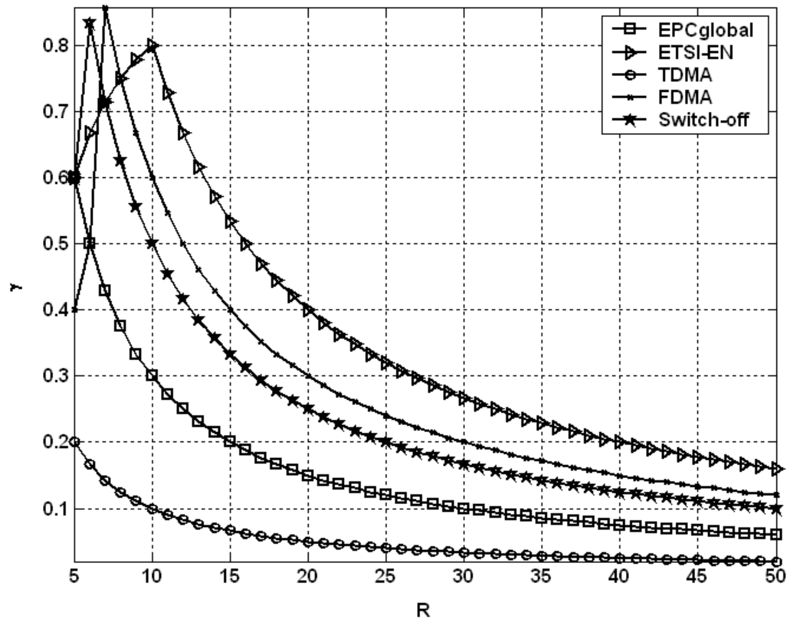

Figure 4.4: Efficiency vs. number of readers

4.4.2 Simulation Results

The scenario in consideration has been simulated in MATLAB using the Montecarlo method. We have considered the following schedulers (due to their feasibility):

- Switch-off interfering readers: [HsuCH07]
- Based on TDMA: [ChenN09][Waldr03][LiuL08]
- Based on FDMA: [DaiH07]
- Regulation: [ETSI302]
- Standard: [EPCgl05]

These proposals have been implemented and simulated in the scenario depicted in Figure 4.3, taking the parameters of Table 4.3. Note that the initial scenario consists of a single cluster with two separated sets at distance d_{RTC} :$\{R_4\}$ and $\{R_1, R_2, R_3, R_5\}$. In the evaluations, the number of readers increases up to R= 50, with each new reader at a distance between d_{RTC} and d_{RRC} of all the previous readers. The number of resources available is extracted from equation (4.1), and β_i and r_i are measured using the simulator. A time slot is considered collision-less if it is exclusively used by only one reader.

Figure 4.4 shows the resulting scheduler efficiency. Note that [ETSI302] and [EPCgl05] work at 10 and 5 frequencies, respectively. The rest of the schedulers have been set to F=5 (number of frequencies defined by the standard [EPCgl05]). The best scheduler efficiency is achieved by [ETSI302], only surpassed by FDMA [DaiH07] and switch-off [HsuCH07]

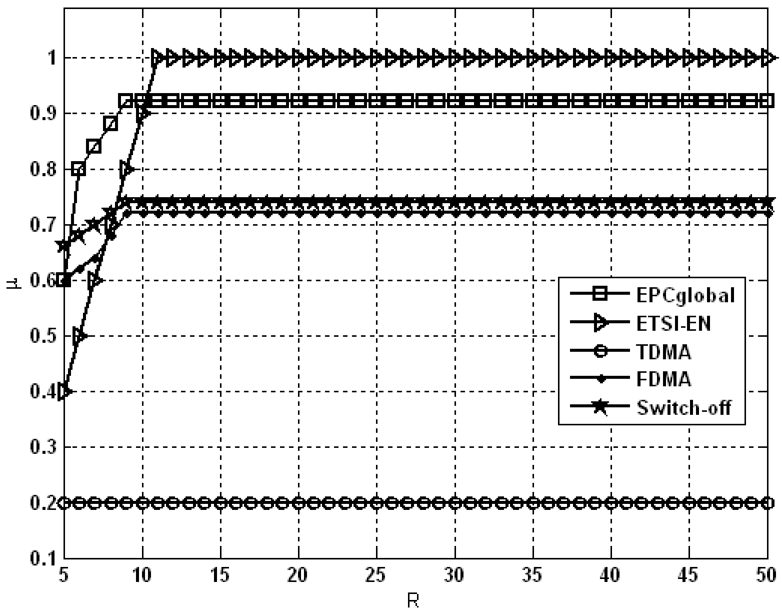

Figure 4.5: Network usability vs. number of readers

when R is lower than 8 and 7, respectively. Note that, although [DaiH07] shows a better response than [EPCgl05], its implementation in a real reader is not feasible because it uses an available frequency as control channel, not compatible with current standards. The worst efficiency is achieved by the proposals based on TDMA. This is because in this work we have studied the worst case, when a reader i requires r_i slots, it is allocated in a frequency and other readers can use it. In other cases the TDMA proposals will have a better response.

Figure 4.5 shows the resulting network usability per scheduler. In this case, the worst usability is achieved by TDMA, independently of the number of readers, because only one of the five available frequencies is occupied. [ETSI302] has a low usability when R<10 because the resources required is lower than the frequencies available ([ETSI302] sets F=10). When R>10, this scheduler has the best network usability. Standard in [EPCgl05] has a good usability but lower than regulation [ETSI302] because one of the available frequencies is used as control channel. In the results it can be easily checked that a high number of frequencies is mandatory when the number of readers is high, in order to obtain both a good efficiency and a good usability. However, since the number of available channels is limited, TDMA techniques must be used in coordination with frequency multiplexing.

4.5 Conclusions

In this chapter we have reviewed the Redundant Reader Problems and the solutions proposed by the current standard for passive RFID, the European regulation, as well as the related proposals. We have checked that, most of them are focused on reducing only one type of collision (RTC or RRC) but not both. Besides, most of the proposals require extra hardware in readers and/or tags, or are incompatible with current standards. We have evaluated the proposals compatible with the standards and the results have demonstrated that most of them have a low efficiency in scenarios with a high number of readers. The network usability of schedulers is also low, motivated by the exclusive use of FDMA or TDMA, but not the combination of both techniques. Hence, from the results we deduce that combining TDMA and FDMA could be a good strategy to improve the scheduler efficiency and the network usability. This approach requires that the scheduler solves, for each iteration, a mathematical problem to assign readers to frequencies and slots in order to minimize the Reader Collision Problems, with several constraints.

Chapter 5

Anti-collision protocols in active RFID systems

The anti-collision protocols for active RFID systems are studied in this chapter. Although the capabilities of active tags highly surpass those of passive counterparts, the basic identification procedure is similar. In this chapter, anti-collision methods which takes advantage of already available capacities in active devices are proposed: a non-persistent CSMA based on Sift [TayYC04] and a p-persistent CSMA. The former outperforms the current standards in terms of identification delay. The latter is a good strategy when the energy saving in active tags takes priority.

5.1 Introduction

Active RFID is an attractive technology in scenarios where passive technology limits implementation, *e.g.* product traceability with control of external factors: temperature, vibrations and cargo opening. Active tags have an autonomous power source and incorporate circuits with a microprocessor and a memory to read, write, rewrite or erase data from an external device, sensors, etc. The main advantage of active tags is the long reading distance, more than 100 meters.

In contrast to passive RFID, active RFID have attracted little academic attention in the topic of anti-collision procedures. The main reason for this lack of interest is that active tags do not present the hardware constraints of passive tags, and the anti-collision protocols can be more sophisticated. A typical active tag may use Bluetooth [Siege03] or IEEE

802.11 protocols or MAC protocols designed for WSN [Vales08b]. The battery power of these devices is enough to operate sensors and perform calculations. However, the cost of active tags is still too high for their massive adoption (see Chapter 1). Therefore, the options are either very simple approaches suitable for passive RFID, or very sophisticated proposals for active RFID.

Independently of the final application, both active and passive RFID must implement an anti-collision protocol for avoiding/handling collisions to ensure readers communicate with tags as quickly and reliably as possible, ensuring the whole tag population is identified. However, active RFID has an additional goal: to save energy in order to maximize the battery lifetime in active tags. Therefore, the tag identification problem deals with identifying multiple objects with minimal delay and power consumption, reliability, line-of-sight independence, scalability, etc.

As well as passive RFID, Aloha family protocols are practically the unanimous choice for active RFID anti-collision procedures, including the standards EPC-C1G2 [EPCgl05] and ISO/IEC 18000-7 [ISO03]. The former proposes the same FSA and DFSA procedures in both passive and active RFID (see Chapter 2). In the passive systems, EPC-C1G2 is the *de facto* standard. However, in active RFID EPC-C1G2 has not been introduced due to the lack of energy saving mechanisms. in contrast, the latter, ISO/IEC 18000-7, is widely deployed for active RFID and it proposes an anti-collision mechanism based on FSA which address the energy problem, turning off devices after successful identification. Besides, DFSA is suggested to adjust the contention frame length but no particular algorithm is endorsed, and ISO/IEC 18000-7 leaves the selection open to vendors. Most of the DFSA algorithms studied in Chapter 2 can be easily implemented in ISO/IEC 18000-7. The main problem of ISO/IEC 18000-7 protocol is its simple default identification procedure, similar to EPC-C1G2, which does not exploit the active tags capabilities to improve identification performance. For instance, carrier sense capabilities of active tags, which do not add any additional costs, would permit to operate CSMA seamlessly.

Hence, in this chapter we propose the use of non-persistent CSMA based on Sift [TayYC04] CSMA and p-persistent CSMA as anti-collision procedures for active RFID systems. On the one hand, the former is fully compatible with the standard. It is based on applying the quasi-optimal Sift distribution along with CSMA for active tag identification. We evaluated analytically the average identification time of this procedure and compared the results with the current ISO/IEC 18000-7 and EPC-C1G2 standard. The results reveal that the non-persistent Sift-based CSMA outperforms both procedures [EgeaE07a]. Moreover, it also scales much better, without the need for further adaptation mechanisms. On the other hand, a p-persistent CSMA approach is also considered for active RFID systems. This alternative allows noticeable energy savings since tags withdraw from contention in the very beginning of the slots, sleeping until next time slot, thus minimizing consumption.

Before addressing the non-persistent and p-persistent CSMA proposals, we describe the anti-collision procedure of ISO/IEC 18000-7 and the related works in the field.

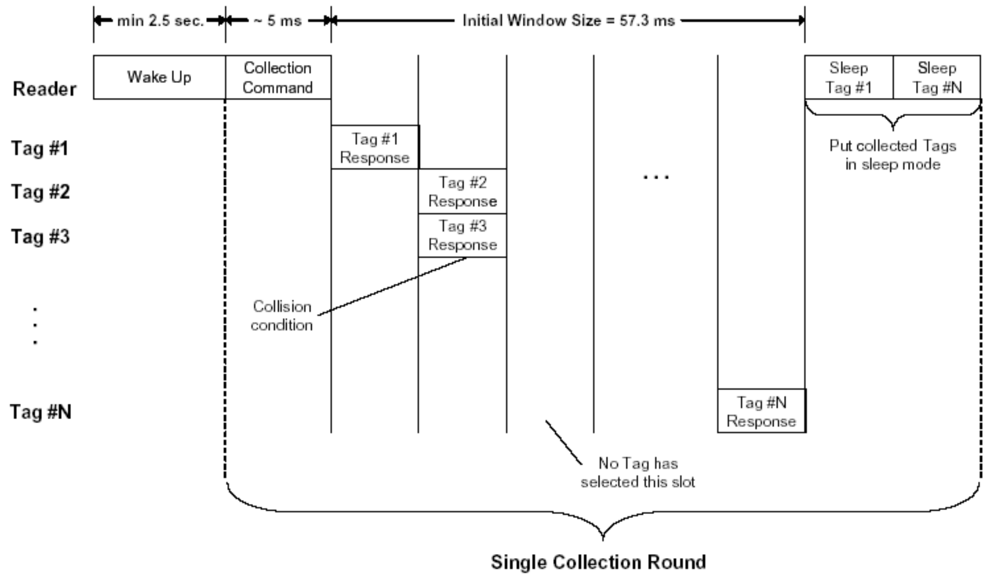

Figure 5.1: Anti-collision procedure of ISO/IEC 18000-7 (from [ISO03])

5.2 ISO/IEC 18000-7

ISO/IEC 18000-7 (or DASH7) is the *de facto* global standard for active UHF RFID solutions. As we introduced in Chapter 1, ISO/IEC 18000-7 was first used by the DoD in USA, and later consolidated in non military sectors. With the aim of improving ISO/IEC 18000-7 and extending its use, several RFID vendors, users and researchers formed the Dash-7 Alliance [Dash7], an independent industry action group whose purpose is to promote the use of ISO/IEC 18000-7 in active RFID technology.

ISO/IEC 18000-7 defines the Physical MAC layer requirements, as well as the communication protocol for active RFID systems communicating at 433 MHz. ISO/IEC 18000-7 was ratified in 2004, and underwent modifications in 2008 and 2009.

5.2.1 Anti-collision procedure

The anti-collision algorithm defined in ISO/IEC 18000-7 is based on a FSA procedure. Figure 5.1 illustrates the identification sequence. Before the reader initiates the identification procedure, a *Wake-Up* signal is sent by the reader to wake up the N tags within its coverage range. Tags move to *idle* mode, listening to the channel. Then, the reader initiates a collection round (or identification cycle) by sending a *Collection* command, with two parameters:

- The time the reader will be listening to the channel, waiting for tag responses. The standard denotes this parameter as the *Window Size* (W_S).
- The length of the tag responses (T_{tag}), determined by the field *type* in the *Collection* command. Note that this parameter determines the type of tag response (*e.g.* only identifier, only specific data, etc.)

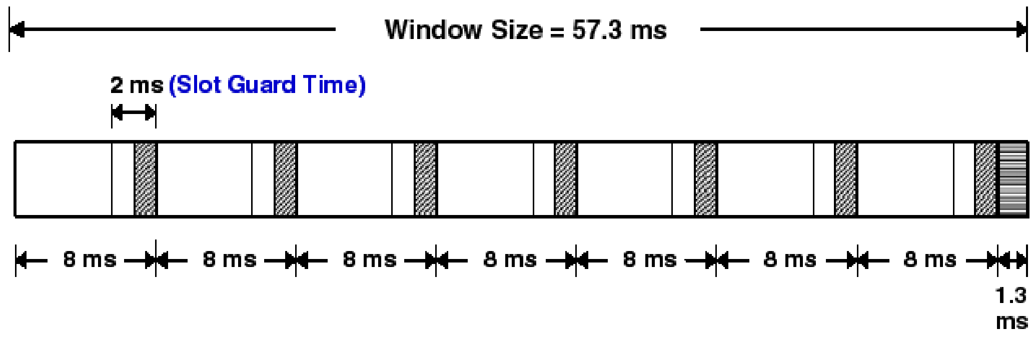

Figure 5.2: Collection round of ISO/IEC 18000-7 (reproduced from [ISO03])

After transmitting the *Collection* command, the reader senses carrier signals during the *Windows Size* time waiting for tag responses. Every time a tag response is detected, it is processed and the corresponding tag identifier is inserted into a buffer, commonly called *sleep queue*. After the collection round, the reader extracts the identifiers stored in the sleep queue one by one, and, for each identifier, the reader transmits a unicast *Sleep* command (see Figure 5.1). When tags receive the *Sleep* command, they change to the sleep mode (saving energy mode) and do not participate again in the following collection rounds. Afterwards, the reader starts a new collection round, resuming the identification process, which eventually finishes after three consecutive collection rounds without reply.

Tags operate as follows: when they receive a *Collection* command, they extract the value of *Windows Size* parameter (in seconds) and calculate the number of slots (K) and the slot size (T_{slot}). The latter is calculated as follows,

$$T_{slot} = T_{tag} + T_{proc} \tag{5.1}$$

being T_{proc} the time the reader needs to process the data received from a tag and the time to be ready to listen to the following tag response. By default, the standard sets T_{proc}=2 ms. Once T_{slot} is calculated, the tag uses it to calculate K as follows,

$$K = \left\lceil \frac{W_S}{T_{slot}} \right\rceil \tag{5.2}$$

K is rounded up to the nearest integer.

The process continues with tags selecting a random slot (with a uniform distribution) to send their *Response* packet. Each tag controls when the slot selected starts by means of an internal clock. Let us remark that carrier sensing is not performed in this procedure. When the selected slot starts, tags change to the transmit mode and send their identifier. After that, tags change to receive mode and listen to the channel. If tags are identified, they will receive a *Sleep* command to change to the sleep mode. If tags are not identified (*e.g.* due to collisions, transmission errors, etc.) they will receive a new *Collection* command.

5.2.2 Operational modes

As we stated in the introduction, ISO-18000-7 offers two operational modes: *(i)* fixed frame window size procedure, where the same window size is used for every collection round, and *ii* variable window size procedure, where the reader, at the end of every collection round, decides whether to increase, decrease or maintain the window size in the subsequent collection round. Both procedures are studied in depth in the following sections.

5.2.2.1 Fixed window size procedure

In this case, the reader uses the same window size for every collection round i. The window size is calculated by the reader as follows:

$$W_{S_i} = W_{F_i} \cdot 57.3 \tag{5.3}$$

for i= 1,2,$\ldots, C$.

W_{F_i} is defined by the standard as the *Window Factor*. W_{F_i} takes the same value for every collision round i. Figure 5.2 shows an example of constant window size in a collection round i with W_{F_i}=1, the default value recommended by the standard.

As discussed in Chapter 2, the fixed window size provides a low degree of flexibility. Table 5.1 shows the average number of collection rounds versus the initial number of tags in coverage (N) for different K values. With a fixed window size the number of collection rounds increases steeply with the number of tags. Therefore, a simple mechanism like FSA does not scale well, suggesting a window size adaptation mechanism as the number of tags increases.

5.2.2.2 Variable window size procedure

In this operation mode, the reader modifies the window size at the end of every collection round i for the subsequent collection round (i+1) as follows:

$$W_{S_{i+1}} = W_{F_i} \cdot 57.3 \tag{5.4}$$

for $i \geq 1$.

In this procedure W_{F_i} is variable and determines the *Window Size* adjustment. W_{F_i} is calculated as follows:

$$W_{F_i} = f(c_i) = f(g(n_i)) \tag{5.5}$$

As seen in equation (5.5), W_{F_i} is a mapping ($f()$) of the number of collisions slots c_i in a collection round i and, in turn, c_i is a mapping ($g()$) of the number of tags participating in that round (n_i). The standard does not provide the $f()$ and $g()$ functions, leading to different proposals, most of them suggested previously for passive RFID.

5.2.3 Performance analysis

The identification process of ISO/IEC 18000-7 is determined by the number of remaining unidentified tags. Like in EPC-C1G2, the identification process can be modeled as a homogeneous DTMC (*Discrete Time Markov Chain*). In fact, the markovian analysis of ISO/IEC 18000-7 for fixed window size mechanisms and assuming a static scenario, is the same as the one developed for EPC-C1G2 (see Section 3.2).

K \ N	10	20	30	40	50	60	70	80	90	100
4	8.2	60	630	8159	$1.1\ 10^{5}$	$1.6\ 10^{6}$	$2.5\ 10^{7}$	$3.8\ 10^{8}$	$6.0\ 10^{9}$	$9.6\ 10^{10}$
8	3.67	8.56	19.6	49.4	138.0	413.9	1304.2	4244.6	14127	47797
16	2.44	4.11	6.15	8.93	13.03	19.3	29.41	46.0	73.81	121.3
32	1.89	2.76	3.60	4.47	5.424	6.50	7.76	9.26	11.0	13.2
64	1.54	2.15	2.61	3.06	3.465	3.90	4.32	4.77	5.23	5.72

Table 5.1: Average number of collection rounds versus number of tags

5.3 Related works

Active RFID systems are still in an early stage and only a small bunch of works has recently appeared related to ISO/IEC 18000-7. In [Jones07, ChoH06] the authors suggest new tags and readers designed to save energy, and compatible with the standard. However, they do not propose any mechanisms to improve the identification performance.

In [JangS07] the authors focus their proposal on the sleep round (see Figure 5.1), suggesting a mechanism to reduce the number of *Sleep* commands to exchange between reader and tags. However, this procedure does not reduce collisions. In [YoonW08] it is proposed to modify the content of the *Collection* commands to improve the performance. The reader, instead of sending the window size value in the collection command, sends the values of T_{slot} and K, previously calculated by it. Hence, tags only have to calculate the guard time T_{proc}. This solution has some drawbacks: the maximum K value is limited to 256 slots. Therefore, if the number of tags in coverage (N) is higher than the maximum K (a likely condition due to the large communication range of active devices), collisions will raise up and the number of collection rounds will increase. Besides, the proposal forces tags to calculate T_{proc}, though they do not suggest any procedures to do it. Finally, [YoonW08] also suggests to use the variable window size mechanism proposed in [ChaJR05]. However, as we demonstrated in [Bueno09c], it is not efficient.

In [YoonW09] the authors propose a mechanism where the reader, while is listening to the channel waiting for tag responses, recognizes empty slots and uses them to transmit *Sleep* commands to the previously identified tags. Despite this enhancement, there are several issues: the standard defines different time parameters that authors do not consider in their calculations: the time a tag needs to start transmitting its identifier (T_{tt} =1 ms), that is, the reader should listen at least T_{listen}>T_{tt} before detecting an empty slot. Moreover, they do not consider the time required to change from reception to transmission mode (T_{rt} =1.05 ms), and from transmitting the *Sleep* command and time to return to reception mode (T_{tr}=1.05 ms). Since the *Sleep* command is T_{sleep}=4.908 ms long, the implementation of this proposal requires that the time slot size be at least T_{slot}=T_{listen}+T_{rt}+T_{sleep}+T_{tr} $\geq$8.008 ms. However, the standard defines T_{slot}=8 ms (see Figure 5.2).

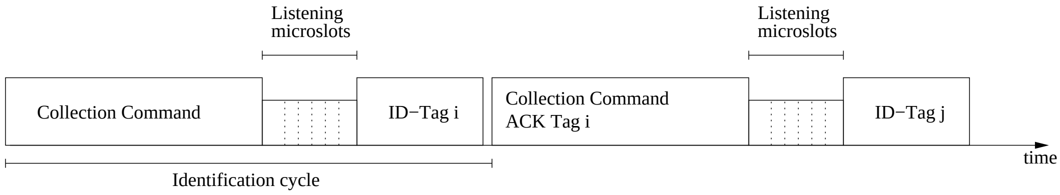

Figure 5.3: Anti-collision procedure with CSMA

5.4 Non-persistent Sift based Carrier Sense Multiple Access proposal

Since active tags have carrier sense capabilities, we propose the non-persistent Sift based CSMA mechanism to improve the identification procedure of ISO/IEC 18000-7, reducing the identification delay. The operation mode is as follows: the reader transmits the *Collection* command, indicating the *Window Size*. Tags calculate the number of contention micro-slots (using the same procedure defined by the standard) and select one of them randomly (see Figure 5.3). Each tag listens to the channel (carrier sense) up to the number of micro-slot chosen. If the channel remains idle after the number of selected micro-slot, the tag sends its ID. If there is no collision, the reader sends an *ACK-Collection* command, which confirms the tag has been identified, and then the reader asks for more IDs. The tag identified changes to sleep mode (saving energy mode) and the remaining tags start the process again. If a collision occurs, the tags withdraw until the next *Collection* command. Figure 5.3 illustrates this mechanism.

The duration of each micro-slot (denoted as T_{m-slot}) depends on the duration and accuracy of carrier sensing Clear Channel Assessment (CCA), which depends on the technology, device and implementation [Ramac07]. There are many possibilities, but we assume that devices use coherent CCA, that is, the channel is busy when the packet preamble is detected. Thus, we set the micro-slot time to the duration of the preamble ($T_{preamble}$) plus the time a tag needs to start transmitting its identifier (T_{tt}). Therefore,

$$T_{m-slot} = T_{tt} + T_{preamble} \tag{5.6}$$

For ISO/IEC 18000-7, $T_{preamble}$=1 ms and T_{tt}=1 ms [ISO03]. Hence, T_{m-slot}=2 ms can be considered as a conservative value, since current devices can perform this task in less time [Ramac07]. Tags calculate the number of contention micro-slots K as follows,

$$K = \left\lceil \frac{W_S - T_{tag} - T_{proc}}{T_{m-slot}} \right\rceil \tag{5.7}$$

As in the standard, W_S and T_{tag} values are extracted from *Collection* command. K is rounded up to the nearest integer.

Our proposal includes not only to use the typical *Collection* command (see Figure 5.4) but also the *Collection with data format* command defined by the standard (see Figure 5.5). The latter is modified to be adapted to our proposal, replacing *Start Address* and *Number of Data bytes* fields by *Tag ID* field. The result is the *ACK-Collection* command (see Figure. 5.6).

Command Code	Windows size	Reserved
‘10’	2 bytes	1 bytes

Figure 5.4: Collection command format (from [ISO03])

Command Code	Windows size	Start Address (M)	Number of Data bytes (N)
‘11’	2 bytes	3 bytes	1 byte

Figure 5.5: Collection with data command format (from [ISO03])

5.4.1 Performance analysis

We address the performance analysis of the identification procedure in a static scenario (tags enter the reader coverage and do not leave until all tags are identified). The identification process can be modeled as a homogeneous DTMC, X_s, where each state in the chain represents the number of unidentified tags, being s the cycle number. Thus, the state space of the Markov process is $N, N-1, \ldots, 0$, being N the total number of tags to identify. The initial state is $X_0 = N$. The transitions between states represent the probability of success $\pi_p(t)$ when t tags ($t \in [0, \ldots, N]$) select a contention micro-slot using probability distribution p_r, that is, the probability each contender picks the slot r independently. The probability of success $\pi_p(t)$, was introduced in [TayYC04]:

$$\pi_p(t) = t \sum_{s=1}^{K-1} p_s (1 - \sum_{r=1}^{s} p_r) \tag{5.8}$$

The transition matrix P for the Markov process $\{X_s\}$ is

$$p_{ij} = \begin{cases} \pi_p(i), \, i = j+1 \\ \\ 1 - \pi_p(i), \, i = j \\ \\ 0, \text{ otherwise} \end{cases} \tag{5.9}$$

The average number of steps until absorption is computed with the same method applied in Section 3.2.1.

Command Code	Windows size	Tag ID
‘11’	2 bytes	4 bytes

Figure 5.6: ACK-Collection command

Let us assume that the micro-slots are chosen uniformly. In this case $p_r = \frac{1}{K}$. Figures 5.7 and 5.8 show the results using a uniform distribution for different numbers of micro-slots. FSA, this proposal does not scale well. In fact, its performance is worse and together with the additional device complexity it may be one of the reasons why it has never been proposed as an anti-collision procedure for RFID systems.

Now let us assume the Sift distribution, which is an approximation to the optimized distribution derived in reference [TayYC04], is used. Sift is based on the concept that when we are interested in low identification delay for the first x tag identification reports, it is important for the first few successful slots to be contention free. Sift uses a fixed window size, but, in contrast to typical FSA procedures, Sift uses a non-uniform, geometrically-increasing probability distribution for picking a transmission slot in the window. Hence, the key difference between Sift and FSA protocols is that the probability of selecting a slot in the window size interval is not uniform. Instead, with a carefully-chosen fixed window size and fixed probability distribution, Sift can perform well in RFID systems.

Therefore, with Sift distribution, the probability to select a slot r is given by:

$$p_r = \frac{\alpha^{-r}(1-\alpha)\alpha^K}{1-\alpha^K} \tag{5.10}$$

for $r = 1 \ldots K$ and $\alpha = M^{\frac{-1}{K-1}}$.

M is a parameter of the Sift distribution, pre-configured before deployment and representing the maximum number of contenders (expected by the designer). The results shown in Figures 5.9 and 5.10 reveal that the number of collection rounds increases almost linearly with the number of tags, unlike the exponential increment of FSA. Therefore, this procedure scales well. In addition, by increasing the number of micro-slots the number of collection rounds tends to the minimum (N collection rounds). However, the duration of a collection round increases and may even be counterproductive. As seen in Figure 5.10, K=8 is enough to handle the entire range of tags.

These results show that after selecting carefully the distribution for the contention window, non-persistent Sift based CSMA becomes an scalable technique for the identification of RFID tags.

5.4.2 Performance Evaluation

In order to compare the different proposals the collection rounds are translated to absolute time, since the actual duration of a collection round depends on the number of slots. First, we compare non-persistent CSMA with the Sift distribution versus ISO/IEC 18000-7. The parameters in ISO/IEC 18000-7 are chosen from the specification [ISO03]. A collection round lasts a *Collection* command (5 ms) plus the slots (8 ms each). Finally, for every identified tag the interrogator sends an *Ack* packet (5 ms) before starting a new collection round. For the CSMA collection round, we set the same duration for the *Collection* command (5 ms) and an *ACK-Data* packet (8 ms) plus the time for *all* the micro-slots, calculated in Section 5.4.

As can be seen in Figure 5.11, non-persistent Sift-based CSMA with 8 micro-slots (and Sift parameter M=64) outperforms the procedure proposed by ISO/IEC 18000-7 for every value of K. When the number of tags is low, the improvement is not important but,

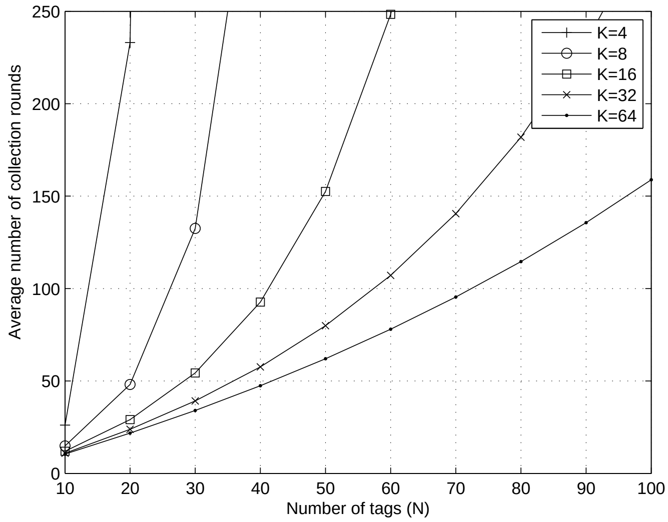

Figure 5.7: Average number of collection rounds with uniform distribution

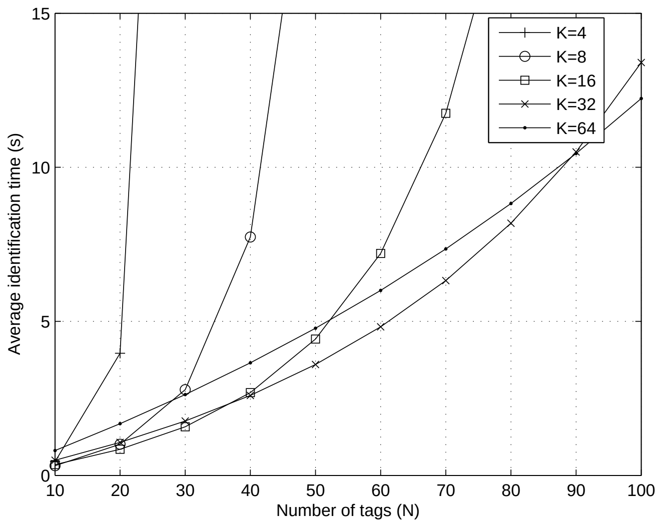

Figure 5.8: Average time with uniform distribution

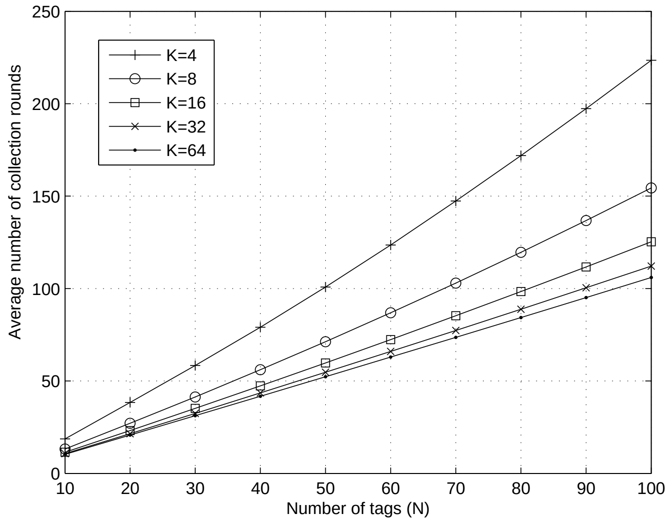

Figure 5.9: Average number of cycles with Sift (M=64)

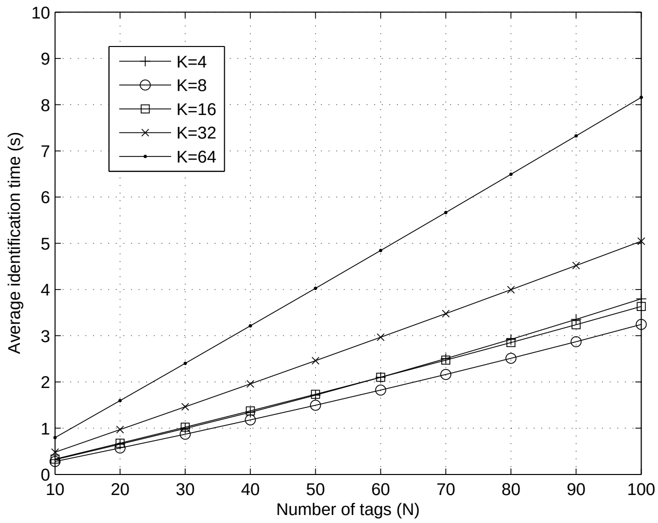

Figure 5.10: Average time with Sift distribution

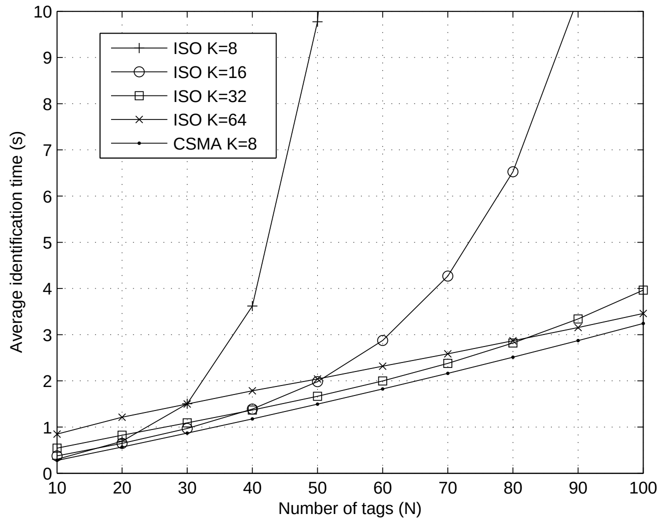

Figure 5.11: Comparison of ISO/IEC 18000-7 versus CSMA with Sift distribution

as the number increases, FSA becomes unstable and the frame length must be adapted. On the contrary, non-persistent Sift-based CSMA can handle all the range of tags seamlessly.

Finally, we compare non-persistent Sift-based CSMA (M=64) with EPC-C1G2. In this case, according to the standard [EPCgl05], empty slots and slots with collision are shorter than slots with successful packets (*Data* packets). However, we provide an approximation of the average identification time, assuming that the duration of all the slots is the same and equals 2.505 ms, which is the time needed for the correct identification of a single tag at 40 Kbps [EPCgl05]. Thus, this is a conservative estimate, since empty and collision slots are actually shorter (0.575 ms). For non-persistent Sift-based CSMA, we set the same values as in the previous comparison. In Figure 5.12 we show the results. In addition to the average number of collection rounds previously computed, we have simulated the EPC-C1G2 with the variable frame length procedure deeply explained in Chapter 2. It is also included in Figure 5.12 labeled as “Adaptive”. Obviously, for a fixed frame length the results are the same as in Figure 5.11 but with another time scale. However, this figure also shows that non-persistent Sift-based CSMA outperforms EPC-C1G2 with frame adaptation as well. Moreover, in this case, the improvement is even better (around 50 % for almost all tag domain) due to the micro-slot length, as discussed before.

In summary, non-persistent Sift-based CSMA makes possible a quick identification of tags in all the cases. The actual improvement depends on the duration of the contention micro-slot. However, it is more important to remark that non-persistent Sift-based CSMA also scales much better than ISO/IEC 18000-7 and EPC-C1G2, even with its variable frame length procedure (variable EPC-C1G2), which simplifies the implementation of readers and tags.

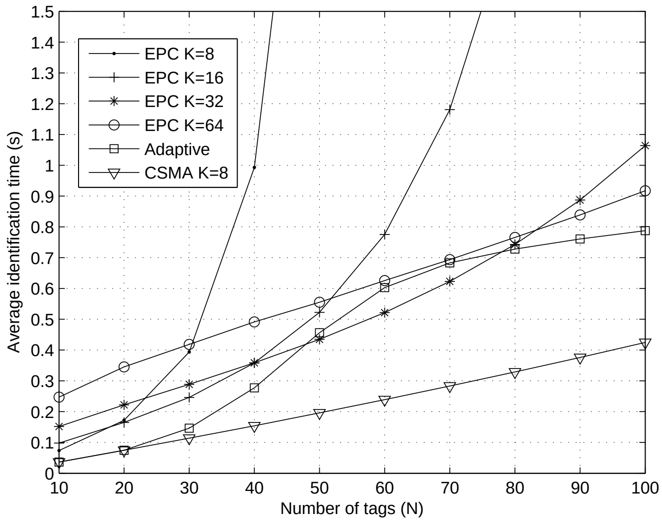

Figure 5.12: Comparison of EPC-C1G2 versus CSMA with Sift distribution

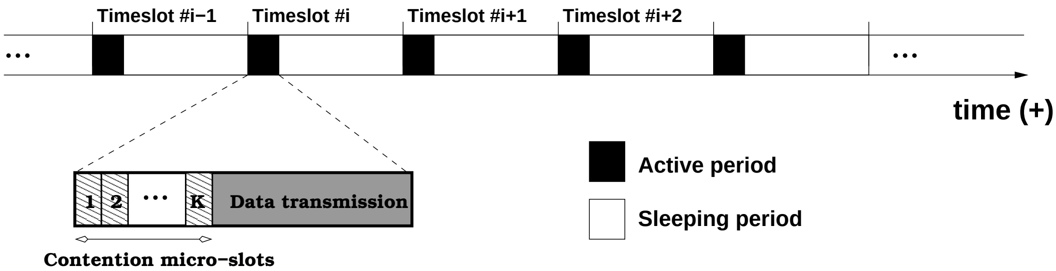

Figure 5.13: Identification procedure with p-persistent CSMA proposal

5.5 p-persistent Carrier Sense Multiple Access proposal

The p-persistent CSMA proposal has been designed for those scenarios where saving energy in active tags is a priority. In contrast to the previous proposal, we assume the tags are always in the sleep mode and, at each contention slot, tags decide wether they wake up (with probability p) or they keep on in the sleeping mode (probability 1-p) (see Figure 5.13). Hence, the goal is to calculate the optimal p value that maximizes energy saving but getting a reasonable identification delay. It is clear that, for low values of p, a considerable saving of energy can be obtained.

Note that this proposal was designed for WSN in [Vales08b]. In that scenario, a population of n nodes monitor an event, and the goal is to minimize the delay of the first notification of the event. In this section, that proposal is extended to RFID as follows: if n tags are in coverage with a reader, the goal is to minimize the delay of the n tag identifications, maximizing the energy saving. The "event" corresponds with an identification order from the reader, an alarm detected by the tag, etc.

5.5.1 Performance analysis

In this section we compute the optimal p for the p-persistent mechanism that minimizes the delay of the first identification, that is, the time elapsed from the moment the reader begins identification procedure to tag identification reaches the reader. Note that this analysis can be seamlessly extended to n identifications with slight modifications.

Before carrying out this analysis, it is necessary to assume a network model, since the optimal p depends on the expected number of tags in coverage.

5.5.1.1 Average notification time

At the beginning of each activity period, all the tags (N) contend in the *Collection* round to transmit their identifiers. Let K be the number of contention micro-slots, and let $\boldsymbol{q}$ be the random variable which selects the initial contention micro-slot for tag $i = 1, \ldots, N$. Let us assume the number of contention micro-slots is a *r.v.* chosen uniformly, q=$Uniform(1, K)$ for all nodes. Let us denote q_k = $Pr(q = k)$ = $\frac{1}{K}$ for every $k \in [1, \ldots, K]$.

The probability of success in contention (one tag sends its identifier successfully) is a function of the number of tags competing (N). Obviously, for N=1 the probability is 1, and for $N \geq 2$ it is given by (see [TayYC04]):

$$\begin{aligned}\pi(N) &= N \sum_{s=1}^{K-1} q_s (1 - \sum_{r=1}^{s} q_r)^{(N-1)} = \\ &= \frac{N}{K} \sum_{s=1}^{K-1} (1 - \frac{s}{K})^{(N-1)}\end{aligned} \tag{5.11}$$

Now, let us consider persistence in the MAC algorithm; in this case the probability of success is computed in expression (5.12).

$$\pi(N, p) = \sum_{c=1}^{N} \pi(c) \binom{N}{c} p^c (1-p)^{N-c} \tag{5.12}$$

For a given number of contending tags (N), we can define the *r.v.* T_N representing the "number of time slots until one of the N tags wins the contention and transmits". The mass probability function of T_N is given by the following equation:

$$Pr(T_N = j) = \pi(N, p)(1 - \pi(N, p))^{j-1} \tag{5.13}$$

for all $j \geq 0$.

In the last expressions we have considered parameter N as a constant. However, as we discuss in the following section, there are scenarios where N can be a *r.v.* N. In this case, the average number of time slots until a tag wins the contention ($\bar{T}$), for a random number of contenders N is

$$\bar{T}(p) = \sum_{i=1}^{n} \bar{T}_i Pr(N = i) \tag{5.14}$$

Note that $Pr(N = i)$ depends on the scenario considered (see section 5.5.1.2, equation (5.15)).

Let us notice that the previous expression gives the average number of time-slots required for the transmission of the first notification.

5.5.1.2 N as random variable. Example of network model

In some active RFID scenarios tags are configured to send data to the reader once they have detected an alarm or an extraordinary event, *e.g.* when active tags used in product traceability detect an increase of temperature which can degrade the product to which they are attached to. These types of scenarios are modeled as follows:

There is a RFID system formed by N tags, densely and randomly deployed in a large area (of size A), and we consider that events occur equiprobability in the area A. Therefore the number of tags that capture each event is given by a *r.v.* N, taking values on $[0, 1, \ldots, n]$. Let us consider a uniform tag distribution into the target area. To compute N, we assume that events are captured by tags within a certain radio r from the point where the event takes place (*e.g.* a reader at distance r starts a Collection round), and that the radio communication coverage radius is R. The size of the area where the event takes place is given by $a = \pi r^2 \ll A$.

If all the tags that receive the event contend for its simultaneous transmission to the reader, then, the probability mass function of N is given by equation (5.15).

$$\begin{aligned} Pr(N = i) &= \binom{n}{i}\left(\frac{a}{A}\right)^i\left(1 - \frac{a}{A}\right)^{n-i} \approx \\ &\approx \frac{(n\frac{a}{A})^i e^{-n\frac{a}{A}}}{i!} \\ &\Rightarrow N \approx Poisson\{n\frac{a}{A}\} \end{aligned} \tag{5.15}$$

In this equation we have employed the Poisson approximation for the binomial distribution. This approximation is correct if $\frac{a}{A} \ll n\frac{a}{A} \ll n$, which is clearly fulfilled since n is expected to be very large and the ratio $\frac{a}{A}$ very low. Based on the Poisson distribution nomenclature, let us define $\lambda = n\frac{a}{A}$. Therefore, in our model λ can be interpreted as the *average number of tags that detect an event or alarm*.

In addition, there is a relationship between λ and the event coverage probability (α), which the probability that at least one tag captures an event,

$$\begin{aligned} 1 - \alpha = Pr(N) = 0 \Rightarrow \alpha = 1 - e^{-\lambda} \Rightarrow \\ \Rightarrow \begin{cases} \lambda = -ln(1-\alpha) \\ n = -\frac{A}{a}ln(1-\alpha) \end{cases} \end{aligned} \tag{5.16}$$

Hence, for a given coverage probability target we can compute the number of tags to be deployed, and the λ associated to such network configuration. Figure 5.14 shows the λ value *versus* a coverage probability target from 95% to almost 100%.

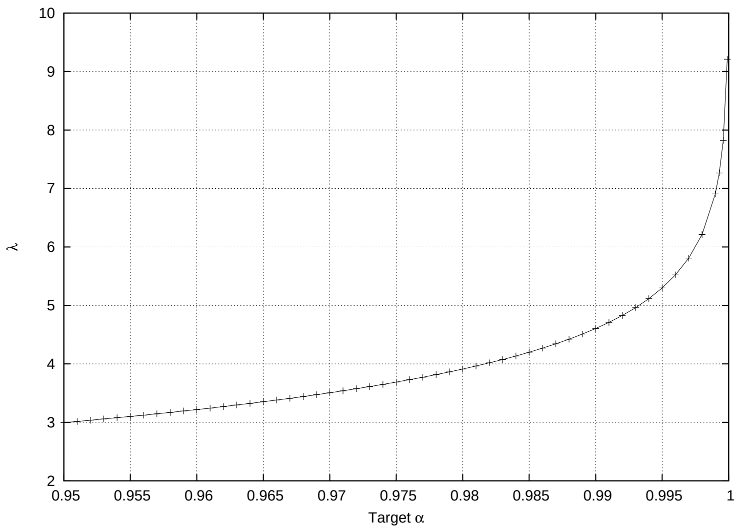

Figure 5.14: λ versus target α

5.5.1.3 p optimization

From the previous analysis we can express our minimization criterion as,

$$
\begin{aligned}
p &= \arg\min_p \left\{\bar{T}(p)\right\} = \\
&= \arg\min_p \left\{\sum_{i=1}^{n} \bar{T}_i Pr(N=i)\}\right\} = \\
&= \arg\min_p \left\{\sum_{i=1}^{n}\left(\sum_{j=1}^{\infty} jPr(T_i=j)\right)Pr(N=i)\right\}
\end{aligned}
$$

Simplifying,

$$
\begin{aligned}
\bar{T}(p) &= \frac{1}{p}\sum_{i=1}^{n}\left(\frac{1}{\sum_{c=1}^{i}\pi(c)\binom{i}{c}p^{c-1}(1-p)^{i-c}}\frac{\lambda^i e^{-\lambda}}{i!}\right) \\
&= \frac{f(p)}{p}
\end{aligned}
\tag{5.17}
$$

Deriving the previous equation and equalling to zero to compute the minimum, we obtain,

$$
\frac{d\bar{T}(p)}{dp} = \frac{d(f(p)/p)}{dp} = 0 \Rightarrow p = \frac{f(p)}{f'(p)} = g(p) \tag{5.18}
$$

From equation (5.18) the optimal p can be computed using the Banach's fixed point theorem [Debna90]. This theorem states that for a contraction mapping $g(x)$ from a closed subset F of a Banach space E into F, a unique x exists in F such that $g(x) = x$. In our problem the contraction mapping is $g(p) = \frac{f(p)}{f'(p)}$. In addition, the theorem provides a

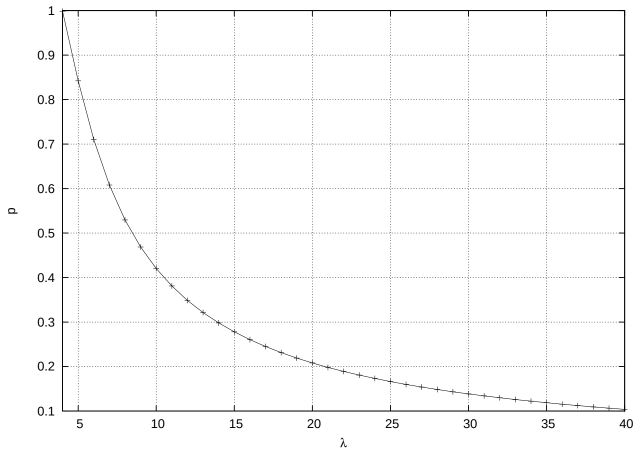

Figure 5.15: Optimal p versus λ

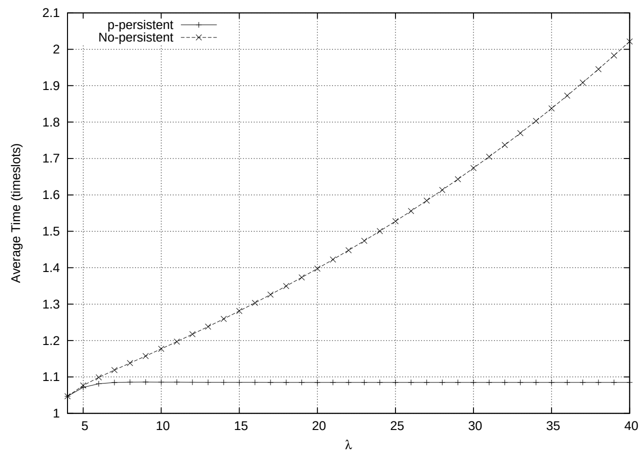

Figure 5.16: $\overline{\boldsymbol{T(p)}}$ versus λ for the optimal p

constructive method to find out the fixed point: setting an arbitrary initial p_0 we compute $p_{i+1} = g(p_i) = \frac{f(p_i)}{f'(p_i)}$. Eventually, the succession p_i converges to the optimal p. Furthermore, since the theorem guarantees that the solution is unique this point is the minimum we look for.

5.5.2 Results

Figure 5.15 shows the optimal p obtained using the fixed point theorem. For values of λ lower than 3.5 we obtain a p>1, which has no physical meaning. In these cases, we have to select p=1 to achieve the best performance. That is, the mechanism behaves as a 1-persistent algorithm. However, note that in any practical deployment the number of tags must be selected so that the probability of losing events is low enough (usually target values should be less than 1%). Looking at Figure 5.14, we conclude that in this case λ >4. For these values of λ we obtain p<1, and the use of the p-persistent approach makes sense.

Figure 5.16 shows the average number of activity periods (time-slots) required for the

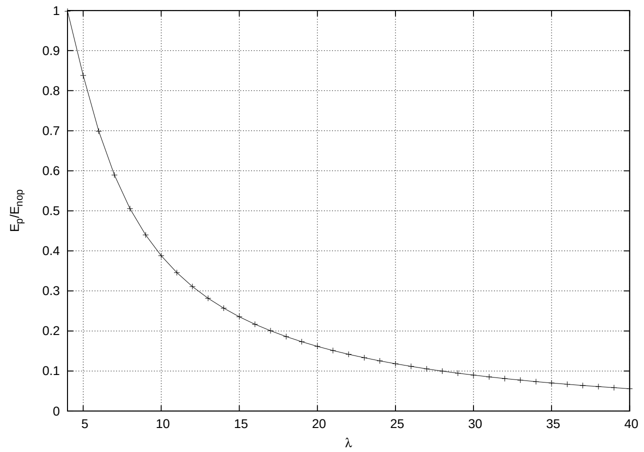

Figure 5.17: Ratio of energy consumption by p-persistent and no persistent protocols versus λ for the optimal p

event notification for both, the p-persistent and 1-persistent variant (*i.e.*, no persistence mechanism used) of the protocol respectively. As it is shown, the use of persistence controls and adjusts contention, keeping the notification delay almost constant. On the contrary, with 1-persistence, delay increases as the number of contenders raises (higher λ). In fact, the increase may be higher, depending on the size of the contention window, that is, the available number of micro-slots (these results have been computed for K=32).

Finally, the energy saving can be approximated as follows. Let us assume some energy consumption per awake tag and activity period, G. If no persistence is employed, the energy consumed for the transmission of an identifier is $E_{p=1} \approx \overline{\boldsymbol{T(1)}}\lambda G$ (let us recall that λ represents the average number of tags trying to compete). Whereas if p-persistence is used the energy consumed is $E_p \approx p\overline{\boldsymbol{T(p)}}\lambda G$. Let us notice that the average time $\overline{\boldsymbol{T(p)}}$ is different in each case. Thus, the benefit is twofold since energy is reduced because of both the asleep tags and the fewer number of time slots needed. As shown in figure 5.17, using p-persistence the energy consumed can be as just a 5% of the energy wasted by the common approach for high density networks.

5.6 Conclusions

In this chapter we have studied how the current identification procedures in active devices have a low performance due to the use of anti-collision techniques from passive RFID (based on FSA). Since active technology already includes carrier sense capabilities, the use of non-persistent Sift-based CSMA and p-persistent CSMA as anti-collision procedures is suggested. To support the former proposal we have evaluated its identification performance, and we have compared it with the current ISO/IEC 18000-7 and EPC-C1G2 standards. The results show that non-persistent Sift based CSMA outperforms both standards. For instance, the average identification time can be decreased by 50% compared to variable EPC-C1G2. In both cases, non-persistent Sift-based CSMA also scales much better: configured with 8 micro-slots CSMA, can effectively handle a range that spans from a few tags to hundreds of them. Besides, p-persistent CSMA has also been proposed as a solution to reduce identification delays and, specially, to save energy. The p-persistent approach notably reduces energy consumption since: (i) the number of collisions is minimized, and (ii) tags do not wake up in many contention rounds. The optimal persistence (p) according to the expected number of tags trying to send their identifiers has been computed by means of a numerical algorithm based on the Banach's fixed point theorem, for different realistic network configurations. Results show a remarkable improvement, in the order of 95%, in terms of energy saving.

Chapter 6

Conclusions

In this chapter we summarize the main outcomes of this thesis, as well as the possible issues that may be addressed in future works.

6.1 Conclusions

Chapter 1 provides an overview of the RFID foundations and describes the major technical issues related to the technology and its standardization. The main research fields in RFID are summarized, together with a brief introduction on the topics related to anti-collision mechanisms.

In Chapter 2 we have studied the collision resolution methods based on FSA and DFSA. Some flaws have been detected in former proposals, and a computational cost analysis reveals that some mechanisms, such as SbS [Knerr08] and *Floerker* [Floer06], are not feasible. Other proposals, like Variable EPC and Heuristic families, are computationally more efficient due to their intrinsic nature. Besides, it is concluded that DFSA proposals based on ML estimators, such as *Chen-3* [ChenW09], achieve the closest approach to the optimal algorithm for large values of N, and that the mixed ML-Bayesian strategy of *Floerker* estimator in [Floer06] has an excellent performance for lower values of N, but it degrades as the initial population grows.

In addition, a new algorithm (MFML-DFSA) was developed. It mixes statistical information from several frames to improve the estimation of the number of tags via a ML estimator. The results have demonstrated that MFML-DFSA outperforms other DFSA proposals with a low computational cost.

Chapter 3 analyzes the identification process of passive RFID systems to find optimal configurations. Optimal parameters depend on the type of traffic and on the underlying anti-collision scheme in use. Criteria are provided to select either the best frame length (K) or the best population (N) in static and dynamic scenarios (Table 3.3 and Figure

3.14), whereas in semi-static case the required sojourn time is also characterized (see Figures 3.6 and 3.10). Empirical results have matched the analysis prediction. Finally, the static scenario was also analyzed considering the realistic Capture Effect phenomenon. The identification time is around 35% less.

In Chapter 4 the collision problems in Dense Reader Environments have been reviewed. Related proposals aim at minimizing either Reader-Tag collisions or Reader-Reader collisions. Besides, most of them require extra hardware in tags and/or readers, or are incompatible with current standards. An evaluation was carried out comparing these mechanisms. The conclusion is that efficiency is low in scenarios with a high number of readers (see Figure 4.4). Moreover, network usability of schedulers is also low (see Figure 4.5), motivated by the exclusive use of FDMA or TDMA.

Finally, Chapter 5 is devoted to the active RFID anti-collision procedures. The ISO/IEC 18000-7 standard and some related proposals are described. We have extracted the shortcomings of those proposals and have suggested the use of two procedures applied previously in WSN: non-persistent Sift-based CSMA and p-persistent CSMA. We have analyzed both procedures and the results have confirmed that the non-persistent Sift based CSMA outperforms ISO/IEC 18000-7 and EPC-C1G2 in terms of identification delay (see Figure 5.11). Besides, the p-persistent approach may achieve energy savings up to 95% in active tags.

6.2 Future works

To close this work let us comment some open issues and future works that may be of further interest.

The MFML-DFSA estimator proposed in Chapter 2 could be modified to improve the estimate using additional information collected in the Physical layer, using some of the techniques described in section 2.1. Moreover, the Capture Effect phenomenon could be considered to get more accurate results. In both cases, the computational cost should be evaluated to study the impact on the final performance.

The conclusions extracted from Chapter 3 show that there are some open issues related to the identification procedure that have not been addressed yet: the analytical characterization of semi-static and dynamic scenarios considering Capture Effect phenomenon, the study of the identification delay in dynamic scenarios with different incoming traffics, as well as the analysis of the identification procedure in scenarios with more than one reader.

Besides, in Chapter 4 the requirements of dense reader environments have been introduced. A promising area is the development of efficient schedulers.

Bibliography

[Abder07] Abderrazak, H., Slaheddine, B., Ridha, B., Performance Analysis of Aloha Protocol for RFID Communication Systems, *International Journal of Computer Science and Network Security*, vol. 7 (12), 2007, pp. 80-83.

[Abrah02] Abraham, C., Ahuja, V., Ghosh A.K., Pakanati, P., Inventory Management using Passive RFID Tags: A survey, *Department of Computer Science, The University of Texas at Dallas*, Texas (USA), 2002, pp. 1-16.

[Akyld95] Akyldiz, I.F., Kasimoglu, I. H., Wireless sensor and actor networks: Research challenges, *Elsevier Journal of Ad Hoc Networks*, vol. 2 (4), 1995, pp. 351-357.

[Akyld02] Akyildiz, I.F., Su, W., Sankarasubramanian, Y., Cayirci, E., A survey on sensor networks, *IEEE Journal of Communications Magazine*, vol. 40 (8), 2002, pp. 102-116.

[Alien] Documentation available on-line at: http://www.alientechnologies.com

[Al-Jar09] Al-Jaroodi, J., Aziz, J., Mohamed, N., Middleware for RFID systems: An overview, *IEEE International Conference on Computer Software and Applications*, vol. 2, 2009, pp. 154-159.

[Altic09] Documentation available on-line at: http://www.altic.com.mex

[Anger10] Angerer, C., Maier, G., **Bueno Delgado, M.V.**, Rupp, M., Vales Alonso, J., Recovering from Collisions in Multiple Tag RFID Environments, in *Proc. IEEE International Conference on Industrial Technology*, Viña del Mar (Chile), 2010.

[AutoID] Documentation available on-line at: http://www.autoidcenter.org.

[Awid] Documentacion available on-line at: http://www.awid.com

[Birar05] Birari, S. M., Iyer, S., PULSE: A MAC Protocol for RFID Networks, in *Proc. 1st International Workshop on RFID and Ubiquitous Sensor Networks*, Japan, 2005, pp. 1036-1046.

[Bueno08a] **Bueno Delgado, M.V.**, Vales Alonso, J., González Castaño, F.J, Egea López, E., García Haro, J., Análisis de mecanismos anticolisión en sistemas RFID pasivos UHF, in *Proc. II Jornadas sobre RFID*, Cuenca (Spain) 2008, pp. 254-260. (***Best paper award***)

[Bueno08b] **Bueno Delgado, M.V.**, Vales Alonso, J., Egea López, E., García Haro, J., Estudio de la configuración óptima de longitud de ciclo en Sistemas RFID, in *Proc. VII Jornadas de Ingeniería Telemática*, Alcalá de Henares (Spain), 2008, pp. 313-320.

[Bueno09a] **Bueno Delgado, M.V.**, Vales Alonso, J., Egea López, E., García Haro, J., Radio-Frequency Identification Technology, *Handbook of Enterprise Intregration, chapter 19, Auerbach Publications, CRC Press*, 2009, pp. 429-466.

[Bueno09b] **Bueno Delgado, M.V.**, Vales Alonso, J., Egea López, E., García Haro, J, Optimum Frame-Length Configuration in Passive RFID Systems Installations, in *Proc. 3rd International Workshop on RFID Technology-Concepts, Applications and Challenges*, Milan (Italy), 2009, pp. 69-77. (***Best paper award***)

[Bueno09c] **Bueno Delgado, M.V.**, Vales Alonso, J., González Castaño, F.J, Analysis of DFSA Anti-collision Protocols in Passive RFID Environments, in *Proc. 35tn International Conference of the IEEE Industrial Electronics Society*, Porto (Portugal), 2009, pp. 2630-2637.

[Bueno09d] **Bueno Delgado, M.V.**, Vales Alonso, J., Estudio de mecanismos de convivencia de lectores en Sistemas RFID pasivos, in *Proc. III Jornadas Científicas sobre RFID*, Bilbao (Spain) 2009, pp. 65-72. (***Best Paper award***)

[Bueno10a] **Bueno Delgado, M.V.**, Vales Alonso, J., Angerer, C., Rupp, M., A comparative study of RFID Schedulers in Dense Reader Environments, in *Proc. IEEE International International Conference on Industrial Technology*, Viña del Mar (Chile), 2010.

[Bueno10b] **Bueno Delgado, M.V.**, Vales Alonso, J., On the Optimal Configuration on Passive RFID Systems, *Journal of Networks and Computer Applications* (pending of publication).

[Caen] Documentation available on-line at: http://www.caen.it/rfid

[ChaJR05] Cha, J-R., Kim, J-H., Novel Anti-collision Algorithms for Fast Object Identification RFID System, in *Proc. 11th Conference on Parallel and Distributed Systems*, vol. 2, 2005, pp. 63-67.

[ChaJR06] Cha, J-R., Kim, J-H, Dynamic Frame Slotted Aloha Algorithms using Fast Tag Estimation Method for RFID System, in *Proc. IEEE Consumer Communications and Networking Conference*, vol. 2, 2006, pp. 768-772.

[Chara05] Charalambides, Ch. A., Derivation of a joint occupancy distribution via a bivariate inclusion and exclusion formula, *Metrica 62*, no.2-3, 2005, pp.149-160.

[Charl73] Charles, W., Portable radio frequency emitting identifier, US. Patent 4384288, 1973.

[ChenW06a] Chen, W-T., An efficient Anti-Collision Method for Tag Identification in a RFID System, *IEICE Journal of Transactions on Communications*, vol. E89-B, no. 12, 2006, pp. 3386-3392.

[ChenW06b] Chen, W-T., Lin, G-H., An Efficient Scheme for multiple access in a RFID System, in *Proc. International Conference on Wireless Networks*, 2006, pp. 160-163.

[ChenW09] Chen, W-T., An Accurate Tag Estimate Method for Improving the Performance of an RFID Anti-collision Algorithm Based on Dynamic Frame Length ALOHA, *IEEE Journal of Transactions on Automation Science and Engineering*, vol. 6 (1), 2009, pp. 9-15.

[ChenY03] Chen, Y., Sirer, E.G., Wicker, S. B., On selection of optimal transmission power for ad-hoc networks, in *Proc. 36th Hawaii International Conference on System Sciences*, 2003, pp. 300-309.

[ChenN09] Chen N.K., Chen, J.L., Lee, C.C., Array-based Reader Anti-Collision Scheme for Highly Efficient RFID Network Applications, *Journal of Wireless Communication and Mobile Computing*, vol. 9, 2009, pp.976-987.

[ChoH06] Cho, H., Choi, H., Lee, W., Jung, Y., Baek, Y., LITeTag: design and implementation of an RFID system for IT-based port logistics, *Journal of Communications*, vol. 1 (4), 2006, pp. 48-57.

[Chung07] Chung, H. B., Mo, H., Kim, N., Pyo, Ch., An advanced RFID system to avoid collision of RFID reader, using channel holder and dual sensitivities, *Microwave and Optical Technology Letters*, vol. 49 (11), 2007, pp. 2643-2647.

[DaiH07] Dai, H., Lai, S., Zhu, H., A Multi-Channel MAC Protocol for RFID Reader Networks, in *Proc. International Conference on Wireless Communications, Networking and Mobile Computing*, 2007, pp. 2093-2096.

[Danes07] Daneshmand, M., Wang, C., Sohraby, K., A New-Count Selection Algorithm for RFID protocol, in *Proc. 2nd International Conference on Communications and Networking China*, 2007, pp. 926-930.

[Dash7] Documentation available on-line at: http://www.dash7.org

[Debna90] Debnath, L. and Mikusinski, P. Introduction to Hilbert Spaces with Applications San Diego, CA: Academic Press, 1990.

[DengX08] Deng, X., Rong, M., Liu, T., Yuan, Y., Yu, D., Tag Count Frame Slotted Aloha: A Novel Anti-Collision Protocol in RFID Systems, in *Proc. IEEE Vehicular Technology Conference*, Marina-Bay (Singapore), 2008, pp. 2666-2670.

[Duque93] Duque Anton, M., Kunz, D., and Ruber, B., Channel assignment for cellular radio using simulated annealing, *IEEE Journal of Transactions on Vehicular Technology*, vol. 42, 1993, pp. 4-21.

[EgeaE06] Egea López, E. , Vales Alonso, J., Martínez Sala, A., Pavón Mariño, P., **Bueno Delgado, M.V.**, A real-time MAC protocol for wireless sensor networks: Virtual TDMA for sensors (VTS), in *Proc. International Conference on Arquitecture of Computing Systems*, LNCS, Frankfurt (Germany), 2006, pp. 382-396.

[EgeaE07a] Egea López, E., Vales Alonso, J., Martínez Sala, A., **Bueno Delgado, M.V.**, García Haro, J., Performance evaluation of non-persistent CSMA as anti-collision protocol for active RFID tags, in *Proc. Wire/Wireless Internet Communication*, LNCS, vol. 4517, Coimbra (Portugal), 2007, pp. 279-289.

[EgeaE07b] Egea López, E., **Bueno Delgado, M.V.**, Vales Alonso, J., García Haro, L., Martínez Sala, A., Costas Rodríguez, S., Gil Castiñeira, F., López Bravo, C., González Castaño, F.J., On the Implementation of a Multi-reader Radio Frequency Identification (RFID) Architecture, in *Proc. IEEE International Symposium on Industrial Electronics*, Vigo (Spain), 2007, pp. 2562-2566.

[EgeaE08] Egea López, E.,Vales Alonso, J.,Martínez Sala, A., García Haro, J., Pavón Mariño, P., **Bueno Delgado, M.V.**, A wireless sensor networks MAC protocol for real-time applications, *Journal of Personal and Ubiquitous Computing*, vol. 12 (2), 2008, pp. 111-122.

[EomJ09] Eom, J. B., Yim, S. B., Lee, T. J., An Efficient Reader Anticollision Algorithm in Dense RFID Networks with Mobile RFID Readers, *IEEE Journal of Transactions on Industrial Electronics*, vol. 56, (7), 2009, pp.2326-2336.

[EPCgl05] EPC Radio-Frequency Identify protocol for communications at 868-960 MHz,Version 1.0.9: EPCglobal Standard Specification, 2005. Available on-line at: http://www.epcglobalinc.org/standards

[EPCne04] EPCglobal Inc. The EPCglobal Network: Overview of Design, Benefits and Security. Available on-line at: http://www.epcglobalinc.org

[ETSI-R] Available on line at: http://www.etsi.org/WebSite/technologies/RFID.aspx

[ETSI302] ETSI-EN-302-208 V1.1.1 (2004-9). Available on line at: http://www.etsi.org

[Feller70] Feller, W., An Introduction to Probability Theory and its Applications, *3rd edition Wiley*, vol. 1, New York, 1970.

[Finke03] Finkenzeller, K., RFID Handbook: Fundamentals and Applications in Contactless Smart Cards and Identification, *2nd Edition, John Wiley and Sons, Chichester, Chapters 1-2,* New York, 2003, pp. 1-28.

[Floer06] Floerkemeier, C., Wille, M., Comparison of Transmission Schemes for Framed Aloha based RFID, in *Proc. Workshop on RFID Extended Network Deployment of Technologies and Applications*, Phoenix (AZ), 2006.

[Harri60] Harris, D.B., Radio transmission system with modulatable passive responder, US. Patent 2927321, 1960.

[HoJ06] Ho, J., Engels, D. W. and Sarma, S.E,. HiQ Hierarchical Q-learning algorithm to solve the reader collision problem, in *Proc. International Symposium on Applications and the Internet Workshops*, SAINT Workshops 2006, pp. 88-91.

[HushD98] Hush, D.R, Wood, C., Analysis of Tree Algorithms for RFID Arbitration, in *Proc. International Symposium on Information Theory,* Massachusetts (USA), 1998, pp. 107-114.

[HsuCH07] Hsu, C-H., Chen, Yi-Min, Yang, C-T., A Layered Optimization Approach for Redundant Reader Elimination in Wireless RFID Networks, in *Proc. 2nd IEEE Asia-Pacific Service Computing Conference*, 2007, pp.138-145.

[ICODE] Documentation available on line at: http://www.semiconductors.philips.com.

[Inter] Documentation available on-line at: http://www.intermec.com.

[Impinj] Documentation available on-line at: http://www.impinj.com.

[ISO03] ISO/IEC 1800-6:2003(E), Part 6: Parameters for Air Interface Communications at 860-960 MHz, 2003. Documentation available on line at: http://www.iso.org

[Jacom99] Jacomet, M., Ehrsam, A. and Gehring, U., Contactless identification device with anti-collision algorithm, in *Proc. IEEE Conference on Circuits, Systems, Computers and Communications,* Athens (Greece), 1999, pp. 269-273.

[JangS07] Jang, S.J., Chung, S.H., Yoon, W.J., Lee, S.J., An effective design of an active RFID reader using a cache of tag memory data, in *Proc. International Workshop on Service, Security and its Data management for Ubiquitous Computing*, vol. 4819, 2007, pp. 584-595.

[Jones07] Jones, A.K., Hoare, R., Dontharaju, S., Tung, S., Sprang, R., Fazekas, J., Cain, J.T., Micke, M.H., An Automated, FPGA-based reconfigurable low-power RFID tag, *Journal of Microprocessors and Mircosystems*, vol. 31 (2), 2007, pp. 116-134.

[JoeI07] Joe, I., Lee, J., A Novel Anti-collision Algorithm with Optimal Frame Size for RFID System, in *Proc. 5th ACIS International Conference on Software Engineering Research, Management and Applications*, 2007, pp. 424-428.

[Juels06] Juels, A., RFID security and privacy: A research survey, *IEEE Journal of Selected Areas in Communications*, vol. 24 (2), 2006, pp. 381-394.

[Juels07] Juels A., Weis, S.A., Defining strong privacy for RFID, in *Proc. IEEE International Conference on Pervasive Computing and Communications Workshop*, pp. 342-347, 2007.

[Jurda07] Jurdak, R., Wireless Ad-Hoc and Sensor Networks: Protocols: A Cross-layer Design Perspective, *Springer Verlang, chapter 2,* New York (USA), 2007.

[Kemen60] Kemeny, J.G., Snell, J.L., Finite Markov Chains, *Van Nostrand*, 1960.

[Khasg09] Khasgiwale, R.S., Adyanthaya, R.U., Engels, D.E. Extracting Information from tag collisions, in *Proc. IEEE International Conference on RFID*, Orlando (USA), 2009, pp. 131-138.

[Khande07] Khandhelwal, G., Lee, K., Yener, A., ASAP: A MAC Protocol for Dense and Time-Constrained RFID Systems, *EURASIP Journal on Wireless Communications and Networking*, vol. 9, 2007, pp. 4028-4033.

[KimJ07] Kim, J., Lee, W., Kim, E., Kim, D., Suh, K., Optimized transmission Power Control of Interrogators for Collision Arbitration in UHF RFID Systems, *IEEE Communications letters*, vol. 11, no.1, 2007, pp. 22-24.

[Klein75] Kleinrock L.and Tobagi, F.A., Packet switching in radio channels: Part I-Carrier sense multiple-access modes and their throughput-delay characteristics, *IEEE Journal of Transactions on Communications*, vol. 23 (12), 1975, pp. 1400-1416.

[Kleis05] Kleist, R., Chapman, T., Sakai, D., Jarvis, B., RFID Labeling: Smart Labeling Concepts and Applications for the Consumer Packaged Goods Supply Chain, *2nd Ed., Banta Book Group, chapter 2*, 2005.

[Knerr08] Knerr, B.Holzer, M., Angerer, C., Rup. M, Slot-by-slot Minimum Squared error estimator for tags populations in FSA protocols, in *Proc. 2nd International EURASIP Workshop on RFID Technology*, 2008, pp. 1-13.

[Knerr08-2] Knerr, B.Holzer, M., Angerer, C., Rup. M., Slot-by-slot Maximum Likelihood estimation of tags populations in frame slotted aloha protocols, in *Proc. International Symposium on Performance Evaluation of Computer and Telecommunication Systems*, Edinburgh (UK) 2008, pp. 303-308.

[Kubic03] Kubich, M. et al., Distributed algorithms for transmission power control in wireless sensor networks, in *Proc. Wireless Communications and Networking Conference*, 1, 2003, pp. 558-563.

[KunzD91] Kunz, D., Channel assignment for cellular radio using neural networks, *IEEE Journal of Transactions on Vehicular Technolgies*, vol. 40, 1991, pp. 188-193.

[Kwang06] Kwang-il, H., Kyung-tae, K., Doo-seop, E., DiCA: Distributed Tag Access with Collision Avoidance among Mobile RFID Readers, in *Proc. International Conference on Computational Science and Engineering*, vol. 2, 2006, pp. 621-626.

[LaiW96] Lai, W. K. and Coghill, G.G., Channel assignment for a homogenous cellular network with genetic algorithms, *IEEE Journal of Transactions on Vehicular Technolgies*, vol. 45, 1996, pp. 91-96.

[LawC00] Law, C., Lee, K. and Siu, K., Efficient memoryless protocol for tag identification, in *Proc. 4th International Workshop on Discrete Algorithms and Methods for Mobile Computing and Communications*, 2000, pp. 75-84.

[LeeD07] Lee, D., Kim, K., Lee, W., Q+- Algorithm: An Enhanced RFID Tag Collision Arbitration Algorithm, in *Proc. Ubiquitous Intelligence and Computing*, LNCS, vol. 4611, 2007, pp. 23-32.

[Leckl05] Lecklider, T., The world of nearfield, Evaluation Engineering, 2005, available on line at http://www.availableengineering.com

[LeonA96] Leon-Garcia A. and Widjaja, I., Communication Networks: Fundamental Concepts and Key Architectures, *McGraw-Hill Press, Boston, Chapter 6, part 1*, 1996, pp. 368-421.

[Leong05] Leong, K.S., Ng, M.L., Cole, P.H., The reader collision problem in RFID systems, in *Proc. IEEE International Symposium on Microwave, Antenna, Propagation and EMC Technologies for Wireless Communications*, 2005, pp. 658-661.

[LiuL08] Liu, L., Yan, D., Lai, X., Lai, S., A New Kind of RFID Reader Anti-collision Algorithm, in *Proc. 4th IEEE International Conference on. Circuits and Systems for Communications*, 2008, pp. 559-563.

[Myung06] Myung, J., Lee, W., Adaptive Splitting Protocols for RFID Tag Collision Arbitration, in *Proc. International Symposium on Mobile Ad-Hoc Networking and Computing*, 2006, pp. 203-213.

[Milen04] Milenkovic, O., Compton, K. J., Probabilistic transforms for combinatorial urn models, *Journal of Combinatorics, probability and Computing*, vol. 13 (4-5), 2004, pp. 645-675.

[Peris06] Peris-Lopez, P., Hernandez-Castro, J.C., Estevez-Tapiador, J.M., Ribagorda, A., RFID Systems: A survey on security threats and proposed solutions, in *Proc. 11th IFIP International Conference on Personal Wireless Communications*, LNCS, vol. 4217, 2006, pp. 912-923.

[PSG09] Available on line at: http://www.pgselectronics.com/PGSRFID.htm

[Ramac07] Ramachandran, I., Das, A., Roy, S., "Clear Channel Assessment in Energy-constrained Wideband Wireless Networks", *IEEE Wireless Communications Magazine*, vol. 14, no. 3, 2007, pp.70-78.

[Rives87] Rivest, R.L, Network Control Bayesian Broadcast, *IEEE Journal of Transactions on Information Theory*, vol. IT-33 (3), 1987, pp. 323-328.

[Rodel07] Rodelgo-Lacruz, M., Gil-Castiñeira, F.J., González-Castaño, F.J., Contreras, J., Gómez, A., **Bueno Delgado, M.V.**, Egea-López, E., Vales-Alonso, J., García-Haro, J., Base technologies for vehicular networking applications: review a case studies, in *Proc. IEEE International Symposium on Industrial Electronics*, 2007, pp. 2567-2572.

[Samsys] Documentation available on-line at: http://www.samsys.com.

[Sarma01] Sarma, S., Brock, D. and Engels, D., Radio frequency identification and the electronic product code, *IEEE Journal of Micro*, vol. 21 (6), 2001, pp. 50-54.

[Sarma03] Sarma, S., Engels, D.W., RFID Systems, Security and Privacy Implications, Auto-ID Center White Paper, February 2003.

[Savi] Documentation available on-line at: http://www.savi.com

[Schou83] Schoute, F.C, Dynamic Frame Length ALOHA, *IEEE Journal of Transactions on Communications*, vol. 31 (4), 1983, pp. 565-568.

[Schur08] Schurgers, C., Li, Y., Thai, M.T. and Wu, W., Wakeup strategies in wireless sensor networks, in Wireless Sensor Networks and Applications, *Eds., Springer Verlang, chapter 8*, 2008, pp. 195-217.

[Shail05] Shailesh B. and Iyer, S., Pulse: A MAC protocol for RFID Networks, in *Proc. 1st International Workshop on RFID and Ubiquitous Sensor Networks*, LNCS, 2005, pp. 1036-1046.

[ShenD09] Shen, D., Woo, G., Reed, D.P., Lippman, A.B., Wang, J., Separation of Multiple Passive RFID Signals Using Software Defined Radio, in *Proc. IEEE International Conference on RFID*, Orlando (USA), 2009, pp. 139-146.

[ShihD06] Shih, D-H., Sun, P-L, Yen, D.C., Huang, S-M, Taxonomy and survey of RFID anti-collision protocols, *Journal of Computer and Communications*, vol. 29, 2006, pp. 2150-2166.

[Siege03] Siegemund, F., Flörkermeier, C., Interaction in Pervasive Computing Settings using Bluetooth-Enabled Active Tags and Passive RFID Technology together with Mobile Phones, *in Proc IEEE Personal Communications*, 2003, pp. 378-387.

[Stemm97] Stemm, M., and Katz, R.H., Measuring and reducing energy consumption of network interfaces in hand-held devices, *IEICE Journal of Transactions on Communications*, vol. E80B, 1997, pp. 1126-1131.

[Stock48] Stockman, H., Communications by means of reflected power, in *Proc. IRE*, vol. 36 (10), 1948, pp. 1196-1204.

[SungK06] Sungjun, K., Sangbin, L., Sunshin, A., Reader Collision Avoidance Mechanism in Ubiquitous Sensor and RFID Networks, in *Proc. International workshop on Wireless network testbeds, Experimental Evaluation and Characterization*, Los Angeles (USA), 2006.

[Symbol] Documentation available on-line at: http://www.symbol.com/rfid

[Takag84] Takagi, H., Kleinrock, L., Optimal transmission ranges for randomly distributed packet radio terminals, *IEEE Journal of Transactions on Communications*, vol. 32 (3), 1984, pp. 246-257.

[TayYC04] Tay, Y.C., Jamieson, K., Balakrishnan, H., Collision-Minimizing CSMA and its Applications to Wireless Sensor Networks, *IEEE Journal on Selected Areas in Communications*, vol. 22(6), 2004, pp. 1048-1057.

[ThingMagic] Documentation available on-line at: http://www.thingmagic.com

[Tobag75] Tobagi, F. A. and Kleinrock, L., Packet Switching in radio channels: Part II- The hidden terminal problem in carrier sense multiple access modes and the busy-tone solution, *IEEE Journal of Transactions on Communications*, vol. 23 (12), 1975, pp. 1417-1433.

[TongQ07] Tong, Q., Zou, X., Liu, D., Dai, Y. Modeling the Anti-collision Process of RFID System by Markov Chain, in *Proc International Conference on Wireless Communications, Networking and Mobile Computing*, 2007, pp. 2054-2057.

[Vales07a] Vales Alonso, J, Egea López, E., Martínez-Sala, A., Pavón Mariño, P., **Bueno Delgado, M.V.**, García Haro, J., Performance evaluation of MAC transmission power control in wireless sensor networks, *Journal of Computer Networks*, vol. 51 (6), 2007, pp. 1483-1498.

[Vales07b] Vales Alonso, J., **Bueno Delgado, M.V.**, Egea López, E., García Haro, J., Analisis mediante simulacion de esquemas de adapatacion de la longitud de trama en escenarios RFID con tags dinámicos, in *Proc. VI Jornadas de Ingeniería Telemática*, 2007, pp. 313-320.

[Vales07c] Vales Alonso, J., González Castaño, F.J., Egea López, E., **Bueno Delgado, M.V.**, Martínez Sala, A., García Haro, J., Evaluación de CSMA no persistente como protocolo anticolisión en sistemas RFID activos, in *Proc. I Jornadas Científicas sobre RFID*, Ciudad Real (Spain), 2007, pp. 313-320. (***Best paper award***)

[Vales08a] Vales Alonso, J., **Bueno Delgado, M.V.**, Egea López, E., García Haro, J., Tag Loss Probability Evaluation for a Continuos Flow of Tags in the EPC-Global Standard, in *Proc. 2nd International Workshop on RFID Technology*, Barcelona (Spain), 2008, pp. 115-126.

[Vales08b] Vales Alonso, J., Egea López, E., **Bueno Delgado, M.V.**, Sieiro Lomba, J.L., García Haro, J., Optimal p-persistent MAC algorithm for event-driven Wireless Sensor Networks, in *Proc. 4th EURO-NGI Conference on Next Generation Internet Networks*, Kraków (Poland), 2008, pp. 203-208.

[Vales08c] Vales Alonso, J., Egea López, E., Sieiro Lomba, J.L., **Bueno Delgado, M.V.**, García Haro, J., Evaluación de un mecanismo MAC p-persistente para redes inalámbricas de sensores con tráficos por eventos, in *Proc. Jornadas de Ingeniería Telemática*, Alcalá de Henares (Spain), 2008, pp. 254-260.

[Vales08d] Vales Alonso, J., Costas Rodriguez, S., **Bueno Delgado, M.V.**, Egea López, E., Gil Castiñerira, F., Rodriguez Fernandez, P.S., García Haro, J., Gonzalez Castaño, F.J., An Analytical Approach to the Optimal Deployment of Wireless Sensor Networks in *Computational Intelligence for Remote Sensing SCI 133*, M. Graña and R.J. Duro (Eds.), Springer Verlag Berlin Heidelberg, 2008, pp. 145-161.

[Vales09] Vales Alonso, J., **Bueno Delgado, M.V.**, Egea López, E., García Haro, J., Markovian Model for Computation of Tag Loss Ratio in Dynamic RFID Systems, in *Proc. 4th European Workshop on RFID Systems and Technologies*, Bremen (Alemania), 2009. (***Best paper award***)

[Vales10a] Vales Alonso, J., **Bueno Delgado, M.V.**, Egea López, E., Alcaraz Espín, J.J., Gonzalez Castaño, F.J., Characterization of the identification process in RFID systems, *Chapter in Radio Frequency Identification: Fundamental and Applications book* (pending of publication).

[Vales10b] Vales Alonso, J., Egea López, E., **Bueno Delgado, M.V.**, Alcaraz Espín, J.J., Analysis of Tag Loss Ratio in Dynamic RFID Systems, *International Journal of RF Technologies* (pending of publication).

[Vales10c] Vales Alonso, J., **Bueno Delgado, M.V.**, Egea López, E., Alcaraz-Espin, J.J., Gonzalez-Castaño, F.J., RFID Multi-Frame Maximum Likelihood Dynamic FSA Anti-collision Algorithm, *IEEE Journal of Transactions on Industrial Electronics* (under review).

[Varga01] A. Vargas, The OMNeT++ Discrete Event Simulation System, in *Proc. European Simulation Multiconference*, Prague (Czech Republic), 2001.

[Verno52] Vernon F.L., Applications of the microwave Homodyne, *Journal of Transactions of the IRE Professional Group on Antennas and Propagation*, vol. 4 (1), 1952, pp. 110-116.

[Vogt02] Vogt, H., Efficient Object Identification with Passive RFID Tags, in *Proc. International Conference on Pervasive Computing*, LNCS, vol. 2414, 2002, pp. 98-113.

[Waldr03] Waldrop, J., Engels, D.W. and Sarma, S.E., Colorwave: An anti-collision algorithm for the reader collision problem, in *Proc. IEEE Wireless Communications and Networking Conference*, 2003, pp. 1206-1210.

[Wang07] Wang, B-S., Zhang, Q-S., Yang, D-K., Di, J-S., Transmission Control Solutions Using Interval Estimation Method for EPC C1G2 RFID Tag Identification, in *Proc. International Conference on Wireless Communications, Networking and Mobile Computing*, 2007, pp. 2105-2108.

[WangD06] Wang, D., Wang, J., and Zhao, Y., A novel solution to the reader collision problem in RFID system, in *Proc. IEEE International Conference on Wireless Communications, Networking and Mobile Computing*, Montreal (Canada), 2006, pp. 1-4.

[Weise88] Wieselthier, J.E., Ephremides, A., Michaels, L.A., An exact analysis and performance evaluation of framed ALOHA with capture, *IEEE Journal of Transactions on Communications*, vol. 37 (2), 1988, pp. 125-137.

[Wentz06a] Chen, W.T., An efficient Anti-Collision Method for Tag Identification in a RFID System, *IEICE Journal of Transactions on Communications*, vol. E89-B, no. 12, 2006, pp. 3386-3392.

[Wentz06b] Chen, W.T., Lin, G.H., An Efficient Scheme for multiple access in a RFID System, in *Proc. International Conference on Wireless Networks*, 2006, pp. 160-163.

[Wentz08] Chen, W.T., An Accurate Tag Estimate Method for Improving the Performance of an RFID Anti-collision Algorithm Based on Dynamic Frame Length ALOHA, *IEEE Journal of Transactions on Automation Science and Engineering*, vol. 6 (1), 2008, pp. 9-15.

[YeW04] Ye, W., Heidemann, J. and Estrin, D., Medium access control with coordinated adaptive sleeping for wireless sensor networks, *ACM/IEEE Journal of Transactions on Networking*, vol. 12, 2004, pp. 493-506.

[YoonW08] Yoon, W.J., Chung, S.H., Lee, S.J., Implementation and performance evaluation of an active RFID system for fast tag collection, *Journal on Computer Communications*, vol 31, 2008, pp. 4107-4116.

[YoonW09] Yoon, W.J., Chung, S.H., Park, S.J., An efficient tag collection algorithm utilizing empty time slots in active RFID systems, *IEICE Electronics Express*, vol 6, no. 7, 2009, pp. 361-367.

[ZhouF04] Zhou, F., Chen, C., Jin, D., Huang, C., Min, C., Evaluating and optimizing power consumption for anti-collision protocols for applications in RFID systems, in *Proc. International Symposium on Low Power Electronics and Design*, 2004, pp. 357-362.

Acronyms and abreviations

ASK *Amplitude Shift Keying*

CCA *Clear Channel Assessment*

CDMA *Code Division Multiple Access*

CE *Capture Effect*

CEPT *European Conference of Postal and Telecommunications*

CFR *Code of Federal Regulations*

CICL *Complete Identification Confidence Level*

CPU *Central Processing Unit*

CSMA *Carrier Sense Multiple Access*

CTS *Clear To Send*

DFSA *Dynamic Frame Slotted Aloha*

DoD *Department of Defense*

DTMC *Discrete Time Markov Chains*

DSP *Digital Signal Processor*

EAN *European Article Numbering*

EAS *Electronic Article Surveillance*

EPC *Electronic Product Code*

ETSI *European Telecommunications Standards Institute*

FCC *Federal Communications Commission*

FDMA *Frequency Division Multiple Access*

FeliCa *Felicity Card*

FFC *Far Field Communications*

FHSS *Frequency Hopping Spread Spectrum*

FMCG *Fast Moving Consumer Goods*

FSK *Frequency Shift Keying*

FSA *Frame Slotted Aloha*

GFLOPS *Giga FLOating Point Operations per Second*

GTIN *Global Trade Item Number*

HF *High Frequency*

ICL *Identification Confidence Level*

IFF *Identification Friend or Foe*

IQ *In-phase Quadrature*

ISM *Industrial, Scientific and Medical Equipement*

ISO *International Organization for Standardization*

ITU-R *International Telecommunication Union-Radiocommunication*

LBT *Listen Before Talk*

LF *Low Frequency*

MAC *Medium Access Control*

MDD *Minimum Distance Detector*

MFFP *Multi-Frame Full-Parameter*

MFML-DFSA *Multi Frame Maximum Likelihood Dynamic Frame Slotted Aloha*

MFSP *Multi-Frame Single-Parameter*

MIT *Massachusetts Institute of Technology*

ML *Maximum Likelihood*

MPHPT *Ministry of Public Management, Home Affairs, Post and Telecommunication*

MSE *Minimum Squared Error*

NFC *Near Field Communications*

OSPF *Open Shorter Path First*

PSK *Phase Shift Keying*

RCS *Radar Cross Section*

RF *Radio Frequency*

RFID *Radio Frequency Identification*

RRC *Reader to Reader Collision*

RTC *Reader to Tag Collision*

RTS *Request To Send*

SDMA *Space Division Multiple Access*

SFSP *Single-Frame Single-Parameter*

SFFP *Single-Frame Full-Parameter*

SRD *Short Range Devices*

TDMA *Time Division Multiple Access*

TLR *Tag Loss Ratio*

UCC *Uniform Code Council*

UHF *Ultra High Frequency*

WF *Window Factor*

WLAN *Wireless Local Area Network*

WS *Window Size*

WSN *Wireless Sensor Networks*

Alphabetic Index

This work has been supported by project DEP2006-56158-C03-03/EQUI, funded by the Spanish Ministerio de Ciencia y Educación, project TEC2007-67966-01/TCM (CONPARTE-1) and also by the framework of “Programa de Ayudas a Grupos de Excelencia de la Region de Murcia”, funded by Fundacion Seneca, Agencia de Ciencia y Tecnologia de la Region de Murcia (Plan Regional de Ciencia y Tecnologia 2007/2010).

GOBIERNO DE ESPAÑA
MINISTERIO DE CIENCIA E INNOVACIÓN